NASA Technical Memorandum 78629

ROTOR SYSTEMS RESEARCH AIRCRAFT SIMULATION MATHEMATICAL MODEL

JACOB A. HOUCK, FREDERICK L. MOORE,
JAMES J. HOWLETT, KENNETH S. POLLOCK,
AND MARY M. BROWNE

NOVEMBER 1977

National Aeronautics and Space Administration

Langley Research Center
Hampton, Virginia 23665

1. Report No.	2. Government Accession No.	3. Recipient's Catalog No.
NASA TM 78629		

4. Title and Subtitle	5. Report Date
ROTOR SYSTEMS RESEARCH AIRCRAFT SIMULATION MATHEMATICAL MODEL	November 1977
	6. Performing Organization Code
7. Author(s) Jacob A. Houck, Frederick L. Moore, James J. Howlett, Kenneth S. Pollock and Mary M. Browne	8. Performing Organization Report No.
	10. Work Unit No. 745-01-01-01
9. Performing Organization Name and Address NASA Langley Research Center Hampton, VA 23665	11. Contract or Grant No.
	13. Type of Report and Period Covered Technical Memorandum
12. Sponsoring Agency Name and Address National Aeronautics and Space Administration Washington, DC 20546	14. Sponsoring Agency Code

15. Supplementary Notes

James J. Howlett is associated with Sikorsky Aircraft Division of United Technologies Corporation.

16. Abstract

The Rotor Systems Research Aircraft (RSRA) has been built for use in evaluating and verifying advanced rotor and control concepts. This report documents the analytical model developed for performance and handling qualities evaluations. It was used during the RSRA design in both open-loop and real-time man-in-the-loop simulation. It will be used in the future for pilot training, preflight of test programs, and the evaluation of promising concepts before their implementation on the flight vehicle.

17. Key Words (Suggested by Author(s))	18. Distribution Statement
Rotor Systems Research Aircraft Helicopter Mathematical Model Real-Time Simulation	Unclassified - Unlimited Subject Category 05

19. Security Classif. (of this report)	20. Security Classif. (of this page)	21. No. of Pages	22. Price*
Unclassified	Unclassified	207	

* For sale by the National Technical Information Service, Springfield, Virginia 22161

ROTOR SYSTEMS RESEARCH AIRCRAFT SIMULATION

MATHEMATICAL MODEL

Jacob A. Houck, Frederick L. Moore,
James J. Howlett*, Kenneth S. Pollock,
and Mary M. Browne

Langley Research Center

SUMMARY

The Rotor Systems Research Aircraft (RSRA) has been built for use in evaluating and verifying advanced rotor and control concepts. This report documents the analytical model developed for performance and handling qualities evaluations. It was used during the RSRA design in both open-loop and real-time man-in-the-loop simulation. It will be used in the future for pilot training, preflight of test programs, and the evaluation of promising concepts before their implementation on the flight vehicle.

INTRODUCTION

The Rotor Systems Research Aircraft (RSRA, reference 1) has been built for use in evaluating and verifying advanced rotor and control concepts. The RSRA is a versatile flying test platform which can be flown as a single rotor helicopter, compound helicopter, and as a fixed wing aircraft (figure 1).

---

*Sikorsky Aircraft Division of United Technologies Corporation

During the design and development phase of the RSRA, an analytical model* of the aircraft was formulated and used to generate performance and stability and control characteristics. This mathematical model will continue to be used for predicting the flying characteristics during the current development flight tests and during the aircraft's future operations. The mathematical model originated from Sikorsky Aircraft's General Helicopter simulation model where it has been used extensively in the design of helicopters. The model has been converted to the Langley Research Center computer system and can be used for general helicopter simulation studies as well as support of the RSRA operations.

This report documents the present version of the mathematical model.

*Howlett, J.J.: RSRA Simulation Model-Volumes I & II. Sikorsky Aircraft - SER 72009. NASA/ARMY Contract NAS1-13000, 1974.

SYMBOLS

Equations and data in this report were derived in the U.S. Customary Units to expedite development of the flight vehicles by Sikorsky Aircraft. Subsequent reports of studies using this mathematical model will be published in the International System of Units (SI). Reference 2 contains the standard conversions for the U.S. Customary Units to SI Units.

Some of the symbols used herein are not standard but were adopted from Sikorsky Aircraft notation and from the FORTRAN notation used in the digital computer program representing this mathematical model.

A_{1S}	deg	total lateral cyclic input
A_{1SL}	deg	lower lateral cyclic limit
A_{1SU}	deg	upper lateral cyclic limit
A_{1S1}	deg	lateral cyclic series trim input
A_{1S2}	deg	lateral cyclic SAS input
A_{1S3}	deg	collective mixing input, lateral cyclic
a	ft/sec	speed of sound
a_{TR}	rad^{-1}	tail rotor blade two dimensional lift curve slope
a_{XP}, a_{YP}, a_{ZP}	ft/sec^2	body axes accelerations at the pilot station
a_{0F}, a_{1SF}, b_{1SF}	deg	Fourier series coefficients, flapping
a_{0L}, a_{1SL}, b_{1SL}	deg	Fourier series coefficients, lagging

$B_{CPULG}, B_{CPULT}, B_{CPUDR}$	%/sec	CPU beeper input-longitudinal, lateral, directional
B_{MR}		main rotor blade tip loss factor
B_{TR}		tail rotor blade tip loss factor
B_{1S}	deg	total longitudinal cyclic input
B_{1SL}	deg	lower longitudinal cyclic limit
B_{1SU}	deg	upper longitudinal cyclic limit
B_{1S1}	deg	longitudinal cyclic series trim input
B_{1S2}	deg	longitudinal cyclic SAS input
B_{1S3}	deg	collective mixing input, longitudinal cyclic
BL_E	in	buttline station for TF-34 engine
BL_{MR}	in	buttline station for main rotor
BL_{PS}	in	buttline station for pilot's head
BL_{TR}	in	buttline station for tail rotor
b_E	ft	TF-34 engine moment arm, Y-body axis
b_{MR}	ft	main rotor moment arm, Y-body axis
b_{NMR}		number of blades in main rotor

b_{NTR}		number of blades in tail rotor
b_{PS}	ft	pilot station moment arm, Y-body axis
b_S		number of blades simulated
b_{TR}	ft	tail rotor moment arm, Y-body axis
C_{A1S}	deg/deg	CPU gain for lateral cyclic control
C_{B1S}	deg/deg	CPU gain for longitudinal cyclic control
C_{DELA}	deg/deg	CPU gain for aileron control
C_{DELE}	deg/deg	CPU gain for elevator control
C_{DELR}	deg/deg	CPU gain for rudder control
C_{DY}		blade segment drag coefficient
C_{LY}		blade segment lift coefficient
C_{THTR}		tail rotor thrust coefficient
C_{TTR}	deg/deg	CPU gain for tail rotor control
C_{TW}	deg	gearing parameter, wing to lower horizontal tail
CPU		control phasing unit
CPU_{DIR}	%	directional CPU input
CPU_{DIR1}	%	directional CPU series trim input

CPU_{LAT}	%	lateral CPU input
CPU_{LAT1}	%	lateral CPU series trim input
CPU_{LON}	%	longitudinal CPU input
CPU_{LON1}	%	longitudinal CPU series trim input
c_R	ft	blade root chord
c_T	ft	blade tip chord
c_{TR}	ft	tail rotor blade chord
$c_{y(n)}$	ft	mean chord of blade segment
c_{75}	ft	blade chord at 75% radius station
$\cos\gamma$		blade segment flow skew angle
D_{DB}	lb	drag brake drag
D_{HT}	lb	lower horizontal tail drag
D_{HTU}	lb	upper horizontal tail drag
D_{TOT}	lb	airframe drag less empennage
D_{VT}	lb	vertical tail drag
D_{WMP}, D_{WMS}	lb	wind-mill drag on TF-34 port and starboard engines
D_{WMR}		main rotor downwash

D_{WTR}		tail rotor downwash
DFCPU	%	breakpoint on pitch and roll fixed wing CPU profiles
DHCPU	%	breakpoint on pitch and roll rotary-wing CPU profiles
DMPARM	in	lag damper arm
EK_{TR}		tail rotor wash factor on vertical tail
EK_{TX}, EK_{TZ}		rotor wash factors on lower horizontal tail
EK_{TXU}, EK_{TZU}		rotor wash factors on upper horizontal tail
EK_{WFX}, EK_{WFZ}		rotor wash factors on the wing-fuselage
e	ft	main rotor hinge offset from center of rotation
e'	ft	distance from hinge to start of blade
F_P, F_T, F_R	lb	blade segment forces-perpendicular, tangential, radial
F_{PB}, F_{TB}, F_{RB}	lb	blade shear forces-perpendicular, tangential, radial, blade span axes
F_{XA}, F_{YA}, F_{ZA}	lb	blade aerodynamic shear forces, rotating shaft axes

F_{XI}, F_{YI}, F_{ZI}	lb	blade inertia shear forces, rotating shaft axes
F_{XT}, F_{YT}, F_{ZT}	lb	blade total shear forces, rotating shaft axes
F_{ζ}	ft lb/rad	lagging hinge damper constant (spring)
$F_{\dot{\zeta}}$	$\frac{\text{ft lb sec}}{\text{rad}}$	lagging hinge damper constant (damper)
FS_{CG}	in	fuselage station for total aircraft C.G.
FS_{CGB}	in	fuselage station of C.G. for total aircraft less main rotor blades
FS_{DB}	in	fuselage station for drag brake
FS_{E}	in	fuselage station for TF-34 engine
FS_{EI}	in	fuselage station for TF-34 engine inlet
FS_{HT}	in	fuselage station for lower horizontal tail
FS_{HTU}	in	fuselage station for upper horizontal tail
FS_{MR}	in	fuselage station for main rotor
FS_{PS}	in	fuselage station for pilot's head
FS_{TR}	in	fuselage station for tail rotor
FS_{VT}	in	fuselage station for vertical tail

FS_{WT}	in	fuselage station for wind tunnel data reference point
g	ft/sec^2	gravitational acceleration
H	lb	main rotor drag, shaft axes
HSCPU	%	breakpoint on pitch and roll fixed-wing CPU profiles
h_{DB}	ft	drag brake moment arm, Z-body axis
h_E	ft	TF-34 engine moment arm, Z-body axis
h_{HT}	ft	lower horizontal tail moment arm, Z-body axis
h_{HTU}	ft	upper horizontal tail moment arm, Z-body axis
h_{MR}	ft	main rotor moment arm, Z-body axis
h_{PS}	ft	pilot station moment arm, Z-body axis
h_{TR}	ft	tail rotor moment arm, Z-body axis
h_{VT}	ft	vertical tail moment arm, Z-body axis
h_{WT}	ft	wind tunnel reference point moment arm, Z-body axis
I_R	slugs ft^2	inertia of main rotor drive less rotor blades

I_X, I_Y, I_Z, I_{XZ}	slugs ft^2	inertias about body axes
I_b	slugs ft^2	main rotor blade inertia about hinge
i_E	deg	engine shaft angle
i_{HT}	deg	lower horizontal tail incidence
i_{HTLL}	deg	lower horizontal tail incidence lower limit
i_{HTU}	deg	upper horizontal tail incidence
i_{HTUL}	deg	lower horizontal tail incidence upper limit
i_W	deg	wing incidence
i_{WL}	deg	wing incidence lower limit
i_{WU}	deg	wing incidence upper limit
i_θ	deg	main rotor longitudinal shaft tilt
i_ϕ	deg	main rotor lateral shaft tilt
J	lb	main rotor side force, shaft axes
K_{AG}	deg/deg	gearing coefficient, ailerons
K_{ASAIL}	deg/deg	asymetric gearing ratio, ailerons
K_{ASTHO}	deg/deg	collective mixing gain, lateral cyclic

K_{LSTHO}	deg/deg	collective mixing gain, longitudinal cyclic
K_{CPULG},K_{CPULT},K_{CPUDR}	%/%	CPU lever gearing-longitudinal, lateral, directional
K_{CTA}	deg/%	basic control gearing to lateral cyclic
K_{CTAIL}	deg/%	basic control gearing to ailerons
K_{CTB}	deg/%	basic control gearing to longitudinal cyclic
K_{CTC}	deg/%	basic control gearing to collective
K_{CTDB}	deg/%	basic control gearing to drag brake
K_{CTE}	deg/%	basic control gearing to elevator
K_{CTF}	deg/%	basic control gearing to flaps
K_{CTPE}	%/%	basic control gearing to TF-34 engine throttles
K_{CTRE}	%/%	basic control gearing to rotor speed
K_{CTRUD}	deg/%	basic control gearing to rudder
K_{CTT}	deg/%	basic control gearing to lower horizontal tail
K_{CTTR}	deg/%	basic control gearing to tail rotor
K_{CTW}	deg/%	basic control gearing to wing

K_{GL}		first harmonic inflow coefficient
K_{QDB}		dynamic pressure loss factor-drag brake
K_{QHT}		dynamic pressure loss factor-lower horizontal tail
K_{QHTU}		dynamic pressure loss factor-upper horizontal tail
K_{QVT}		dynamic pressure loss factor-vertical tail
K_{RDTH0}	deg/deg	collective mixing gain, rudder
K_{RPM}		main rotor speed ratio, = Ω/Ω_T if rotor speed degree of freedom not utilized
K_{TLIN1}	deg/deg	gearing coefficient, lower horizontal tail
K_{TMAIL}	deg/sec	fixed rate series trim beeper input, ailerons
K_{TMA1S}	deg/sec	fixed rate series trim beeper input, lateral cyclic
K_{TMB1S}	deg/sec	fixed rate series trim beeper input, longitudinal cyclic
K_{TMELV}	deg/sec	fixed rate series trim beeper input, elevator
K_{TMJET}	%/sec	fixed rate series trim beeper input, TF-34 engines

K_{TMRE}	%/sec	fixed rate series trim beeper input, rotor speed
K_{TMRUD}	deg/sec	fixed rate series trim beeper input, rudder
K_{TMTTR}	deg/sec	fixed rate series trim beeper input, tail rotor
K_{TRBLK}		fin-tail rotor blockage factor
K_{TRTH0}	deg/deg	collective mixing gain, tail rotor
K_{TW1}	deg/deg	gearing coefficient, wing to lower horizontal tail
K_{1X}		cosine component of first harmonic inflow
K_{1Y}		sine component of first harmonic inflow
$K_{\alpha 0}$	deg	α_1 hinge constant
$K_{\alpha 1}$		α_1 hinge coefficient
$K_{\alpha 2}$	deg^{-1}	α_1 hinge coefficient
K_{β}	ft lb/rad	flapping hinge spring constant
$K_{\beta}^{\bullet}$	$\frac{\text{ft lb sec}}{\text{rad}}$	flapping hinge rate damper constant
K_{λ}		modified downwash filter constant
K_{λ}'		downwash loop filter constant

L_{BODY}	ft lb	total aircraft body axes rolling moment
L_{DB}	lb	drag brake lift
L_E	ft lb	TF-34 engine body axes rolling moment
L_H	ft lb	main rotor rolling moment, shaft axes
L_{HT}	lb	lower horizontal tail lift
L_{HTU}	lb	upper horizontal tail lift
L_L	ft	lag damper arm
L_{MR}	ft lb	main rotor body axes rolling moment
L_{MTOT}	ft lb	airframe rolling moment less empennage
L_T	ft lb	empennage body axes rolling moment
L_{TOT}	lb	airframe lift less empennage
L_{TR}	ft lb	tail rotor body axes rolling moment
L_{VT}	lb	vertical tail lift
L_{WF}	ft lb	wing-fuselage body axes rolling moment
l_{DB}	ft	drag brake moment arm, X-body axis
l_L	ft	TF-34 engine moment arm, X-body axis
l_{EI}	ft	TF-34 engine inlet moment arm, X-body axis

l_{HT}	ft	lower horizontal tail moment arm, X-body axis
l_{HTU}	ft	upper horizontal tail moment arm, X-body axis
l_{MR}	ft	main rotor moment arm, X-body axis
l_{PS}	ft	pilot station moment arm, X-body axis
l_{TR}	ft	tail rotor moment arm, X-body axis
l_{VT}	ft	vertical tail moment arm, X-body axis
l_{WT}	ft	wind tunnel reference point moment arm, X-body axis
M		Mach number
M_{BODY}	ft lb	total aircraft body axes pitching moment
M_E	ft lb	TF-34 engine body axes pitching moment
M_{FA}	ft lb	aerodynamic moment about flapping hinge
M_{FD}	ft lb	flap damper moment
M_H	ft lb	main rotor pitching moment, shaft axes
M_{LA}	ft lb	aerodynamic moment about lagging hinge
M_{LD}	ft lb	lag damper moment

M_{MR}	ft lb	main rotor body axes pitching moment
M_{MTOT}	ft lb	airframe pitching moment less empennage
M_{PEP}	slugs/sec	TF-34 port engine mass flow
M_{PES}	slugs/sec	TF-34 starboard engine mass flow
M_T	ft lb	empennage body axes pitching moment
M_{TR}	ft lb	tail rotor body axes pitching moment
M_{WF}	ft lb	wing-fuselage body axes pitching moment
M_b	slugs ft	blade first mass moment about hinge
MFCPU	%	breakpoint on pitch and roll fixed-wing CPU profiles
MHCPU	%	breakpoint on pitch and roll rotary-wing CPU profiles
N_{BODY}	ft lb	total aircraft body axes yawing moment
N_E	ft lb	TF-34 engine body axes yawing moment
N_{MR}	ft lb	main rotor body axes yawing moment
N_{MTOT}	ft lb	airframe yawing moment less empennage
N_T	ft lb	empennage body axes yawing moment
N_{TR}	ft lb	tail rotor body axes yawing moment

N_{WF}	ft lb	wing-fuselage body axes yawing moment
n_S		number of blade segments simulated
p	rad/sec	body axes roll rate
$\dot{p}$	rad/sec^2	body axes roll acceleration
p_S	rad/sec	shaft axes roll rate
$\dot{p}_S$	rad/sec^2	shaft axes roll acceleration
Q	ft lb	main rotor torque, shaft axes
Q_E	ft lb	T-58 engine torque
q	rad/sec	body axes pitch rate
$\dot{q}$	rad/sec^2	body axes pitch acceleration
q_{DB}	lb/ft^2	dynamic pressure at drag brake
q_{HT}	lb/ft^2	dynamic pressure at lower horizontal tail
q_{HTU}	lb/ft^2	dynamic pressure at upper horizontal tail
q_S	rad/sec	shaft axes pitch rate
$\dot{q}_S$	rad/sec^2	shaft axes pitch acceleration
q_{VT}	lb/ft^2	dynamic pressure at vertical tail

q_{WF}	lb/ft^2	dynamic pressure at wing-fuselage
R_{MR}	ft	main rotor radius
R_{TR}	ft	tail rotor radius
r	rad/sec	body axes yaw rate
$\dot{r}$	rad/sec^2	body axes yaw acceleration
r_S	rad/sec	shaft axes yaw rate
$\dot{r}_S$	rad/sec^2	shaft axes yaw acceleration
S_W	ft^2	wing area
s		Laplace Operator
T	lb	main rotor thrust, shaft axes
T_A	lb	main rotor aerodynamic thrust
T_{HRL}	deg	lower tail rotor blade pitch limit
T_{HRU}	deg	upper tail rotor blade pitch limit
T_{HOL}	deg	lower collective pitch limit
T_{HOU}	deg	upper collective pitch limit
T_J	lb	total TF-34 engine thrust (T_P+T_S)
T_P	lb	TF-34 port engine net thrust

T_{RG}	sec	main rotor speed response time constant
T_S	lb	TF-34 starboard engine net thrust
T_{TR}	lb	tail rotor thrust
T_{TR1}	deg	tail rotor series trim input
T_{TR2}	deg	tail rotor SAS input
T_{TR3}	deg	collective mixing input, tail rotor
u_P		blade segment perpendicular velocity
u_{PIWR}		perpendicular interference of wing on main rotor
u_R		blade segment radial velocity
u_T		blade segment tangential velocity
u_{TIWR}		tangential interference of wing on main rotor
u_{YAW}		blade segment resultant velocity
V_{DB}	ft/sec	resultant velocity at drag brake
V_E	ft/sec	inertial axes velocity, east direction
V_{HT}	ft/sec	resultant velocity at lower horizontal tail
V_{HTU}	ft/sec	resultant velocity at upper horizontal tail

V_N	ft/sec	inertial axes velocity, north direction
V_{NOW}		wing on main rotor normal velocity interference factor
V_{TOW}		wing on main rotor tangential velocity interference factor
V_{VT}	ft/sec	resultant velocity at vertical tail
V_{XB}	ft/sec	X-body axis translational velocity
$\dot{V}_{XB}$	ft/sec^2	X-body axis translational acceleration
V_{XDB}	ft/sec	drag brake X-body axis velocity
V_{XHT}	ft/sec	lower horizontal tail X-body axis velocity
V_{XHTU}	ft/sec	upper horizontal tail X-body axis velocity
V_{XP}	ft/sec	pilot station X-body axis velocity
$\dot{V}_{XS}$	ft/sec^2	main rotor X-shaft axis translational acceleration
V_{XTP}	ft/sec	tail rotor X-shaft axis velocity
V_{XTRB}	ft/sec	tail rotor X-body axis velocity
V_{XVT}	ft/sec	vertical tail X-body axis velocity
V_{XWF}	ft/sec	wing-fuselage X-body axis velocity

V_{YB}	ft/sec	Y-body axis translational velocity
$\dot{V}_{YB}$	ft/sec^2	Y-body axis translational acceleration
V_{YDB}	ft/sec	drag brake Y-body axis velocity
V_{YHT}	ft/sec	lower horizontal tail Y-body axis velocity
V_{YHTU}	ft/sec	upper horizontal tail Y-body axis velocity
V_{YIW}	ft/sec	wing sidewash velocity at vertical tail, Y-body axis
V_{YP}	ft/sec	pilot station Y-body axis velocity
$\dot{V}_{YS}$	ft/sec^2	main rotor Y-shaft axis translational acceleration
V_{YTR}	ft/sec	tail rotor Y-shaft axis velocity
V_{YTRB}	ft/sec	tail rotor Y-body axis velocity
V_{YVT}	ft/sec	vertical tail Y-body axis velocity
V_{YWF}	ft/sec	wing-fuselage Y-body axis velocity
V_Z	ft/sec	inertial axes velocity, vertical direction
V_{ZB}	ft/sec	Z-body axis translational velocity
$\dot{V}_{ZB}$	ft/sec^2	Z-body axis translational acceleration

V_{ZDB}	ft/sec	drag brake Z-body axis velocity
V_{ZHT}	ft/sec	lower horizontal tail Z-body axis velocity
V_{ZHTU}	ft/sec	upper horizontal tail Z-body axis velocity
V_{ZIW}	ft/sec	wing downwash velocity at lower horizontal tail, Z-body axis
V_{ZIWU}	ft/sec	wing downwash velocity at upper horizontal tail, Z-body axis
V_{ZP}	ft/sec	pilot station Z-body axis velocity
$\dot{V}_{ZS}$	ft/sec^2	main rotor Z-shaft axis translational acceleration
V_{ZTR}	ft/sec	tail rotor Z-shaft axis velocity
V_{ZTRB}	ft/sec	tail rotor Z-body axis velocity
V_{ZVT}	ft/sec	vertical tail Z-body axis velocity
V_{ZWF}	ft/sec	wing-fuselage Z-body axis velocity
W	lb	aircraft gross weight
W_b	lb	main rotor blade weight
W_{bd}	lb	aircraft weight less main rotor blades
WL_{CG}	in	waterline station for total aircraft C.G.

WL_{CGB}	in	waterline station of C.G. for total aircraft less main rotor blades
WL_{DB}	in	waterline station for drag brake
WL_{E}	in	waterline station for TF-34 engines
WL_{HT}	in	waterline station for lower horizontal tail
WL_{HTU}	in	waterline station for upper horizontal tail
WL_{MR}	in	waterline station for main rotor
WL_{PS}	in	waterline station for pilot's head
WL_{TR}	in	waterline station for tail rotor
WL_{VT}	in	waterline station for vertical tail
WL_{WT}	in	waterline station for wind tunnel data reference point
WRL	deg/sec	wing motion rate limit
X_A	%	lateral stick position
X_B	%	longitudinal stick position
X_{BODY}	lb	total aircraft body axes longitudinal force
X_C	%	collective stick position

X_{CPUDR}	%	directional CPU lever position
X_{CPULG}	%	longitudinal CPU lever position
X_{CPULT}	%	lateral CPU lever position
X_{DB}	lb	drag brake body axes longitudinal force
X_{DRAG}	%	drag brake lever position
X_{E}	lb	TF-34 engine body axes longitudinal force
X_{FLAP}	%	flap lever position
X_{HT}	lb	lower horizontal tail body axes longitudinal force
X_{HTU}	lb	upper horizontal tail body axes longitudinal force
X_{MR}	lb	main rotor body axes longitudinal force
X_{P}	%	pedal position
X_{PRE}	%	main rotor speed lever position
X_{RPMJTP}	%	TF-34 port engine throttle position
X_{RPMJTS}	%	TF-34 starboard engine throttle position
X_{T}	lb	total empennage body axes longitudinal force

X_{TR}	lb	tail rotor body axes longitudinal force
X_{VT}	lb	vertical tail body axes longitudinal force
X_{WF}	lb	wing-fuselage body axes longitudinal force
X_{WING}	%	wing lever position
Y_{BODY}	lb	total aircraft body axes lateral force
Y_{DB}	lb	drag brake body axes lateral force
Y_{E}	lb	TF-34 engine body axes lateral force
Y_{HT}	lb	lower horizontal tail body axes lateral force
Y_{HTU}	lb	upper horizontal tail body axes lateral force
Y_{MR}	lb	main rotor body axes lateral force
Y_{T}	lb	total empennage body axes lateral force
Y_{TOT}	lb	airframe side force less empennage
Y_{TR}	lb	tail rotor body axes lateral force
Y_{VT}	lb	vertical tail body axes lateral force
Y_{WF}	lb	wing-fuselage body axes lateral force

y		generalized nondimensional distance along main rotor blade
$y_{2(n)}$		center of lift position of n th blade segment from hinge
Z_{BODY}	lb	total aircraft body axes vertical force
Z_{DB}	lb	drag brake body axes vertical force
Z_{E}	lb	TF-34 engine body axes vertical force
Z_{HT}	lb	lower horizontal tail body axes vertical force
Z_{HTU}	lb	upper horizontal tail body axes vertical force
Z_{MR}	lb	main rotor body axes vertical force
Z_{T}	lb	total empennage body axes vertical force
Z_{TR}	lb	tail rotor body axes vertical force
Z_{VT}	lb	vertical tail body axes vertical force
Z_{WF}	lb	wing-fuselage body axes vertical force
α_{DB}	deg	angle of attack of drag brake
α_{HT}	deg	angle of attack of lower horizontal tail
α_{HTT}	deg	total angle of attack of lower horizontal tail

α_{HTU}	deg	angle of attack of upper horizontal tail
α_{HTTU}	deg	total angle of attack of upper horizontal tail
α_{TRANS}	rad	blade function angle of attack map entry
α_{VT}	deg	angle of attack of vertical tail
α_{VTT}	deg	total angle of attack of vertical tail
α_{W}	deg	angle of attack of wing
α_{WF}	deg	angle of attack of wing-fuselage
α_{Y}	rad	blade segment angle of attack
β	rad	blade flapping angle
$\dot{\beta}$	rad/sec	blade flapping velocity
$\ddot{\beta}$	rad/sec^2	blade flapping acceleration
β_{WF}	deg	angle of sideslip of wing-fuselage
Γ_{TR}	deg	tail rotor cant angle
Δ_{SP}	deg	main rotor swash plate rotation
ΔC_D		two-dimensional blade drag coefficient increment
Δt	sec	integration step size

$\Delta y_{(n)}$		blade segment width
$\Delta\psi$	deg	main rotor azimuthal advance angle
δ	rad	blade lagging angle
$\dot{\delta}$	rad/sec	blade lagging velocity
$\ddot{\delta}$	rad/sec^2	blade lagging acceleration
δ_A	deg	aileron deflection angle
δ_{AFT}	rad	blade lagging angle aft limit
δ_{AL}	deg	aileron deflection angle lower limit
δ_{AU}	deg	aileron deflection angle upper limit
δ_{A1}	deg	series trim input to ailerons
δ_{A2}	deg	lateral SAS input to ailerons
δ_{DB}	deg	drag brake deflection angle
δ_{DBL}	deg	drag brake deflection angle lower limit
δ_{DBU}	deg	drag brake deflection angle upper limit
δ_E	deg	elevator deflection angle
δ_{EL}	deg	elevator deflection angle lower limit
δ_{EU}	deg	elevator deflection angle upper limit

δ_{E1}	deg	series trim input to elevator
δ_{E2}	deg	longitudinal SAS input to elevators
δ_{F}	deg	flap deflection angle
δ_{FL}	deg	flap deflection angle lower limit
δ_{FU}	deg	flap deflection angle upper limit
δ_{FWD}	rad	blade lagging angle forward limit
δ_{PE}	%	TF-34 engine fan speed demanded
δ_{PED}	%	δ_{PE} after response delay
δ_{PEL}	%	TF-34 engine idle fan speed
δ_{PEU}	%	TF-34 engine maximum allowable fan speed
δ_{PE1}	%	series trim input to TF-34 engines
δ_{R}	deg	rudder deflection angle
δ_{RE}	%	main rotor speed selector
δ_{REL}	%	main rotor speed selector lower limit
δ_{REU}	%	main rotor speed selector upper limit
δ_{RE1}	%	series trim input to main rotor speed selector
δ_{RL}	deg	rudder deflection angle lower limit

δ_{RU}	deg	rudder deflection angle upper limit
δ_{R1}	deg	series trim input to rudder
δ_{R2}	deg	directional SAS input to rudder
δ_3	deg	main rotor blade hinge effective skew angle, pitch-flap coupling
δ_{3TR}	deg	tail rotor blade hinge effective skew angle, pitch-flap coupling
ϵ_{WT}	deg	wing downwash angle at lower horizontal tail
ϵ_{WTU}	deg	wing downwash angle at upper horizontal tail
θ	deg	blade segment pitch angle
θ_A	rad	blade segment pitch angle
θ_{BODY}	deg	body Euler angle, pitch
$\dot{\theta}_{BODY}$	deg/sec	body Euler angle rate, pitch
θ_{CTR}	deg	impressed tail rotor collective pitch angle
θ_{CUFF}	deg	impressed main rotor collective pitch angle
θ_{TR}	deg	actual tail rotor collective pitch angle

θ_1	deg/unit radius	main rotor blade twist
θ_{1TR}	deg/unit radius	tail rotor blade twist
λ_{MR}		main rotor inflow
λ_{TR}		tail rotor inflow
μ_{TR}		tail rotor resultant velocity
μ_{XH}		X-body axis translational velocity at main rotor hub
μ_{XS}		X-shaft axis translational velocity at main rotor hub
μ_{XTR}		X-shaft axis translational velocity at tail rotor hub
μ_{YH}		Y-body axis translational velocity at main rotor hub
μ_{YS}		Y-shaft axis translational velocity at main rotor hub
μ_{YTR}		Y-shaft axis translational velocity at tail rotor hub
μ_{ZH}		Z-body axis translational velocity at main rotor hub
μ_{ZS}		Z-shaft axis translational velocity at main rotor hub

μ_{ZTR}		Z-shaft axis translational velocity at tail rotor hub
ξ		e/R_{MR}
ξ'		e'/R_{MR}
ρ	slugs/ft^3	air density
σ_{TR}		tail rotor solidity
σ_{WT}	deg	wing sidewash angle at vertical tail
τ_T	sec	time lag in wing flow reaching lower horizontal tail
τ_{TU}	sec	time lag in wing flow reaching upper horizontal tail
ϕ_{BODY}	deg	body Euler angle, roll
$\dot{\phi}_{BODY}$	deg/sec	body Euler angle rate, roll
χ	deg	main rotor wake skew angle
ψ	deg	main rotor blade azimuthal position
ψ_{BODY}	deg	body Euler angle, yaw
$\dot{\psi}_{BODY}$	deg/sec	body Euler angle rate, yaw
ψ_{WF}	deg	$-\beta_{WF}$
Ω	rad/sec	actual main rotor rotational velocity

$\dot{\Omega}$	rad/sec^2	main rotor rotational acceleration
Ω_T	rad/sec	main rotor nominal trimmed rotational velocity
Ω_{TR}	rad/sec	tail rotor rotational velocity

Subscripts

i	current mathematical model iteration
i - 1	past iteration

Special symbols

$(C_T/\sigma)'$		main rotor thrust coefficient based on aerodynamic loading only. Used in calculation of D_{WMR}
(r/R_{MR})		nondimensional main rotor radius
(da_o/dT)	deg/lb	rate of change of cone angle with thrust
f( )		indicates function of ( )

GENERAL DESCRIPTION OF MATHEMATICAL MODEL

The overall structure of the mathematical model is shown by the simplified block diagram in figure 2. This modular format allows selection of desired aircraft configurations or dynamic configuration changes, such as, blade severance, by input logic. The aircraft configurations which can be modeled are: a helicopter, a compound helicopter, and a fixed wing aircraft with or without a tail rotor. Mutual interference effects link the various component parts of the aircraft together.

The aircraft equations of motion are solved iteratively by summing the forces and moments of each module relative to the aircraft center of gravity. From the subsequent body axes accelerations, the resulting velocities and displacements then condition the environment for each module in subsequent calculations of the mathematical model. The body axes system used is shown in figure 3. The final aircraft motions can be transferred into the earth inertial axes for use in driving simulator cockpits in real-time man-in-the-loop simulation studies. The remainder of this report will discuss in detail each module of the mathematical model.

MAIN ROTOR MODULE

The rotor mathematical model is a rotating blade element model of an articulated rotor system. The total forces and moments are developed from a combination of the aerodynamic, mass, and inertia loads acting on each

blade simulated. The aerodynamic loads are determined from blade element theory as a function of local blade angle of attack and Mach number. The summation of the aerodynamic, mass, and inertia loads gives the shear loads on the blade root hinge pins. The total rotor forces are obtained by summing all the blade shear loads. The total moments at the hub are based on the hinge offset from the center of the shaft. The forces and moments are then transferred to the body axes system for solving the aircraft's equations of motion. The following basic assumptions are made in the rotor representation:

1. Rotor blade and airframe flexibility are not taken into account.
2. Air mass flow degree of freedom through the rotor can be represented by applying a simple lag to the calculation of downwash. The only nonuniform flow considered results from increases in forward speed. This causes a redistribution of the uniform flow from the front to the back of the disk.
3. Simple sweep theory.
4. The aerodynamic loads are quasi-static.
5. The distributed blade mass characteristics can be represented as a total blade first mass moment and a total blade inertia about the hinge.
6. The flapping and lagging hinges are coincident.

The details of the main rotor module will be discussed in the following sections. The corresponding equations and data are presented in appendix A and tables 1-4, respectively.

Rotor Geometric Parameters - The rotor geometric parameters are listed in table 1. The calculation of the effect of the rotor blade weight on the aircraft center of gravity position is presented in section A-1 of appendix A.

The simulated rotor blades are divided into segments based on equal annulii areas of the rotor disk. This allows the number of segments to be minimized, input data to be reduced, and the segments to be distributed toward the high dynamic pressure areas of the blade. This becomes important when real-time simulation is required as is shown in references 3 and 4. The equations used to define the blade segments are presented in section A-2.

Velocity Components at Each Blade Segment - The total air velocity components at the blade segments are made up of the body velocities, rotor downwash, blade motion, and up-wash from the wings.

Before calculations at the blade segment can be executed, several axes transformations must be implemented. Initially body axes angular and translational accelerations and velocities are transferred to the rotor hub and rotated through the shaft inclination angles i_θ and i_ϕ into the rotor shaft axes. These angles are Euler angles with positive rotation of i_θ about the Y_H axis followed by rotation of i_ϕ about the resulting X_S axis (figure 4 and section A-3). The body translational accelerations and velocities at the rotor hub are presented in sections A-4 and A-5 respectively. Sections A-6 and A-7 present the body translational and angular accelerations and velocities at the rotor hub in the shaft axes system.

Sections A-8 and A-9 present the rotor azimuthal advance angle calculations and rotor speed degree of freedom calculations respectively.

The uniform rotor downwash is calculated by application of momentum theory to the rotor thrust (section A-10). To approximate an air mass degree of freedom, the downwash is passed through a first order lag with a time constant of 0.1 seconds. The resulting uniform downwash is distributed first harmonically around the azimuth as a cosine function depending on the inclination of the rotor wake. This results in uniform downwash at hover and a weighted distribution toward the aft portion of the rotor disk at high forward velocities. The first harmonic inflow coefficients are presented in section A-11. Since this effect is really dependent on the resultant velocity vector a lateral velocity term is also added. The velocities at the blade segments are obtained by transforming the fixed shaft vectors into the rotating hub axes system, then transferring to the blade hinge position, transforming into blade span axes through the Euler angles β (flapping) and δ (lagging) and finally transferring to the segment position on the blade. These transformations are illustrated on figure 5.

The lifting wing under the rotor (compound helicopter only) influences the flow field in the plane of the rotor disk. This effect is introduced into the rotor model by distributing normal and tangential velocity functions, dependent on forward speed and wing lift, (approximated to wing and body lift) around the azimuth and along the radius of the blade (section A-12). These data were obtained from the Sikorsky Aircraft potential flow program. While not rigorous, it was considered within the accuracy of the

data to add these effects to the other components without resolution through the flapping and lagging angles. Data for the velocity functions are provided in table 2.

The final contribution to the velocities at the blade segments is that due to blade motion. Sections A-13 and A-14 present the blade flapping and lagging equations respectively. Blade flapping and lagging velocities and angles are obtained by application of a Fourier prediction technique, rather than by direct integration of the accelerations. The total velocity components (section A-15) are subsequently used to calculate the resultant velocity (section A-16), local Mach number (section A-17), yawed angle of attack (section A-18), and flow yaw angle (section A-18). It should be noted that the segment Mach number which is used in the aerodynamic function tables is based on the perpendicular and tangential velocities. Previous studies indicate that Mach number should be based on the unyawed component of flow.

Blade Aerodynamic Data - The total local segment angle of attack (section A-18) is the summation of blade geometric pitch angle (section A-19) and the yawed angle of attack on the blade. The former is made up of collective pitch (θ_{CUFF}), lateral cyclic (A_{1S}), longitudinal cyclic (B_{1S}), blade twist contribution, a component due to blade pitch-flap coupling (δ_3), and components for effective α_1 hinge contributions. A_{1S} and B_{1S} are distributed as cosine and sine functions dependent on blade azimuth and swashplate setting. The collective pitch, θ_{CUFF}, is defined in this equation as applied at the start of the blade, i.e., $\xi + \xi'$ from the center of rotation.

Twist is assumed to washout at the rate of θ_1 per unit radius from that point. The yawed angle of attack is complicated by the requirement to resolve blade pitch into the local stream direction as shown in figure 6. The resulting equation assumes the series approximation (to the 5th power) for the tangent of blade pitch.

The treatment of the blade segment aerodynamic force calculation is completely non-linear. Lift and drag characteristics are provided for the range $-180^\circ \leq \alpha \leq +180^\circ$. Bivariate tables as a function of angle of attack and Mach number are used in the range $-30^\circ \leq \alpha \leq +30^\circ$ allowing good definition of blade stall. A univariate table is used for the remainder of the range. The complete coverage of angle of attack allows good definition of aerodynamic characteristics on the retreating blade side of the disk. This is important at high advance ratios. The blade segment lift coefficient is determined by applying simple sweep theory to the unyawed blade aerodynamic data. This is rigorously applied in the linear lift range where the entry to the unyawed lift coefficient is transformed by the cosine of the yaw angle (i.e., $\alpha_{TRANS} = \alpha_Y \cos\gamma$) and the entry Mach number is a function of the unyawed component of flow. At higher angles of attack some liberties are taken where sweep theory is not valid. These steps are taken to avoid discontinuities in blade lift data as the blade proceeds around the azimuth. Discontinuities can result in an unstable flapping and lagging solution. The application of sweep theory to the determination of drag is not well established. For this model, drag is determined by entering the drag data with the actual yawed angle of attack, ($\alpha_{TRANS} = \alpha_Y$). Univariate and bivariate tables of blade lift and drag coefficients as a function of α_{TRANS} and Mach number are tabulated in

table 3. Table entry logic is shown in section A-20. It should be noted that a tip loss factor is applied to the tip segment.

The aerodynamic segmental loads are resolved into blade span axes (section A-21), and summed along each simulated blade (section A-22). Finally, they are resolved into rotating shaft axes (section A-23), as aerodynamic shears at the hinge. It should be noted that the angles β and δ are Euler angles and order of treatment must be observed.

Blade Motion About the Flapping and Lagging Hinges - The contributions to flapping and lagging accelerations, about the corresponding hinges, are aerodynamic moments, hinge restraint moments, and inertia moments. The aerodynamic moments are simply obtained from the segment forces multiplied by the segment moment arms and summed along the blade (section A-24).

The hinge restraint moments (section A-25) are represented by spring and damping resistance to motion. The flapping restraint moment derivatives are set to zero for an articulated rotor system. These terms can be used to represent a hingeless system using the virtual hinge approach. The lagging hinge restraint derivatives are derived from damper tests. For the RSRA rotor system, the damping characteristics are presented in table 4.

The derivation of the inertia loads on the blades is a lengthy process and is not presented in this report. The inertia shears at the hinge are presented in section A-26. Normally some inertia terms integrate to zero around the rotor azimuth and are eliminated. In this case they are retained in order that the rotor model can be used for evaluating out-of-balance loads following blade severance. The final blade flapping and lagging acceleration equations are given in sections A-13 and A-14 respectively.

Total Rotor Forces and Moments - The total blade forces (section A-27) at the hinge in the rotating shaft axes are obtained by summing the aerodynamic and inertia shears. Total rotor forces (section A-28) are then obtained by resolving the forces into the fixed shaft axes and summing them over the simulated number of blades. At this point, the compensation for the actual number of blades is applied if necessary. It should be noted that the rotor thrust, T_A (used in the calculation of $(C_T/\sigma)'$, and subsequently the downwash on the next iteration through the equations), is based on the aerodynamic shears alone. Total rotor hub moments (section A-29) are developed from the total blade shears and the blade restraint moments, transferred into the fixed shaft axes, and summed over the number of simulated blades. As with the blade forces, the compensation for the actual number of blades is added at this point if necessary. If the blade lagging degree of freedom is eliminated, the alternate equation for calculating rotor torque is applied. Figure 7 presents the total rotor forces and moments in the fixed shaft axes system. The final rotor forces and moments are obtained by transforming the shaft axes forces and moments into body axes with the origin at the center of gravity (section A-30). These are eventually summed with other component outputs to give the total external forces and moments.

Section A-31 presents the flapping and lagging Fourier coefficients, and section A-32 presents the rotor wake skew angle (figure 8). The rotor wake skew angle is the angle that the center line of the rotor wake makes with the rotor shaft. It is this parameter which is used to establish the variation of rotor wash on the fuselage, wing, and tail.

Figure 9 presents a detailed block diagram of the equations which make up the rotor mathematical model. References 3, 4, and 5 provide an insight into the problems associated with using this rotor mathematical model for real-time man-in-the-loop simulations.

FUSELAGE MODULE

In this module, the tail-off aerodynamics for the fuselage only (helicopter) and for the fuselage/wing/nacelles combination (fixed wing) are represented. The aerodynamic data are presented in the wind axes system and in parametric format (ex $L/q = Ft^2$). The associated equations for generating the forces and moments for the selected configuration are presented in appendix B. Unless otherwise noted fixed wing refers to the compound configuration also.

The effects of rotor wash on the airframe has been treated in gross terms. The technique used provides the essential effects of increased interference velocity with increased rotor load and varies as the rotor wake deflects rearward with increased forward speed. The normalized rotor wash in the vicinity of the wing and fuselage as a function of rotor wake skew angle (χ) is given in section B-1 and table 5.

For entry into the aerodynamic data functions, the angles of attack and sideslip, sections B-2 and B-3 respectively, are derived from the wing-fuselage body axes components of velocity (section B-4). These velocity components include additions for rotor downwash effects. Following these calculations, the aerodynamics of the desired configuration are determined as a function of these calculated angles, wing incidence, flap setting,

aileron setting, thrust setting, and the body pitch, roll, and yaw rates. The total forces and moments, section B-5, are generated based on the aerodynamic data in tables 6 to 17. The aerodynamic data are based on wind tunnel tests conducted to post stall conditions and are extended with analytical justification to $\pm$ 90° to cover the low speed flight regimes. Contributions due to aerodynamic damping are derived using a derivative approach. These derivatives are presented in table 18.

The total aerodynamic forces and moments are resolved from wind axes to the body axes at the center of gravity in section B-6. The wind tunnel mounting positions are presented in table 1 and in figure 10. Because α_{WF} and β_{WF} are not Euler angles, when they approach 90° the transformation in section B-6 gives invalid body axes forces and moments. To avoid these conditions, section B-7 is introduced which fades out the transformation and introduces fixed body axes parameters estimated specifically for hover and low speed flight. These parameters are presented in table 19.

EMPENNAGE MODULE

The empennage has been modeled separately from the airframe to facilitate tail configuration changes. The separate empennage formulation allows good definition of non-linear tail characteristics and allows changes to the empennage without regenerating complete airframe data functions. Two tail configurations were used for the RSRA simulation. The first configuration, for the helicopter, was a T-tail with ground adjustable incidence. The second configuration was used for the compound and fixed wing versions. This consisted of a fixed upper T-tail, and a lower horizontal tail with variable incidence

and geared elevator. The empennage also includes the vertical tail with a rudder and a lower vertical fin with a drag brake. The geometry associated with the empennage is presented in section C-1 of appendix C, table 1, and figure 11. Table 20 presents an effective longitudinal moment arm for the vertical tail which is variable as a function of α_{WF}, ψ_{WF}, i_W, and δ_F. This is a convenient means for portraying the nonlinear aerodynamic characteristics.

The rotor downwash at the tail (section C-2 and table 21), which depends on rotor loading and rotor wake skew angle, is derived in a similar manner to the downwash at the body. The vertical tail is assumed to experience the same downwash as the lower horizontal tail. The downwash, from the fuselage/wing/nacelles combination (section C-3 and tables 22 and 23), is derived from wind tunnel test data in terms of the downwash angle ε. Small angles are assumed, allowing the Z component of velocity to be obtained without changes to the X component. Sidewash (section C-3 and tables 24 and 25) at the vertical tail is treated in a similar fashion. The basic lift dependent downwash from the nacelles and fairings is included in the basic downwash data. The engine efflux is represented as a change in dynamic pressure at the tail. Finally, the interference effects are modified by a pure time delay based on tail arm and forward speed. This is presented in section C-4.

The dynamic pressure at the tail is expressed as a velocity ratio factor rather than a pressure ratio factor. Provision is made for dynamic pressure ratio corrections to be applied to each empennage component (section C-5 and tables 26-28). By necessity, these are average effects at each component.

The total velocity components for the lower horizontal tail (section C-6) are made up of contributions from the basic body axes translational and angular velocities, rotor wash, and fuselage/wing/nacelle downwash and sidewash. Dynamic pressure loss is introduced by factoring out the X component from the basic body velocity. The actual dynamic pressure at the tail is calculated from the resultant velocity vector. This allows a more representative definition of dynamic pressure at low speeds where downwash from the rotor dominates the flow at the tail. Section C-7 presents the definition of angle of attack for the lower horizontal tail. This and control setting, δ_E, define the lower horizontal tail aerodynamic forces (section C-8 and table 29), using isolated tail data. The aerodynamic forces are then resolved from wind axes into body axes at the tail (section C-9).

A similar procedure is used to define the velocities, angles, and forces for the upper horizontal tail, the vertical tail, and the drag brake. Section C-10 through section C-21 and tables 30-33 present the equations and data for these components.

Finally, all components of the empennage are summed, section C-22, to provide the tail forces at the aircraft center of gravity. Moments about the center of gravity due to the tail forces are obtained by multiplying the forces by the appropriate tail moment arms. Figure 12 presents an overall detailed block diagram of the empennage model.

TAIL ROTOR MODULE

The tail rotor model is a simplification of the linearized closed form Bailey theory developed in reference 6. Terms in tip speed ratio greater than μ-squared have been eliminated.

The geometry of the tail rotor location is presented in section D-1 of appendix D, table 1, and figure 13.

The airflow impinging on the tail rotor (section D-2) is calculated in a similar manner to the velocities at the empennage. These are normalized by tip speed (section D-3) for the Bailey calculation. The basic Bailey equations have been retained with some additions. In order to obtain the actual tail rotor collective, θ_{TR} (section D-4), it is necessary to modify the value used in the Bailey formulation by a contribution due to δ_{3TR} (pitch-flap coupling). It has been shown by Sikorsky Aircraft data that δ_{3TR} effects can be conveniently compensated. This method relies on the derivative, (da_o/dT), being constant for a given tail rotor system. With thrust being known from the previous iteration of the equations, the coning, and hence blade pitch can be determined.

The Bailey theory equation, sections D-5 through D-8, is normally presented as the thrust coefficient in terms of the 't' coefficients. It should be noted that the equations have been manipulated to obtain an expression for downwash (section D-6). This was found to be necessary to obtain an unconditionally stable solution. It is important that computer program flow follows the equation flow for a stable tail rotor solution.

A blockage factor K_{TRBLK} is applied to the final thrust output, section D-8, to account for the proximity of the vertical tail. This correction is empirical and based on Sikorsky Aircraft flight test data of other helicopters.

This simplified tail rotor model only calculates thrust. No account of H force is included in the final tail rotor force outputs. The tail rotor thrust is finally resolved into the body axes forces and moments at the aircraft center of gravity which are presented in section D-9.

AUXILIARY ENGINE MODULE

As stated previously, the auxiliary engine associated nacelle aerodynamics are included in the fuselage module. In the auxiliary engine module, the direct thrust, momentum drag effects, and engine out effects are modeled. The engine geometry is presented in section E-1 of appendix E, table 1, and figure 14.

The dynamic response of the auxiliary engines is simulated by a simple time delay and a first order lag as shown by the block diagram in section E-2. After the pilot's commanded RPM is processed through the dynamics, the thrust and mass flow of each engine is calculated from the relationships in section E-3. These equations are a function of RPM and mach number. The thrust relationship presented is based on the RSRA TF-34 engine performance data. Two engines are represented in order that one-engine-out flight characteristics can be simulated.

The final engine force and moment effects at the aircraft's center of gravity are obtained from section E-4. The thrust is resolved through

the engine cant angle and summed with the inlet momentum forces. Since net thrust is represented in section E-3, no momentum effects appear in the X body axis equation.

CONTROL SYSTEM MODULE

The control system represented in this module includes a full compliment of both helicopter and fixed wing controls. This includes the primary system, the secondary system and the stability augmentation system. In simulating the compound vehicle, the helicopter primary control system can be mixed with the fixed wing primary control system. The mixing of controls is accomplished through the control phasing units (CPU). This control phasing capability allows adjustment of the control sensitivity throughout the compound flight envelope. Figure 15 presents the control system sign convention used in this report, and table 1 presents the control system gains and limits.

Figure 16 through 18 present a diagramatic representation of the primary control system for all three axes. For the longitudinal axis (section F-1 of appendix F), the pilot's control stick position is summed with the stability augmentation output. The summation is then processed through the CPU. This provides outputs as a function of the CPU setting which are ratioed to helicopter controls and to fixed wing controls. Next, the output is summed with a series trim system. The series trim is a research control used by the onboard computer and/or pilot. The longitudinal fixed wing control includes an interconnect input for the wing tilt to the horizontal tail. The longitudinal helicopter control

includes a collective mixing input. The lateral and directional control systems are similar to the longitudinal system and are presented in sections F-2 and F-3, respectively. The final primary control for the helicopter is the collective control system which is presented in section F-4. The CPU functions described above are generated from logic driven by the CPU control levers. The control lever equations are presented in section F-5, and the CPU logic is presented in section F-6 and figure 19.

The secondary control systems consist of wing incidence (section F-7), drag brake (section F-8), flaps (section F-9), auxiliary engine throttles (section F-10), and main rotor engine throttles (section F-11).

The block diagrams of the stability augmentation system (SAS) for the pitch, roll, and yaw axes are presented in figures 20 through 22. The SAS model is a simple rate plus lag rate system for pitch and roll with a washout in the pitch channel. The yaw SAS is a simple rate system with washout. Section F-12 presents the equations and gains for the SAS system.

GENERAL EQUATION MODULE

The forces and moments derived from the various simulated components of the aircraft are summed in section G-1 of appendix G. These equations provide the total applied external forces and moments, acting at and about, the center of gravity in the body axes system. These forces and moments are then introduced into the general equations of motion from which the six components of acceleration are solved (section G-2). It should be noted that these are the equations of the aircraft without rotor blades, thus

only the aircraft body mass is used. The rotor blade mass is accounted for in the rotor degree of freedom equations.

The Euler angle rate equations are given in section G-3, and the body axes to inertial axes transformation is presented in section G-4. Large angles are assumed throughout the calculations. At this point the kinematic model of reference 7 is used to calculate the accelerations in the inertial axes. These accelerations are then integrated to form the inertial velocities and positions of the aircraft. The inertial velocities can then be used to form the body axes velocities.

The geometry associated with the pilot's station is presented in section G-5, table 1, and figure 23. The equations are written for the starboard pilot's position. Sections G-6 and G-7 present the accelerations and velocities, respectively, at the pilot's station.

Finally figure 24 presents the total block diagram for the simulation of the Rotor Systems Research Aircraft.

CONCLUDING REMARKS

This report describes the present version of the mathematical model representing the Rotor Systems Research Aircraft. The mathematical model, incorporated into a real-time simulation, provides an excellent method by which evaluation of promising rotor and control concepts can be conducted. The real-time man-in-the-loop simulation also provides a method by which pilot training and preflighting of experiments can be conducted. It is recommended that this mathematical model be continually

updated as the flight vehicle is tested. It is further recommended that studies in the area of mathematical modeling be conducted to provide a more valid representation for each of the various components.

APPENDIX A

MAIN ROTOR MODULE EQUATIONS

A-1 Effect Of Rotor Blade Weight On CG Postions

$$W_{bd} = W - b_{NMR}W_b$$

$$FS_{CGB} = (FS_{CG}W - b_{NMR}FS_{MR}W_b)/W_{bd}$$

$$WL_{CGB} = (WL_{CG}W - b_{NMR}WL_{MR}W_b)/W_{bd}$$

$$l_{MR} = (FS_{CGB} - FS_{MR})/12$$

$$b_{MR} = BL_{MR}/12$$

$$h_{MR} = (WL_{MR} - WL_{CGB})/12$$

A-2 Rotor Blade Definition

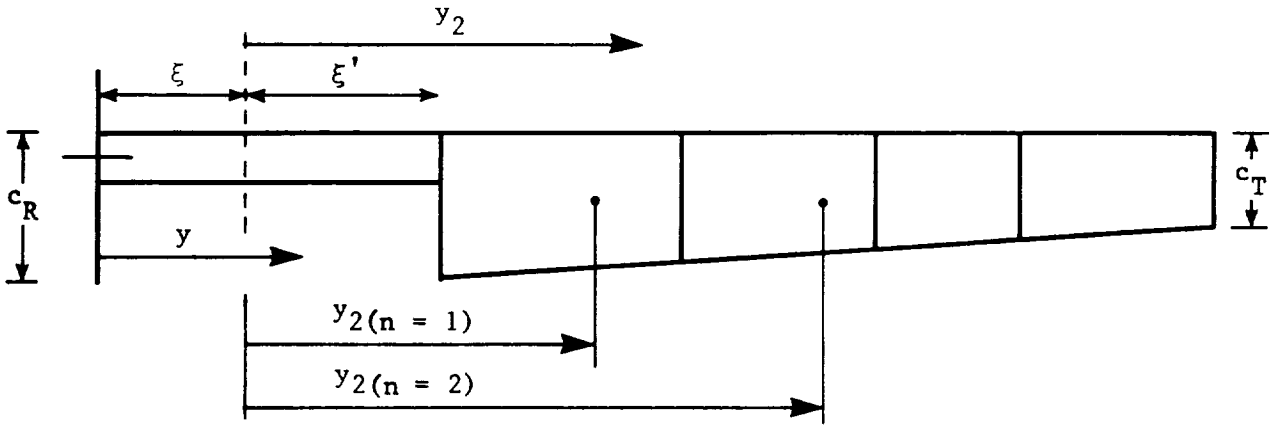

The blade segments are set-up based on equal annulii area.

APPENDIX A

Distance to segment center of lift per unit radius.

First segment -

$$y_{2(n=1)} = \left\{ \left[\frac{1 - (\xi + \xi')^2}{2n_S} \right] + (\xi + \xi')^2 \right\}^{1/2} - \xi$$

Subsequent segments -

$$y_{2(n)} = \left\{ \left[\frac{1 - (\xi + \xi')^2}{n_S} \right] + (\xi + y_{2(n-1)})^2 \right\}^{1/2} - \xi$$

Distance to inboard end of segment from centerline

$$y_{INB(n)} = \left\{ (\xi + y_{2(n)})^2 - \left[\frac{1 - (\xi + \xi')^2}{2n_S} \right] \right\}^{1/2}$$

Distance to outboard end of segment from centerline

$$y_{OUTB(n)} = \left\{ (\xi + y_{2(n)})^2 + \left[\frac{1 - (\xi + \xi')^2}{2n_S} \right] \right\}^{1/2}$$

Segment width

$$\Delta y_{(n)} = y_{OUTB(n)} - y_{INB(n)}$$

Mean chord of segment

$$c_{y(n)} = \left[\frac{y_{OUTB(n)} + y_{INB(n)} - 2(\xi + \xi')}{2(1 - \xi + \xi')} \right] (c_T - c_R) + c_R$$

Offset

$$\xi = e/R_{MR}$$

Spar length

$$\xi' = e'/R_{MR}$$

APPENDIX A

A-3 Body Axes To Shaft Axes Transformation Matrix

$$[A_{BS}] = \begin{bmatrix} \cos i_\theta & 0 & -\sin i_\theta \\ \sin i_\theta \sin i_\phi & \cos i_\phi & \cos i_\theta \sin i_\phi \\ \sin i_\theta \cos i_\phi & -\sin i_\phi & \cos i_\theta \cos i_\phi \end{bmatrix}$$

where i_θ and i_ϕ are Euler angles with positive rotations of i_θ about the Y-hub axis and then i_ϕ about the resulting X-shaft axis.

Shaft axes to body axes transformation matrix

$$[A_{SB}] = [A_{BS}]^T$$

since $[A_{BS}]$ is an orthogonal matrix.

A-4 Body Translational Accelerations At The Rotor Hub

$$\dot{V}_{XH} = \dot{V}_{XB} - rV_{YB} + qV_{ZB} - l_{MR}(q^2 + r^2) + b_{MR}(pq - \dot{r})$$
$$- h_{MR}(pr + \dot{q}) + g \sin \theta_{BODY}$$

$$\dot{V}_{YH} = \dot{V}_{YB} - pV_{ZB} + rV_{XB} + l_{MR}(pq + \dot{r}) - b_{MR}(p^2 + r^2)$$
$$- h_{MR}(qr - \dot{p}) - g \sin \phi_{BODY} \cos \theta_{BODY}$$

$$\dot{V}_{ZH} = \dot{V}_{ZB} - qV_{XB} + pV_{YB} + l_{MR}(pr - \dot{q}) + b_{MR}(qr + \dot{p})$$
$$+ h_{MR}(p^2 + q^2) - g \cos \phi_{BODY} \cos \theta_{BODY}$$

gravity terms are added for convenience at this point. They are normally found in the $\ddot{\beta}$ and $\ddot{\delta}$ equations.

A-5 Body Translational Velocities At The Rotor Hub

(non-dimensionalized by $\Omega_T R_{MR}$)

$$\mu_{XH} = \left[\frac{1}{\Omega_T R_{MR}}\right][V_{XB} - qh_{MR} - rb_{MR}]$$

$$\mu_{YH} = \left[\frac{1}{\Omega_T R_{MR}}\right][V_{YB} + ph_{MR} + rl_{MR}]$$

$$\mu_{ZH} = \left[\frac{1}{\Omega_T R_{MR}}\right][V_{ZB} - ql_{MR} + pb_{MR}]$$

A-6 Body Translational And Angular Accelerations At The Hub In Shaft Axes

$$\begin{bmatrix} \dot{V}_{XS} \\ \dot{V}_{YS} \\ \dot{V}_{ZS} \end{bmatrix} = [A_{BS}] \begin{bmatrix} \dot{V}_{XH} \\ \dot{V}_{YH} \\ \dot{V}_{ZH} \end{bmatrix}$$

$$\begin{bmatrix} \dot{p}_S \\ \dot{q}_S \\ \dot{r}_S \end{bmatrix} = [A_{BS}] \begin{bmatrix} \dot{p} \\ \dot{q} \\ \dot{r} \end{bmatrix}$$

A-7 Body Translational And Angular Velocities At The Hub In Shaft Axes

$$\begin{bmatrix} \mu_{XS} \\ \mu_{YS} \\ \mu_{ZS} \end{bmatrix} = [A_{BS}] \begin{bmatrix} \mu_{XH} \\ \mu_{YH} \\ \mu_{ZH} \end{bmatrix}$$

$$\begin{bmatrix} p_S \\ q_S \\ r_S \end{bmatrix} = [A_{BS}] \begin{bmatrix} p \\ q \\ r \end{bmatrix}$$

A-8 Rotor Azimuthal Advance Angle

$$\psi_i = \psi_{i-1} + 57.3\Omega\ \Delta t$$

where $\Delta\psi = 57.3\Omega\ \Delta t$.

A-9 Rotor Speed Degree Of Freedom

If rotor speed is governed perfectly

$$\Omega = \Omega_T K_{RPM}$$

$$\dot{\Omega} = 0.$$

If rotor speed degree of freedom is released

$$\Omega_i = \Omega_{i-1} + \left[\frac{Q_E - Q}{I_R}\right]\Delta t$$

where $$\dot{\Omega}_i = \left[\frac{Q_E - Q}{I_R}\right]$$

A-10 Rotor Uniform Inflow Velocity And Downwash

$$D_{WMR_i} = \left[\frac{K_\lambda - 1}{K_\lambda}\right] D_{WMR_{i-1}} + \left[\frac{1}{K_\lambda}\right]\left[\frac{\left(\frac{b_{MR}c_{75}}{2\pi R_{MR}}\right)\left(\frac{C_T}{\sigma}\right)'}{(\mu_{XS}^2 + \mu_{YS}^2 + \lambda_{MR_{i-1}}^2)^{1/2}}\right]$$

where $$\lambda_{MR_i} = \mu_{ZS} - D_{WMR_i}$$

$$K_\lambda = K'_\lambda \left[\frac{.02}{\Delta t}\right]$$

and K'_λ is an input constant normally set to 6.0 which gives an approximate air mass lag of 0.1 seconds for D_{WMR}.

A-11 First Harmonic Inflow Coefficients

$$K_{GL} = \frac{[\mu_{XS}^2 + \mu_{YS}^2]^{1/2}}{[\mu_{XS}^2 + \mu_{YS}^2 + \lambda_{MR_i}^2]^{1/2}}$$

$$K_{1X} = K_{GL}\left\{\frac{\mu_{XS}}{[\mu_{XS}^2 + \mu_{YS}^2 + \lambda_{MR_i}^2]^{1/2}}\right\}$$

$$K_{1Y} = K_{GL}\left\{\frac{\mu_{YS}}{[\mu_{XS}^2 + \mu_{YS}^2 + \lambda_{MR_i}^2]^{1/2}}\right\}$$

A-12 Wing Interference Airflow At The Rotor

If the vehicle is configured as a helicopter do not calculate this section and set $u_{PIWR} = u_{TIWR} = 0.$

Normal induced velocity -

$$V_{NOW} = f(r/R_{MR}, \psi_{MAP})$$

if $0^o \leq \psi \leq 180^o$

$$\psi_{MAP} = \psi$$

$$u_{PIWR} = -V_{NOW}\left(\frac{V_{XB}}{\Omega_T R_{MR}}\right) 0.03608$$

if $180^o \leq \psi \leq 360^o$

$$\psi_{MAP} = 360^o - \psi$$

$$u_{PIWR} = -V_{NOW}\left(\frac{V_{XB}}{\Omega_T R_{MR}}\right) 0.03608$$

Tangential induced velocity -

$$V_{TOW} = f(r/R_{MR}, \psi_{MAP})$$

if $0^o \leq \psi \leq 180^o$

$$\psi_{MAP} = \psi$$

$$u_{TIWR} = -V_{TOW}\left(\frac{V_{XB}}{\Omega_T R_{MR}}\right)\ 0.03608$$

if $180^\circ \leq \psi \leq 360^\circ$

$$\psi_{MAP} = 360^\circ - \psi$$

$$u_{TIWR} = V_{TOW}\left(\frac{V_{XB}}{\Omega_T R_{MR}}\right)\ 0.03608$$

The values for V_{NOW} and V_{TOW} are presented in the data section of this paper.

A-13 Blade Flapping Equations (Rotating Shaft Axes)

$$\begin{aligned}\ddot{\beta} = \frac{M_b}{I_b}\Big[&\cos\beta\{\dot{V}_{ZS} + e[2\Omega(p_S\cos\psi - q_S\sin\psi) \\ &+ \dot{p}_S\sin\psi + \dot{q}_S\cos\psi]\} + \sin\beta\cos\delta\{\dot{V}_{YS}\sin\psi \\ &- \dot{V}_{XS}\cos\psi - e(r_S - \Omega)^2\}\Big] + \cos^2\beta\Big[\cos\delta\{\dot{p}_S\sin\psi \\ &+ \dot{q}_S\cos\psi - 2(\dot{\delta} + \Omega)(q_S\sin\psi - p_S\cos\psi)\} \\ &- 2\Omega\sin\delta(p_S\sin\psi + q_S\cos\psi)\Big] \\ &+ \cos\beta\sin\beta\left[2\dot{\delta}(r_S - \Omega) - (r_S - \Omega)^2\right] + \frac{M_{FA}}{I_b} + \frac{M_{FD}}{I_b}\end{aligned}$$

$$\dot{\beta}_i = \dot{\beta}_{i-1}\cos\Delta\psi + \frac{1}{\Omega}\ddot{\beta}_{i-1}\sin\Delta\psi$$

$$\beta_i = \beta_{i-1} + \frac{1}{\Omega}\dot{\beta}_{i-1}\sin\Delta\psi + \frac{1}{\Omega^2}\ddot{\beta}_{i-1}(1 - \cos\Delta\psi)$$

A-14 Blade Lagging Equations (Rotating Shaft Axes)

Continued on next page.

$$\ddot{\delta} = \frac{M_b}{I_b \cos\beta}\Big[\sin\delta\{\dot{V}_{YS}\sin\psi - \dot{V}_{XS}\cos\psi - e(r_S - \Omega)^2\}$$

$$-\cos\delta\{\dot{V}_{XS}\sin\psi + \dot{V}_{YS}\cos\psi + e(\dot{\Omega} - \dot{r}_S)\}\Big]$$

$$+ \frac{\sin\beta}{\cos\beta}[2\dot{\beta}(\Omega + \dot{\delta} - r_S) + \dot{q}_S\sin(\psi + \delta)$$

$$- \dot{p}_S\cos(\psi + \delta)] + (\dot{r}_S - \dot{\Omega})$$

$$+ 2\dot{\beta}[\cos\delta(q_S\sin\psi - p_S\cos\psi)$$

$$+ \sin\delta(p_S\sin\psi + q_S\cos\psi)] - \frac{M_{LA}}{I_b\cos\beta} - \frac{M_{LD}}{I_b\cos\beta}$$

$$\dot{\delta}_i = \dot{\delta}_{i-1}\cos\Delta\psi + \frac{1}{\Omega}\ddot{\delta}_{i-1}\sin\Delta\psi$$

$$\delta_i = \delta_{i-1} + \frac{1}{\Omega}\dot{\delta}_{i-1}\sin\Delta\psi + \frac{1}{\Omega^2}\ddot{\delta}_{i-1}(1 - \cos\Delta\psi)$$

limit δ_i to $\delta_{AFT} \leq \delta_i \leq \delta_{FWD}$

if no lag degree of freedom $\delta = \dot{\delta} = \ddot{\delta} = M_{LD} = 0$.

A-15 Blade Element Velocities

$$u_P = \lambda_{MR}\cos\beta + \mu_{YS}\sin\beta\sin(\psi + \delta) - \mu_{XS}\sin\beta\cos(\psi + \delta)$$

$$+ \xi\cos\beta[(\frac{q_S}{\Omega_T} - K_{1X}D_{WMR})\cos\psi + (\frac{p_S}{\Omega_T} + K_{1Y}D_{WMR})\sin\psi]$$

$$- \xi\sin\beta\sin\delta(\frac{r_S - \Omega}{\Omega_T})$$

$$+ y_{2(n)}[-\frac{\dot{\beta}}{\Omega_T} + (\frac{q_S}{\Omega_T} - K_{1X}D_{WMR}\cos\beta)\cos(\psi + \delta)$$

$$+ (\frac{p_S}{\Omega_T} + K_{1Y}D_{WMR}\cos\beta)\sin(\psi + \delta)]$$

$$+ u_{PIWR}$$

$$u_T = \mu_{XS} \sin(\psi + \delta) + \mu_{YS} \cos(\psi + \delta) - \xi \cos \delta \left(\frac{r_S - \Omega}{\Omega_T}\right)$$

$$+ y_{2(n)} \left[\frac{\dot{\delta}}{\Omega_T} + \left(\frac{p_S}{\Omega_T} \cos(\psi + \delta) - \frac{q_S}{\Omega_T} \sin(\psi + \delta)\right) \sin \beta \right.$$

$$\left. - \cos \beta \left(\frac{r_S - \Omega}{\Omega_T}\right)\right]$$

$$+ u_{TIWR}$$

$$u_R = \lambda_{MR} \sin \beta + \mu_{XS} \cos \beta \cos(\psi + \delta) - \mu_{YS} \cos \beta \sin(\psi + \delta)$$

$$+ \xi \sin \beta \left[\left(\frac{q_S}{\Omega_T} - K_{1X} \dot{D}_{WMR}\right) \cos \psi + \left(\frac{p_S}{\Omega_T} + K_{1Y} D_{WMR}\right) \sin \psi\right]$$

$$+ \xi \cos \beta \sin \delta \left(\frac{r_S - \Omega}{\Omega_T}\right)$$

$$+ y_{2(n)} \sin \beta \left[-K_{1X} D_{WMR} \cos(\psi + \delta) + K_{1Y} D_{WMR} \sin(\psi + \delta)\right]$$

A-16 Resultant Velocity At The Blade Segment

$$u_{YAW} = \left(u_T^2 + u_P^2 + u_R^2\right)^{1/2}$$

A-17 Mach Number At The Blade Segment

$$M = \left(u_T^2 + u_P^2\right)^{1/2} \left(\frac{\Omega_T R_{MR}}{a}\right)$$

A-18 Blade Segment Angle Of Attack (Resolved in direction of local segment airflow)

$$\alpha_Y = \tan^{-1} \left\{ \frac{\left[u_T \left(\theta_A + \frac{\theta_A^3}{3} + \frac{2\theta_A^5}{15}\right) + u_P\right] |\cos \gamma|}{u_T - u_P \left(\theta_A + \frac{\theta_A^3}{3} + \frac{2\theta_A^5}{15}\right) \cos^2 \gamma} \right\}$$

where

$$\tan \theta_A = \theta_A + \frac{\theta_A^3}{3} + \frac{2\theta_A^5}{15}$$

$$|\cos \gamma| = \frac{|u_T|}{(u_T^2 + u_R^2)^{1/2}}$$

A-19 Blade Segment Geometric Pitch Angle (Blade Span Axes)

$$\theta = \theta_{COFF} - A_{1S} \cos(\psi + \Delta_{SP}) - B_{1S} \sin(\psi + \Delta_{SP})$$

$$+ \theta_1(y_{2(n)} - \zeta') - 57.3\ \beta \tan \delta_3 + K_{\alpha 0}$$

$$+ K_{\alpha 1}(57.3\ \delta) + K_{\alpha 2}(57.3\ \delta)^2$$

$$\theta_A = \theta/57.3$$

A-20 Rotor Blade Aerodynamic Data

Lift Coefficient, C_{LY}, where

$$0^\circ \leq \alpha_{TRANS} \leq 180^\circ$$

$$0 \leq M \leq 1;\ \text{if}\ M > 1\ \text{set}\ M = 1$$

Definition of α_{TRANS} for C_{LY}

(a) $0^\circ \leq |\alpha_Y| \leq \frac{13.5^\circ}{|\cos \gamma|}$, $\alpha_{TRANS} = |\alpha_Y \cos \gamma|$

(b) $(180^\circ - \frac{8^\circ}{|\cos \gamma|}) \leq |\alpha_Y| \leq 180^\circ$, $\alpha_{TRANS} = |\alpha_Y \cos \gamma|$

(c) if (a) or (b) and $|\alpha_Y| > 90^\circ$,

$$\alpha_{TRANS} = \left|\alpha_Y \cos \gamma + \frac{\alpha_Y}{|\alpha_Y|} 180^\circ(1 - |\cos \gamma|)\right|$$

(d) $\frac{13.5^\circ}{|\cos \gamma|} \leq |\alpha_Y| \leq (180^\circ - \frac{8^\circ}{|\cos \gamma|})$, $\alpha_{TRANS} = |\alpha_Y|$

APPENDIX A

Definition of C_{LY}

if $n < n_S$

$$C_{LY} = \frac{\alpha_Y}{|\alpha_Y|} f(\alpha_{TRANS}, M)$$

if $n = n_S$

$$C_{LY} = \frac{\alpha_Y}{|\alpha_Y|} \left[1 - \frac{(1 - B_{MR})}{\Delta y_{(n=n_S)}} \right] f(\alpha_{TRANS}, M)$$

where n is the particular blade segment being evaluated.

Drag Coefficient, C_{DY}, where

$$0^\circ \leq \alpha_{TRANS} \leq 180^\circ$$

$$0 \leq M \leq 1; \text{ if } M > 1 \text{ set } M = 1$$

Definition of α_{TRANS} for C_{DY}

$$0^\circ \leq |\alpha_Y| \leq 180^\circ, \quad \alpha_{TRANS} = |\alpha_Y|$$

Definition of C_{DY}

$$C_{DY} = f(\alpha_{TRANS}, M) + \Delta C_D$$

where ΔC_D is a constant drag coefficient.
The values for C_{LY} and C_{DY} are presented in the data section of this paper.

A-21 Blade Segmental Forces

$$F_P = \frac{1}{2} \rho \Omega_T^2 R_{MR}^3 (c_{y(n)} \Delta y_{(n)}) u_{YAW} \left(C_{LY} \frac{u_T}{|\cos \gamma|} + C_{DY} u_P \right)$$

$$F_T = \frac{1}{2} \rho \Omega_T^2 R_{MR}^3 (c_{y(n)} \Delta y_{(n)}) u_{YAW} (C_{DY} u_T - C_{LY} u_P |\cos \gamma|)$$

$$F_R = \frac{1}{2} \rho \Omega_T^2 R_{MR}^3 (c_{y(n)} \Delta y_{(n)}) u_{YAW} (C_{DY} - C_{LY} \frac{u_P}{u_T} |\cos \gamma|) u_R$$

A-22 Blade Aerodynamic Shears (Blade Span Axes)

$$F_{PB} = \sum_{n=1}^{n=n_S} F_P$$

$$F_{TB} = \sum_{n=1}^{n=n_S} F_T$$

$$F_{RB} = \sum_{n=1}^{n=n_S} F_R$$

A-23 Blade Aerodynamic Shears (Rotating Shaft Axes)

$$F_{XA} = F_{RB} \cos \beta \sin \delta - F_{TB} \cos \delta - F_{PB} \sin \beta \sin \delta$$

$$F_{YA} = F_{RB} \cos \beta \cos \delta + F_{TB} \sin \delta - F_{PB} \sin \beta \cos \delta$$

$$F_{ZA} = -(F_{RB} \sin \beta + F_{PB} \cos \beta)$$

A-24 Aerodynamic Moments About The Blade Hinges (Rotating Shaft Axes)

Flapping hinge

$$M_{FA} = R_{MR} \sum_{n=1}^{n=n_S} y_{2(n)} F_P$$

Lagging hinge

$$M_{LA} = R_{MR} \sum_{n=1}^{n=n_S} y_{2(n)} F_T$$

A-25 Blade Hinge Constraint Moments (Rotating Shaft Axes)

Flapping hinge

$$M_{FD} = -(K_\beta \beta + K_{\dot\beta} \dot\beta)$$

Lagging hinge

$$M_{LD} = L_L (F_\delta + F_{\dot\delta})$$

where

$$F_\delta = f(\delta)$$

$$F_{\dot\delta} = \frac{\dot\delta}{|\dot\delta|} F'_{\dot\delta}$$

The values for K_β, $K_{\dot\beta}$, F_δ, and $F'_{\dot\delta}$ are presented in tables 1 and 4.

A-26 Blade Inertia Shears At Hinge (Rotating Shaft Axes)

Normally many inertia acceleration terms integrate to zero around the azimuth and are eliminated. This rotor model will be used to evaluate rotor out-of-balance loads following blade release and all significant terms are retained.

$$F_{XI} = M_b \{\cos\beta \cos\delta(\dot r_S - \dot\Omega - \ddot\delta) + 2 \sin\beta \cos\delta[\dot\delta\dot\beta - (r_S - \Omega)\dot\beta] + \cos\beta \sin\delta[\dot\delta^2 + \dot\beta^2 - 2(r_S - \Omega)\dot\delta + (r_S - \Omega)^2] + 2\dot\beta \cos\beta(p_S \cos\psi - q_S \sin\psi) + \ddot\beta \sin\beta \sin\delta\} - \frac{W_b}{g}(\dot V_{XS} \sin\psi + \dot V_{YS} \cos\psi)$$

$$F_{YI} = M_b\{\cos\beta\cos\delta[\dot{\delta}^2 + \dot{\beta}^2 - 2(r_S - \Omega)\dot{\delta} + (r_S - \Omega)^2]$$

$$+ \ddot{\beta}\sin\beta\cos\delta + \ddot{\delta}\cos\beta\sin\delta - 2\dot{\beta}\cos\beta(p_S\sin\psi$$

$$+ q_S\cos\psi) + \frac{W_b e}{gM_b}(r_S - \Omega)^2\} + \frac{W_b}{g}(\dot{V}_{XS}\cos\psi$$

$$- \dot{V}_{YS}\sin\psi)$$

$$F_{ZI} = M_b\{\ddot{\beta}\cos\beta - \dot{\beta}^2\sin\beta + 2\dot{\beta}\sin\beta\cos\delta(p_S\sin\psi$$

$$+ q_S\cos\psi) + \cos\beta\sin\delta[2(\Omega + \dot{\delta})(p_S\sin\psi$$

$$+ q_S\cos\psi) + \dot{q}_S\sin\psi - \dot{p}_S\cos\psi]$$

$$- \cos\beta\cos\delta[2(\Omega + \dot{\delta})(p_S\cos\psi - q_S\sin\psi)$$

$$+ \dot{p}_S\sin\psi + \dot{q}_S\cos\psi] - \frac{W_b e}{gM_b}[2\Omega(p_S\cos\psi - q_S\sin\psi)$$

$$+ \dot{p}_S\sin\psi + \dot{q}_S\cos\psi]\} - \frac{W_b}{g}(\dot{V}_{ZS})$$

A-27 Total Blade Shear Forces At The Hinge (Rotating Shaft Axes)

$$F_{XT} = F_{XA} + F_{XI}$$

$$F_{YT} = F_{YA} + F_{YI}$$

$$F_{ZT} = F_{ZA} + F_{ZI}$$

A-28 Total Rotor Forces (Fixed Shaft Axes)

$$T = -\frac{b_N B}{b_S}\sum_{b=1}^{b=b_S} F_{ZT}$$

$$H = \frac{b_{NMR}}{b_S} \sum_{b=1}^{b=b_S} (F_{YT} \cos \psi - F_{XT} \sin \psi)$$

$$J = -\frac{b_{NMR}}{b_S} \sum_{b=1}^{b=b_S} (F_{XT} \cos \psi + F_{YT} \sin \psi)$$

$$T_A = -\frac{b_{NMR}}{b_S} \sum_{b=1}^{b=b_S} F_{ZA}$$

$$\left(\frac{C_T}{\sigma}\right)' = \frac{T_A}{\rho b_{NMR} c_{75} \Omega_T^2 R_{NR}^3}$$ used in calculation of rotor downwash on next iteration. The use of negative coordinate axes system for shaft forces is to preserve the usual understanding of thrust (T), drag (H), and side force (J) in helicopter practice.

A-29 Total Rotor Hub Moments (Fixed Shaft Axes)

$$L_H = \frac{b_{NMR}}{b_S} \sum_{b=1}^{b=b_S} [(eF_{ZT} + M_{FD} \cos \delta - M_{LD} \sin \beta \sin \delta)\sin \psi + (M_{FD} \sin \delta + M_{LD} \sin \beta \cos \delta)\cos \psi]$$

$$M_H = \frac{b_{NMR}}{b_S} \sum_{b=1}^{b=b_S} [(eF_{ZT} + M_{FD} \cos \delta - M_{LD} \sin \beta \sin \delta)\cos \psi + (M_{FD} \sin \delta + M_{LD} \sin \beta \cos \delta)\sin \psi]$$

$$Q = -\frac{b_{NMR}}{b_S} \sum_{b=1}^{b=b_S} (eF_{XT} + M_{LD} \cos \beta)$$

If no lag degree of freedom

$$Q = -\frac{b_{NMR}}{b_S} \sum_{b=1}^{b=b_S} (eF_{XT} - M_{LA} \cos \beta)$$

A-30 Transformation Of Rotor Forces And Moments Into Body Axes

$$\begin{bmatrix} X_{MR} \\ Y_{MR} \\ Z_{MR} \end{bmatrix} = [A_{SB}] \begin{bmatrix} -H \\ -J \\ -T \end{bmatrix}$$

$$\begin{bmatrix} L_{MR} \\ M_{MR} \\ N_{MR} \end{bmatrix} = [A_{SB}] \begin{bmatrix} L_H \\ M_H \\ Q \end{bmatrix} + \begin{bmatrix} h_{MR}Y_{MR} + b_{MR}Z_{MR} \\ -h_{MR}X_{MR} - l_{MR}Z_{MR} \\ l_{MR}Y_{MR} - b_{MR}X_{MR} \end{bmatrix}$$

A-31 Flapping And Lagging Fourier Coefficients

$$a_{0F} = \frac{57.3}{b_S} \sum_{b=1}^{b=b_S} \beta$$

$$a_{1SF} = -\frac{2(57.3)}{b_S} \sum_{b=1}^{b=b_S} \beta \cos \psi$$

$$b_{1SF} = -\frac{2(57.3)}{b_S} \sum_{b=1}^{b=b_S} \beta \sin \psi$$

$$a_{0L} = \frac{57.3}{b_S} \sum_{b=1}^{b=b_S} \delta$$

$$a_{1SL} = \frac{2(57.3)}{b_S} \sum_{b=1}^{b=b_S} \delta \cos \psi$$

$$b_{1SL} = \frac{2(57.3)}{b_S} \sum_{b=1}^{b=b_S} \delta \sin \psi$$

A-32 Rotor Wake Skew Angle

$$\chi = \tan^{-1} \frac{\mu_{XS}}{|\lambda_{MR}|} + a_{1SF}$$

APPENDIX B

FUSELAGE MODEL

(Includes Wing and Nacelles)

Total configuration aerodynamic force and moment functions are entered depending on the configuration selected. Two configurations are currently available:

(1) Fuselage only

(2) Fuselage plus wing plus nacelles

Note: Unless otherwise stated, fixed wing refers to the compound configuration also.

B-1 Rotor Wash In The Vicinity Of The Fuselage/Wing/Nacelles

EK_{WFX}, EK_{WFZ} } Defined in the data section of this paper

B-2 Angle Of Attack

$$\alpha_{WF} = \tan^{-1}\left(\frac{V_{ZWF}}{V_{XWF}}\right)$$

$$\alpha_W = \alpha_{WF} + i_W; \quad \alpha_{WF} \text{ in degrees}$$

B-3 Angle Of Sideslip

$$\beta_{WF} = \sin^{-1}\left[\frac{V_{YWF}}{(V_{XWF}^2 + V_{YWF}^2 + V_{ZWF}^2)^{1/2}}\right]$$

$$\psi_{WF} = -\beta_{WF}; \quad \beta_{WF} \text{ in degrees}$$

B-4 Velocity Components And Dynamic Pressure

$$V_{XWF} = V_{XB} + EK_{WFX}(D_{WMR}\Omega_T R_{MR})$$

$$V_{YWF} = V_{YB}$$

$$V_{ZWF} = V_{ZB} - EK_{WFZ}(D_{WMR}\Omega_T R_{MR})$$

$$q_{WF} = \frac{1}{2}\rho\,(V_{XWF}^2 + V_{YWF}^2 + V_{ZWF}^2)$$

B-5 Total Fuselage Aerodynamic Forces And Moments In The Wind Axes

(a) Helicopter

$$L_{TOT} = (\frac{L}{q}(\alpha_{WF}) + \frac{L}{q}(\psi_{WF}))q_{WF}$$

$$D_{TOT} = (\frac{D}{q}(\alpha_{WF}) + \frac{D}{q}(\psi_{WF}))q_{WF}$$

$$M_{MTOT} = (\frac{M_M}{q}(\alpha_{WF}) + \frac{M_M}{q}(\psi_{WF}))q_{WF}$$

$$Y_{TOT} = (\frac{Y}{q}(\alpha_{WF}, \psi_{WF}))q_{WF}$$

$$L_{MTOT} = (\frac{L_M}{q}(\alpha_{WF}, \psi_{WF}))q_{WF}$$

$$N_{MTOT} = (\frac{N_M}{q}(\alpha_{WF}, \psi_{WF}))q_{WF}$$

(b) Fixed Wing

$$L_{TOT} = (\frac{L}{q}(\alpha_W, i_W) + \frac{L}{q}(\psi_{WF}, i_W) + \frac{L}{q}(T_J) + \frac{L}{q}(\delta_F, \alpha_W) + \frac{L}{q}(\delta_A))q_{WF}$$

$$D_{TOT} = (\frac{D}{q}(\alpha_W, i_W) + \frac{D}{q}(\psi_{WF}) + \frac{D}{q}(T_J)$$

$$+ \frac{D}{q}(\delta_F, \alpha_W) + \frac{D}{q}(\delta_A))q_{WF}$$

$$M_{MTOT} = (\frac{M_M}{q}(\alpha_W, i_W) + \frac{M_M}{q}(\psi_{WF}, i_W) + \frac{M_M}{q}(T_J)$$

$$+ \frac{M_M}{q}(\delta_F, \alpha_W) + \frac{M_M}{q}(\delta_A) + M_{M_q} q)q_{WF}$$

$$Y_{TOT} = (\frac{Y}{q}(\alpha_W, i_W) + \frac{Y}{q}(\psi_{WF}, i_W) + \frac{Y}{q}(T_J)$$

$$+ \frac{Y}{q}(\delta_F, \psi_{WF}) + \frac{Y}{q}(\delta_A) + Y_p p + Y_r r)q_{WF}$$

$$L_{MTOT} = (\frac{L_M}{q}(\alpha_W, \psi_{WF}) + \frac{L_M}{q}(\psi_{WF}, i_W) + \frac{L_M}{q}(T_J, \psi_{WF})$$

$$+ \frac{L_M}{q}(\delta_F, \psi_{WF}) + \frac{L_M}{q}(\delta_A, \alpha_W) + L_{M_p} p + L_{M_r} r)q_{WF}$$

$$N_{MTOT} = (\frac{N_M}{q}(\alpha_W, i_W) + \frac{N_M}{q}(\psi_{WF}, i_W) + \frac{N_M}{q}(T_J)$$

$$+ \frac{N_M}{q}(\delta_F, \psi_{WF}) + \frac{N_M}{q}(\delta_A, \alpha_W) + N_{M_p} p + N_{M_r} r)q_{WF}$$

where

$$\frac{L}{q}(\delta_A) = \frac{L}{q}(\delta_{AS}) + \frac{L}{q}(\delta_{AP})$$

$$\frac{D}{q}(\delta_A) = \frac{D}{q}(\delta_{AS}) + \frac{D}{q}(\delta_{AP})$$

$$\frac{M_M}{q}(\delta_A) = 0 .$$

$$\frac{Y}{q}(\delta_A) = 0 .$$

$$\frac{L_M}{q}(\delta_A, \alpha_W) = \frac{L_M}{q}(\delta_{AS}, \alpha_W) - \frac{L_M}{q}(\delta_{AP}, \alpha_W)$$

$$\frac{N_M}{q}(\delta_A, \alpha_W) = \frac{N_M}{q}(\delta_{AS}, \alpha_W) - \frac{N_M}{q}(\delta_{AP}, \alpha_W)$$

APPENDIX B

The terms in the equations in sections (a) and (b) are defined in the data section of this paper.

B-6 Transformation Of Forces And Moments From Wind To Body Axes

$$[A_{WB}] = \begin{bmatrix} \cos\beta_{WF}\cos\alpha_{WF} & \sin\beta_{WF}\cos\alpha_{WF} & -\sin\alpha_{WF} \\ \sin\beta_{WF} & -\cos\beta_{WF} & 0 \\ \cos\beta_{WF}\sin\alpha_{WF} & \sin\beta_{WF}\sin\alpha_{WF} & \cos\alpha_{WF} \end{bmatrix}$$

$$\begin{bmatrix} X'_{WF} \\ Y'_{WF} \\ Z'_{WF} \end{bmatrix} = [A_{WB}] \begin{bmatrix} -D_{TOT} \\ -Y_{TOT} \\ -L_{TOT} \end{bmatrix}$$

$$\begin{bmatrix} L'_{WF} \\ M'_{WF} \\ N'_{WF} \end{bmatrix} = [A_{WB}] \begin{bmatrix} L_{MTOT} \\ -M_{MTOT} \\ N_{MTOT} \end{bmatrix} + \begin{bmatrix} -Y'_{WF}h_{WT} \\ -Z'_{WF}l_{WT} + X'_{WF}h_{WT} \\ Y'_{WF}l_{WT} \end{bmatrix}$$

where

$$l_{WT} = (FS_{CG} - FS_{WT})/12 \ .$$

$$h_{WT} = (WL_{CG} - WL_{WT})/12 \ .$$

B-7 Low Speed Phasing Of Body Aerodynamic Data

If $|V_{XWF}| > 25$.

$$X_{WF}, Y_{WF}, Z_{WF} = X'_{WF}, Y'_{WF}, Z'_{WF}$$

$$L_{WF}, M_{WF}, N_{WF} = L'_{WF}, M'_{WF}, N'_{WF}$$

APPENDIX B

If $|V_{XWF}| \leq 25$.

$$X_{WF} = \left|\frac{V_{XWF}}{25}\right| X'_{WF} - \frac{\alpha_{WF}}{|\alpha_{WF}|}\left[1 - \left|\frac{V_{XWF}}{25}\right|\right] X_{LS}q_{WF}$$

$$Y_{WF} = \left|\frac{V_{XWF}}{25}\right| Y'_{WF} - \frac{V_{YWF}}{|V_{YWF}|}\left[1 - \left|\frac{V_{XWF}}{25}\right|\right] Y_{LS}q_{WF}$$

$$Z_{WF} = \left|\frac{V_{XWF}}{25}\right| Z'_{WF} - \frac{\alpha_{WF}}{|\alpha_{WF}|}\left[1 - \left|\frac{V_{XWF}}{25}\right|\right] Z_{LS}q_{WF}$$

$$L_{WF} = \left|\frac{V_{XWF}}{25}\right| L'_{WF} - \frac{V_{YWF}}{|V_{YWF}|}\left[1 - \left|\frac{V_{XWF}}{25}\right|\right] L_{LS}q_{WF}$$

$$M_{WF} = \left|\frac{V_{XWF}}{25}\right| M'_{WF} - \frac{\alpha_{WF}}{|\alpha_{WF}|}\left[1 - \left|\frac{V_{XWF}}{25}\right|\right] M_{LS}q_{WF}$$

$$N_{WF} = \left|\frac{V_{XWF}}{25}\right| N'_{WF} - \frac{V_{YWF}}{|V_{YWF}|}\left[1 - \left|\frac{V_{XWF}}{25}\right|\right] N_{LS}q_{WF}$$

where X_{LS}, Y_{LS}, Z_{LS}, L_{LS}, M_{LS}, N_{LS} are provided in the data section of this paper.

APPENDIX C

EMPENNAGE MODEL

C-1 Empennage Geometry

$$l_{HT} = (FS_{HT} - FS_{CG})/12$$

$$h_{HT} = (WL_{HT} - WL_{CG})/12$$

$$l_{HTU} = (FS_{HTU} - FS_{CG})/12$$

$$h_{HTU} = (WL_{HTU} - WL_{CG})/12$$

$$l_{VT} = (FS_{VT} - FS_{CG})/12$$

$$h_{VT} = (WL_{VT} - WL_{CG})/12$$

$$l_{DB} = (FS_{DB} - FS_{CG})/12$$

$$h_{DB} = (WL_{DB} - WL_{CG})/12$$

C-2 Rotor Wash At The Tail

EK_{TX}, EK_{TZ} } lower horizontal tail

EK_{TXU}, EK_{TZU} } upper horizontal tail

} Defined in the data section of this paper

C-3 Fuselage/Wing/Nacelle Downwash And Sidewash Interference At The Tail

Interference effects at the tail will depend on the selected tail-off configuration and are defined on the next page as:

Downwash —

$\left.\begin{matrix}\varepsilon_{WT} \\ \varepsilon_{WTU}\end{matrix}\right\}$ Defined in the data section of this paper.

$V_{ZIW} = [\frac{\varepsilon_{WT}}{57.3}] V_{XB}$ lower horizontal tail

$V_{ZIWU} = [\frac{\varepsilon_{WTU}}{57.3}] V_{XB}$ upper horizontal tail

Sidewash —

σ_{WT} Defined in the data section of this paper.

$V_{YIW} = [\frac{\sigma_{WT}}{57.3}] V_{XB}$

C-4 Pure Time Delay For Airflow To Reach The Tail

$\tau_T = l_{HT}/V_{XB}$

$\tau_{TU} = l_{HTU}/V_{XB}$

C-5 Dynamic Pressure Loss At The Tail

$\left.\begin{matrix}K_{QHT} \\ K_{QHTU} \\ K_{QVT} \\ K_{QDB}\end{matrix}\right\}$ Defined in the data section of this paper.

C-6 Lower Horizontal Tail Velocities

$V_{XHT} = V_{XB}K_{QHT} - qh_{HT} + EK_{TX}(D_{WMR}\Omega_T R_{MR})$

$$V_{YHT} = V_{YB} - rl_{HT} + ph_{HT} - V_{YIW}f(\tau_T)$$

$$V_{ZHT} = V_{ZB} + ql_{HT} - V_{ZIW}f(\tau_T) - EK_{TZ}(D_{WMR}\Omega_T R_{MR})$$

$$V_{HT}^2 = V_{XHT}^2 + V_{YHT}^2 + V_{ZHT}^2$$

$$q_{HT} = \frac{1}{2}\rho V_{HT}^2$$

where $f(\tau_T)$ is a pure time delay.

C-7 Lower Horizontal Tail Angle Of Attack

$$\alpha_{HT} = \tan^{-1}\left[\frac{V_{ZHT}}{V_{XHT}}\right]$$

$$\alpha_{HTT} = \alpha_{HT} + i_{HT} \; ; \; \alpha_{HT} \text{ in degrees}$$

C-8 Lower Horizontal Tail Aerodynamic Forces

$\left(\frac{L_{HT}}{\bar{q}}\right)$, $\left(\frac{D_{HT}}{\bar{q}}\right)$ — Defined in the data section of this paper.

C-9 Lower Horizontal Tail Forces In Body Axes

$$X_{HT} = -\left[\left(\frac{D_{HT}}{\bar{q}}\right)\cos\alpha_{HT}\cos\alpha_{VT} - \left(\frac{L_{HT}}{\bar{q}}\right)\sin\alpha_{HT}\right]q_{HT}$$

$$Y_{HT} = -\left[\left(\frac{D_{HT}}{\bar{q}}\right)\sin\alpha_{VT}\right]q_{HT}$$

$$Z_{HT} = -\left[\left(\frac{D_{HT}}{\bar{q}}\right)\sin\alpha_{HT}\cos\alpha_{VT} + \left(\frac{L_{HT}}{\bar{q}}\right)\cos\alpha_{HT}\right]q_{HT}$$

C-10 Upper Horizontal Tail Velocities

$$V_{XHTU} = V_{XB}K_{QHTU} - qh_{HTU} + EK_{TXU}(D_{WMR}\Omega_T R_{MR})$$

$$V_{YHTU} = V_{YB} - rl_{HTU} + ph_{HTU} - V_{YIW}f(\tau_{TU})$$

$$V_{ZHTU} = V_{ZB} + ql_{HTU} - V_{ZIWU}f(\tau_{TU}) - EK_{TZU}(D_{WMR}\Omega_T R_{MR})$$

$$V^2_{HTU} = V^2_{XHTU} + V^2_{YHTU} + V^2_{ZHTU}$$

$$q_{HTU} = \frac{1}{2}\rho V^2_{HTU}$$

where $f(\tau_{TU})$ is a pure time delay.

C-11 Upper Horizontal Tail Angle Of Attack

$$\alpha_{HTU} = \tan^{-1}\left[\frac{V_{ZHTU}}{V_{XHTU}}\right]$$

$$\alpha_{HTTU} = \alpha_{HTU} + i_{HTU} \; ; \; \alpha_{HTU} \text{ in degrees}$$

C-12 Upper Horizontal Tail Aerodynamic Forces

$\left(\frac{L_{HTU}}{\bar{q}}\right)$, $\left(\frac{D_{HTU}}{\bar{q}}\right)$ — Defined in the data section of this paper.

C-13 Upper Horizontal Tail Forces In Body Axes

$$X_{HTU} = -\left[\left(\frac{D_{HTU}}{\bar{q}}\right)\cos\alpha_{HTU}\cos\alpha_{VT} - \left(\frac{L_{HTU}}{\bar{q}}\right)\sin\alpha_{HTU}\right]q_{HTU}$$

$$Y_{HTU} = -\left[\left(\frac{D_{HTU}}{\bar{q}}\right)\sin\alpha_{VT}\right]q_{HTU}$$

$$Z_{HTU} = -\left[\left(\frac{D_{HTU}}{\bar{q}}\right)\sin\alpha_{HTU}\cos\alpha_{VT} + \left(\frac{L_{HTU}}{\bar{q}}\right)\cos\alpha_{HTU}\right]q_{HTU}$$

C-14 Vertical Tail Velocities

$$V_{XVT} = V_{XB}K_{QVT} - qh_{VT} + EK_{TX}(D_{WMR}\Omega_T R_{MR})$$

$$V_{YVT} = V_{YB} - rl_{VT} + ph_{VT} - V_{YIW}f(\tau_T) + EK_{TR}(D_{WTR}\Omega_{TR}R_{TR})$$

$$V_{ZVT} = V_{ZB} + ql_{VT} - V_{ZIW}f(\tau_T) - EK_{TZ}(D_{WMR}\Omega_T R_{MR})$$

where

$f(\tau_T)$ is a pure time delay.

$$V_{VT}^2 = V_{XVT}^2 + V_{YVT}^2 + V_{ZVT}^2$$

$$q_{VT} = \frac{1}{2}\rho V_{VT}^2$$

C-15 Vertical Tail Angle Of Attack

$$\alpha_{VTT} = \alpha_{VT} = \sin^{-1}\left[\frac{V_{YVT}}{(V_{XVT}^2 + V_{YVT}^2 + V_{ZVT}^2)^{1/2}}\right]$$

C-16 Vertical Tail Aerodynamic Forces

$\left(\frac{L_{VT}}{\bar{q}}\right)$

$\left(\frac{D_{VT}}{\bar{q}}\right)$

} Defined in the data section of this paper.

C-17 Vertical Tail Forces In Body Axes

$$X_{VT} = -\left[\left(\frac{D_{VT}}{\bar{q}}\right)\cos\alpha_{VT}\cos\alpha_{HT} - \left(\frac{L_{VT}}{\bar{q}}\right)\sin\alpha_{VT}\cos\alpha_{HT}\right]q_{VT}$$

$$Y_{VT} = -\left[\left(\frac{D_{VT}}{\bar{q}}\right)\sin\alpha_{VT} + \left(\frac{L_{VT}}{\bar{q}}\right)\cos\alpha_{VT}\right]q_{VT}$$

$$Z_{VT} = -\left[\left(\frac{D_{VT}}{\bar{q}}\right)\cos\alpha_{VT}\sin\alpha_{HT} - \left(\frac{L_{VT}}{\bar{q}}\right)\sin\alpha_{VT}\sin\alpha_{HT}\right]q_{VT}$$

where $\alpha_{HT} = 0^\circ$ for the helicopter configuration.

C-18 Drag Brake Velocities

$$V_{XDB} = V_{XB}K_{QDB} - qh_{DB} + EK_{TX}(D_{WMR}\Omega_T R_{MR})$$

$$V_{YDB} = V_{YB} - rl_{DB} + ph_{DB} - V_{YIW}f(\tau_T)$$

$$V_{ZDB} = V_{ZB} + ql_{DB} - V_{ZIW}f(\tau_T) - EK_{TZ}(D_{WMR}\Omega_T R_{MR})$$

where $f(\tau_T)$ is a pure time delay.

$$V_{DB}^2 = V_{XDB}^2 + V_{YDB}^2 + V_{ZDB}^2$$

$$q_{DB} = \frac{1}{2}\rho V_{DB}^2$$

C-19 Drag Brake Angle Of Attack

$$\alpha_{DB} = \sin^{-1}\left[\frac{V_{YDB}}{(V_{XDB}^2 + V_{YDB}^2 + V_{ZDB}^2)^{1/2}}\right]$$

C-20 Drag Brake Aerodynamic Forces

$\left(\frac{L_{DB}}{\bar{q}}\right)$

$\left(\frac{D_{DB}}{\bar{q}}\right)$

} Defined in the data section of this paper.

C-21 Drag Brake Forces In Body Axes

$$X_{DB} = -[(\frac{D_{DB}}{\bar{q}})\cos\alpha_{DB}\cos\alpha_{HT} - (\frac{L_{DB}}{\bar{q}})\sin\alpha_{DB}\cos\alpha_{HT}]q_{DB}$$

$$Y_{DB} = -[(\frac{D_{DB}}{\bar{q}})\sin\alpha_{DB} + (\frac{L_{DB}}{\bar{q}})\cos\alpha_{DB}]q_{DB}$$

$$Z_{DB} = -[(\frac{D_{DB}}{\bar{q}})\cos\alpha_{DB}\sin\alpha_{HT} - (\frac{L_{DB}}{\bar{q}})\sin\alpha_{DB}\sin\alpha_{HT}]q_{DB}$$

where $\alpha_{HT} = 0^\circ$ for the helicopter configuration.

APPENDIX C

C-22 Empennage Total Forces And Moments

$$X_T = X_{HT} + X_{HTU} + X_{VT} + X_{DB}$$

$$Y_T = Y_{HT} + Y_{HTU} + Y_{VT} + Y_{DB}$$

$$Z_T = Z_{HT} + Z_{HTU} + Z_{VT} + Z_{DB}$$

$$M_T = -[X_{HT}h_{HT} + X_{HTU}h_{HTU} + X_{VT}h_{VT} + X_{DB}h_{DB}]$$

$$+ Z_{HT}l_{HT} + Z_{HTU}l_{HTU} + Z_{VT}l_{VT} + Z_{DB}l_{DB}$$

$$L_T = \left(\frac{L_{MVT}}{\bar{q}}\right) q_{VT}$$

$$N_T = -[Y_{HT}l_{HT} + Y_{HTU}l_{HTU} + Y_{VT}l_{VT} + Y_{DB}l_{DB}]$$

where $\frac{L_{MVT}}{\bar{q}}$ is defined in the data section of this paper.

APPENDIX D

TAIL ROTOR MODEL

A Bailey type tail rotor model is assumed. This model can be replaced by the main rotor model if necessary at high forward velocities.

D-1 Tail Rotor Geometry

$$l_{TR} = (FS_{TR} - FS_{CG})/12$$

$$h_{TR} = (WL_{TR} - WL_{CG})/12$$

$$b_{TR} = BL_{TR}/12$$

D-2 Tail Rotor Velocities

$$V_{XTRB} = V_{XB}K_{QVT} - qh_{TR} + rb_{TR} + EK_{TX}(D_{WMR}\Omega_T R_{MR})$$

$$V_{YTRB} = V_{YB} - rl_{TR} + ph_{TR} - V_{YIW}f(\tau_T)$$

$$V_{ZTRB} = V_{ZB} + ql_{TR} - pb_{TR} - V_{ZIW}f(\tau_T) - EK_{TZ}(D_{WMR}\Omega_T R_{MR})$$

where $f(\tau_T)$ is a pure time delay.

$$V_{XTR} = V_{XTRB}$$

$$V_{YTR} = V_{YTRB} \cos \Gamma_{TR} + V_{ZTRB} \sin \Gamma_{TR}$$

$$V_{ZTR} = -V_{YTRB} \sin \Gamma_{TR} + V_{ZTRB} \cos \Gamma_{TR}$$

D-3 Nondimensional Velocities

$$\mu_{XTR} = \frac{V_{XTR}}{\Omega_{TR} R_{TR}}$$

$$\mu_{YTR} = \frac{V_{YTR}}{\Omega_{TR} R_{TR}}$$

$$\mu_{ZTR} = \frac{V_{ZTR}}{\Omega_{TR} R_{TR}}$$

$$\mu_{TR}^2 = \mu_{XTR}^2 + \mu_{YTR}^2$$

D-4 Tail Rotor Blade Pitch

$$\theta_{TR} = [\theta_{CTR} - T_{TR_{i-1}} (\frac{da_0}{dT}) \tan \delta_{3TR}]/57.3$$

D-5 Bailey Coefficients

$$t_{31} = \frac{B_{TR}^2}{2} + \frac{\mu_{TR}^2}{4}$$

$$t_{32} = \frac{B_{TR}^3}{3} + (\frac{B_{TR}}{2}) \mu_{TR}^2$$

$$t_{33} = \frac{B_{TR}^4}{4} + (\frac{B_{TR}^2}{4}) \mu_{TR}^2$$

D-6 Tail Rotor Downwash

$$G_{TR} = [\frac{a_{TR}}{2}][\frac{b_{NTR} c_{TR}}{\pi R_{TR}}]$$

$$D_{WTR_i} = \frac{G_{TR}[\mu_{ZTR} t_{31} + \theta_{TR} t_{32} + (\frac{\theta_{1TR}}{57.3}) t_{33}]}{2\left[\mu_{TR}^2 + \lambda_{TR_{i-1}}^2\right]^{1/2} + G_{TR} t_{31}}$$

D-7 Tail Rotor Inflow

$$\lambda_{TR_i} = \mu_{ZTR} - D_{WTR_i}$$

D-8 Tail Rotor Thrust

$$C_{THTR} = 2D_{WTR_i}\left[\mu_{TR}^2 + \lambda_{TR_i}^2\right]^{1/2}$$

$$T_{TR_i} = C_{THTR}\left[\frac{\Omega}{\Omega_T}\right]^2 \rho\pi R_{TR}^4 \Omega_{TR}^2 K_{TRBLK}$$

D-9 Tail Rotor Forces And Moments In Body Axes

$$X_{TR} = -\left(\frac{D}{q}\right)_{TR} \frac{1}{2} \rho (V_{XTR})^2$$

$$Y_{TR} = T_{TR} \sin \Gamma_{TR}$$

$$Z_{TR} = -T_{TR} \cos \Gamma_{TR}$$

$$L_{TR} = Y_{TR} h_{TR} - Z_{TR} b_{TR}$$

$$M_{TR} = Z_{TR} l_{TR} - X_{TR} h_{TR}$$

$$N_{TR} = -Y_{TR} l_{TR} + X_{TR} b_{TR}$$

where $\left(\frac{D}{q}\right)_{TR}$ is an input parameter used to approximately account for the tail rotor H force. It is an attempt to account for the blow back of the rotor resultant thrust vector with forward speed.

APPENDIX E

AUXILIARY ENGINE MODEL

E-1 Engine Geometry

$$l_E = (FS_{CG} - FS_E)/12$$

$$h_E = (WL_{CG} - WL_E)/12$$

$$b_E = BL_E/12$$

$$l_{EI} = (FS_{CG} - FS_{EI})/12$$

E-2 Engine Response

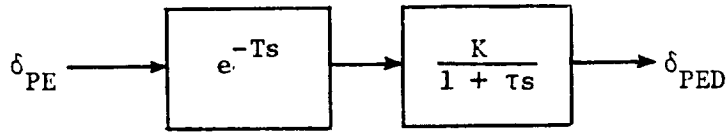

where

$K = 1$

$T = .05$ seconds

$\tau = 2$ seconds

E-3 Engine Thrust And Mass Flow - Normal Operation

$$T_P = 8200\left[\frac{\delta_{PEDP}}{100}\right]^2 - 4000\left[\frac{V_{XWF}}{a}\right] - 2400\left[\frac{V_{XWF}}{a}\right]\left[\frac{\delta_{PEDP}}{100}\right]$$

$$T_S = 8200\left[\frac{\delta_{PEDS}}{100}\right]^2 - 4000\left[\frac{V_{XWF}}{a}\right] - 2400\left[\frac{V_{XWF}}{a}\right]\left[\frac{\delta_{PEDS}}{100}\right]$$

$$M_{PEP} = \left[\frac{1}{32.2}\right]\left[320\left(\frac{\delta_{PEDP}}{100}\right) + 100\left(\frac{V_{XWF}}{a}\right)\right]$$

$$M_{PES} = \left[\frac{1}{32.2}\right]\left[320\left(\frac{\delta_{PEDS}}{100}\right) + 100\left(\frac{V_{XWF}}{a}\right)\right]$$

$$D_{WMP} = D_{WMS} = 0.$$

APPENDIX E

E-4 Engine Forces And Moments In Body Axes

$$X_E = (T_P + T_S)\cos i_E - (D_{WMS} + D_{WMP})$$

$$Y_E = -(M_{PEP} + M_{PES})V_{YWF}$$

$$Z_E = -(T_P + T_S)\sin i_E - (M_{PEP} + M_{PES})V_{ZWF}$$

$$L_E = (T_P - T_S)b_E \sin i_E + (M_{PEP} - M_{PES})b_E V_{ZWF}$$

$$+ (M_{PEP} + M_{PES})h_E V_{YWF}$$

$$M_E = X_E h_E + (T_P + T_S)l_E \sin i_E + (M_{PEP} + M_{PES})l_{EI} V_{ZWF}$$

$$N_E = (T_P - T_S)b_E \cos i_E - (M_{PEP} + M_{PES})l_{EI} V_{YWF}$$

$$- (D_{WMP} - D_{WMS})b_E$$

APPENDIX F

CONTROL SYSTEM MODEL

F-1 Longitudinal Control System

Longitudinal cyclic

$$B_{1S} = [K_{CTB}(X_B + B_{1S2}) + B_{1SL}]C_{B1S} + B_{1S1} + B_{1S3}$$

where

$$K_{CTB} = \left[\frac{B_{1SU} - B_{1SL}}{100}\right]$$

$$B_{1S1_i} = B_{1S1_{i-1}} + K_{TMB1S}\Delta t, \pm 20\% \text{ authority}$$

$$B_{1S3} = K_{BSTH0}[\theta_{CUFF} - T_{HOL}]$$

Flying tail with geared elevator

$$i_{HTS} = [K_{CTT}(X_B + \delta_{E2}) + i_{HTLL}]C_{DELE} + \frac{\delta_{E1}}{K_{EG}} + i_{HTW}$$

where

$$K_{CTT} = \left[\frac{i_{HTUL} - i_{HTLL}}{100}\right]$$

$$\delta_{E1_i} = \delta_{E1_{i-1}} + K_{TMELV}\Delta t, \pm 20\% \text{ authority}$$

$$K_{EG} = \left[\frac{(\delta_{EU} - \delta_{EL})}{(i_{HTUL} - i_{HTLL})}\right]$$

$$i_{HTW} = C_{TW} + K_{TW1}i_W$$

$$i_{HT} = K_{TLIN1}i_{HTS}$$

$$\delta_E = K_{EG}i_{HT}$$

F-2 Lateral Control System

Lateral cyclic

$$A_{1S} = [K_{CTA}(X_A + A_{1S2}) + A_{1SL}]C_{A1S} + A_{1S1} + A_{1S3}$$

where

$$K_{CTA} = [\frac{A_{1SU} - A_{1SL}}{100}]$$

$$A_{1S1_i} = A_{1S1_{i-1}} + K_{TMA1S}\Delta t, \pm 20\% \text{ authority}$$

$$A_{1S3} = K_{ASTHO}[\theta_{CUFF} - T_{HOL}]$$

Aileron

$$\delta_A = [K_{CTAIL}(X_A + \delta_{A2}) + \delta_{AL}]C_{DELA} + \delta_{A1}$$

where

$$K_{CTAIL} = [\frac{\delta_{AU} - \delta_{AL}}{100}]$$

$$\delta_{A1_i} = \delta_{A1_{i-1}} + K_{TMAIL}\Delta t, \pm 20\% \text{ authority}$$

Increments in forces and moments due to aileron deflection are obtained from starboard-side-only wind tunnel data. The following equations define the aileron gearing.

If $\delta_A \geq 0$.

$$\delta_{AP} = -\delta_A K_{AG}$$

$$\delta_{AS} = \delta_A K_{AG} K_{ASAIL}$$

If $\delta_A < 0.$

$$\delta_{AP} = -\delta_A K_{AG} K_{ASAIL}$$

$$\delta_{AS} = \delta_A K_{AG}$$

where δ_{AP} denotes port aileron deflection

δ_{AS} denotes starboard aileron deflection.

F-3 Directional Control System

Tail rotor

$$\theta_{CTR} = [K_{CTTR}(X_P + T_{TR2}) + T_{HRU} + T_{TR3}]C_{TTR} + T_{TR1}$$

where

$$K_{CTTR} = -[\frac{T_{HRU} - T_{HRL}}{100}]$$

$$T_{TR1_i} = T_{TR1_{i-1}} + K_{TMTTR}\Delta t, \pm 20\% \text{ authority}$$

$$T_{TR3} = K_{TRTH0}[\theta_{CUFF} - T_{H0L}]$$

Note: T_{TR1} set to 0 for Langley simulation.

Rudder

$$\delta_R = K_{\delta_R}\{[K_{CTRUD}(X_P + \delta_{R2}) + \delta_{RL} + \delta_{R3}]C_{DELR} + \delta_{R1}\}$$

where

$$K_{\delta_R} = 1.11111$$

$$K_{CTRUD} = [\frac{\delta_{RU} - \delta_{RL}}{100}]$$

$$\delta_{R1_i} = \delta_{R1_{i-1}} + K_{TMRUD}\Delta t, \pm 20\% \text{ authority}$$

$$\delta_{R3} = K_{RDTH0}[\theta_{CUFF} - T_{HOL}]$$

Note: δ_{R1} set to 0 for Langley simulation.

F-4 Collective Control System

$$\theta_{CUFF} = K_{CTC}X_C + T_{HOL}$$

where

$$K_{CTC} = [\frac{T_{HOU} - T_{HOL}}{100}]$$

F-5 CPU Control Levers

$$CPU_{LON} = K_{CPULG}X_{CPULG} + CPU_{LON1}$$

where

$$CPU_{LON1_i} = CPU_{LON1_{i-1}} + B_{CPULG}\Delta t$$

$$CPU_{LAT} = K_{CPULT}X_{CPULT} + CPU_{LAT1}$$

where

$$CPU_{LAT1_i} = CPU_{LAT1_{i-1}} + B_{CPULT}\Delta t$$

$$CPU_{DIR} = K_{CPUDR}X_{CPUDR} + CPU_{DIR1}$$

where

$$CPU_{DIR1_i} = CPU_{DIR1_{i-1}} + B_{CPUDR}\Delta t$$

$CPU_{LON}, CPU_{LAT}, CPU_{DIR}$ range from 0% to 100%

F-6 Control Phasing Units

Longitudinal Cyclic

(a) if $CPU_{LON} < DHCPU$, $C_{B1S} = 0.$

(b) if $DHCPU \leq CPU_{LON} \leq MHCPU$,

$$C_{B1S} = \left[\frac{CPU_{LON} - DHCPU}{MHCPU - DHCPU}\right]$$

(c) if $MHCPU < CPU_{LON}$, $C_{B1S} = 1.0$

Lateral Cyclic

(a) if $CPU_{LAT} < DHCPU$, $C_{A1S} = 0.$

(b) if $DHCPU \leq CPU_{LAT} \leq MHCPU$,

$$C_{A1S} = \left[\frac{CPU_{LAT} - DHCPU}{MHCPU - DHCPU}\right]$$

(c) if $MHCPU < CPU_{LAT}$, $C_{A1S} = 1.0$

Elevator

(a) if $CPU_{LON} < DFCPU$,

$$C_{DELE} = HSCPU + \left[\frac{1.0 - HSCPU}{DFCPU}\right]CPU_{LON}$$

(b) if $DFCPU \leq CPU_{LON} \leq MFCPU$, $C_{DELE} = 1.0$

(c) if $MFCPU < CPU_{LON}$,

$$C_{DELE} = 1.0 - \left[\frac{CPU_{LON} - MFCPU}{100. - MFCPU}\right]$$

Aileron

(a) if $CPU_{LAT} < DFCPU$,

$$C_{DELA} = HSCPU + \left[\frac{1.0 - HSCPU}{DFCPU}\right]CPU_{LAT}$$

(b) if $DFCPU \leq CPU_{LAT} \leq MFCPU$, $C_{DELA} = 1.0$

(c) if $MFCPU < CPU_{LAT}$,

$$C_{DELA} = 1.0 - \left[\frac{CPU_{LAT} - MFCPU}{100. - MFCPU}\right]$$

Tail rotor

if $0. \leq CPU_{DIR} \leq 100.$,

$$C_{TTR} = \frac{CPU_{DIR}}{100.}$$

Rudder

if $0. \leq CPU_{DIR} \leq 100.$,

$$C_{DELR} = \left[1 - \frac{CPU_{DIR}}{100.}\right]$$

F-7 Wing Tilt System

$$i_W = K_{CTW} X_{WNG} + i_{WL}$$

where

$$K_{CTW} = \left[\frac{i_{WU} - i_{WL}}{100}\right]$$

Wing tilt rate limit

$$\frac{\Delta i_W}{\Delta t} < WRL$$

F-8 Drag Brake System

$$\delta_{DB} = K_{CTDB} X_{DRAG} + \delta_{DBL}$$

where

$$K_{CTDB} = \left[\frac{\delta_{DBU} - \delta_{DBL}}{100}\right]$$

F-9 Flap System

$$\delta_F = K_{CTF} X_{FLAP} + \delta_{FL}$$

where

$$K_{CTF} = \left[\frac{\delta_{FU} - \delta_{FL}}{100}\right]$$

APPENDIX F

F-10 Auxiliary Engine Control System

$$\delta_{PE} = K_{CTPE} X_{XRPMJT} + \delta_{PEL} + \delta_{PE1}$$

where

$$K_{CTPE} = \left[\frac{\delta_{PEU} - \delta_{PEL}}{100}\right]$$

$$\delta_{PE1_i} = \delta_{PE1_{i-1}} + K_{TMJET}\Delta t$$

The above equations hold for both port and starboard engines.

F-11 Rotor Speed Control System

$$\delta_{RE} = K_{CTRE} X_{PRE} + \delta_{REL} + \delta_{RE1}$$

where

$$K_{CTRE} = \left[\frac{\delta_{REU} - \delta_{REL}}{100}\right]$$

$$\delta_{RE1_i} = \delta_{RE1_{i-1}} + K_{TMRE}\Delta t$$

Rotor Governor And Speed Schedule

$$K_{RPM} = \frac{\delta_{RE}}{1 + T_{RG}s} \quad , \quad \text{governor setting}$$

$$\frac{\Omega}{\Omega_T} = K_{RPM} \quad \text{unless rotor degree of freedom is released}$$

(a) if $(1.69\ V_{COMMAND} + \Omega_T R_{MR}) \leq 0.9a$

$$K_{RPM} = 1.0$$

(b) if $(1.69\ V_{COMMAND} + \Omega_T R_{MR}) > 0.9a$

$$K_{RPM} = \left[\frac{0.9a - 1.69\ V_{COMMAND}}{\Omega_T R_{MR}}\right]$$

Note: Normal governed operation inhibits the rotor degree of freedom, $Q = Q_E$

F-12 Stability Augmentation System

Pitch

$$B_{1S2}(s) = \delta_{E2}(s)$$

$$\delta_{E2}(s) = 57.3\ qs \left\{ \frac{[(RKQ)(TKQ)]s + (RKQ + LRKQ)}{[(TKQ)s + 1][s + W_{OE}]} \right\}$$

Roll

$$A_{1S2}(s) = \delta_{A2}(s)$$

$$\delta_{A2}(s) = 57.3\ p \left\{ \frac{[(RKP)(TKP)]s + (RKP + LRKP)}{[(TKP)s + 1]} \right\}$$

Yaw

$$T_{TR2}(s) = \delta_{R2}(s)$$

$$\delta_{R2}(s) = -57.3rs \left\{ \frac{RKR}{s + W_{OR}} \right\}$$

where

RKQ = 1.25	RKP = 0.50 (helicopter), 1.00 (fixed wing)
TKQ = 1.00	TKP = 6.50
LRKQ = 2.50	LRKP = 2.60 (helicopter), 2.00 (fixed wing)
W_{OE} = 0.25	
RKR = 1.00	
W_{OR} = 0.50	

APPENDIX G

GENERAL EQUATIONS

G-1 Total Forces And Moments In Body Axes

$$X_{BODY} = X_E + X_{MR} + X_T + X_{TR} + X_{WF}$$

$$Y_{BODY} = Y_E + Y_{MR} + Y_T + Y_{TR} + Y_{WF}$$

$$Z_{BODY} = Z_E + Z_{MR} + Z_T + Z_{TR} + Z_{WF}$$

$$L_{BODY} = L_E + L_{MR} + L_T + L_{TR} + L_{WF}$$

$$M_{BODY} = M_E + M_{MR} + M_T + M_{TR} + M_{WF}$$

$$N_{BODY} = N_E + N_{MR} + N_T + N_{TR} + N_{WF}$$

G-2 Body Axes Accelerations

$$\dot{V}_{XB} = X_{BODY}\left(\frac{g}{W_{bd}}\right) + rV_{YB} - qV_{ZB} - g \sin \theta_{BODY}$$

$$\dot{V}_{YB} = Y_{BODY}\left(\frac{g}{W_{bd}}\right) - rV_{XB} + pV_{ZB} + g \cos \theta_{BODY} \sin \phi_{BODY}$$

$$\dot{V}_{ZB} = Z_{BODY}\left(\frac{g}{W_{bd}}\right) + qV_{XB} - pV_{YB} + g \cos \theta_{BODY} \cos \phi_{BODY}$$

$$\dot{p} = [L_{BODY} + (I_Y - I_Z)qr + I_{XZ}(\dot{r} + pq)]/I_X$$

$$\dot{q} = [M_{BODY} + (I_Z - I_X)pr + I_{XZ}(r^2 - p^2)]/I_Y$$

$$\dot{r} = [N_{BODY} + (I_X - I_Y)pq + I_{XZ}(\dot{p} - rq)]/I_Z$$

APPENDIX G

G-3 Euler Angle Rates

$$\dot{\phi}_{BODY} = [p + \dot{\psi}_{BODY} \sin \theta_{BODY}]57.3$$

$$\dot{\theta}_{BODY} = [q \cos \phi_{BODY} - r \sin \phi_{BODY}]57.3$$

$$\dot{\psi}_{BODY} = \left[\frac{r \cos \phi_{BODY} + q \sin \phi_{BODY}}{\cos \theta_{BODY}}\right] 57.3$$

G-4 Body Axes To Inertial Axes Transformation Matrix

$$[A_{BI}] =$$

$$\begin{bmatrix} \cos\theta_{BODY}\cos\psi_{BODY}, & \sin\theta_{BODY}\sin\phi_{BODY}\cos\psi_{BODY}-\cos\phi_{BODY}\sin\psi_{BODY}, & \sin\theta_{BODY}\cos\phi_{BODY}\cos\psi_{BODY}+\sin\phi_{BODY}\sin\psi_{BODY} \\ \cos\theta_{BODY}\sin\psi_{BODY}, & \sin\theta_{BODY}\sin\phi_{BODY}\sin\psi_{BODY}+\cos\phi_{BODY}\cos\psi_{BODY}, & \sin\theta_{BODY}\cos\phi_{BODY}\sin\psi_{BODY}-\sin\phi_{BODY}\cos\psi_{BODY} \\ -\sin\theta_{BODY}, & \cos\theta_{BODY}\sin\phi_{BODY}, & \cos\theta_{BODY}\cos\phi_{BODY} \end{bmatrix}$$

G-5 Pilot Station Geometry

Written for pilot's head at starboard station.

$$l_{PS} = (FS_{CG} - FS_{PS})/12$$

$$h_{PS} = (WL_{CG} - WL_{PS})/12$$

$$b_{PS} = BL_{PS}/12$$

G-6 Pilot Station Accelerations

$$a_{XP} = X_{BODY}(\frac{g}{W_{bd}}) - l_{PS}(q^2 + r^2) + h_{PS}(pr + \dot{q}) + b_{PS}(pq - \dot{r})$$

$$a_{YP} = Y_{BODY}(\frac{g}{W_{bd}}) + l_{PS}(pq + \dot{r}) + h_{PS}(qr - \dot{p}) - b_{PS}(p^2 + r^2)$$

$$a_{ZP} = Z_{BODY}(\frac{g}{W_{bd}}) + l_{PS}(pr - \dot{q}) - h_{PS}(p^2 + q^2) + b_{PS}(qr + \dot{p})$$

G-7 Pilot Station Velocities

$$V_{XP} = V_{XB} + qh_{PS} - rb_{PS}$$

$$V_{YP} = V_{YB} + rl_{PS} - ph_{PS}$$

$$V_{ZP} = V_{ZB} - ql_{PS} + pb_{PS}$$

REFERENCES

1. Letchworth, Robert, Lt. Col.; and Condon, Gregory W.: Rotor Systems Research Aircraft (RSRA). AGARD Flight Mechanics Panel Symposium (Valloire, France), June 1975.

2. Mechtly, E. A.: The International System of Units. Physical Constants and Conversion Factors. Second Revision. NASA SP-7012, 1973.

3. Houck, Jacob A.; and Bowles, Roland L.: Effects of Rotor Model Degradation on the Accuracy of Rotorcraft Real-Time Simulation. NASA TND-8378, 1976.

4. Houck, Jacob Albert: Computational Aspects of Real-Time Simulation of Rotary Wing Aircraft. M.S. Thesis, George Washington Univ., 1976. (Available as NASA CR-147932.)

5. Cooper, D. E.; and Howlett, J.J.: Ground Based Helicopter Simulation. Symposium on Status of Testing and Model Techniques for V/STOL Aircraft (Essington, Pa), American Helicopter Soc., Oct. 1972.

6. Bailey, F. J., Jr.: A Simplified Theoretical Method of Determining the Characteristics of a Lifting Rotor in Forward Flight. NACA REP. NO. 716, 1941.

7. McFarland, Richard E.: A Standard Kinematic Model for Flight Simulation at NASA-AMES. NASA CR-2497, 1975.

TABLE 1.- RSRA Simulation Input Parameters.

(a) Main Rotor

BL_{MR}	0.	$K_{\alpha 1}$	-0.146
B_{MR}	0.97	$K_{\alpha 2}$	-0.005733
b_{NMR}	5.	K_{β}	0.
b_S	5.	$K_{\beta}^{\cdot}$	0.
c_R	1.52	$K_{\lambda}^{'}$	6.
c_T	1.52	m_b	91.
c_{75}	1.52	n_S	5
DMPARM	7.375	R_{MR}	31.
e	1.05	WL_{MR}	302.
e'	5.4	W_b	276.
F_{δ}	0.	Δ_{SP}	-10.
FS_{MR}	300.	ΔC_D	0.002
I_R	880.	δ_{AFT}	-0.34904
I_b	1824.	δ_{FWD}	0.05236
i_{θ}	-2.	δ_3	0.
i_{ϕ}	0.	θ_1	-8.
$K_{\alpha 0}$	0.581	Ω_T	22.1416

(b) Tail Rotor

a_{TR}	5.73	WL_{TR}	276.5
B_{TR}	0.92	Γ_{TR}	90.
BL_{TR}	24.	δ_{3TR}	45.
b_{NTR}	5.	θ_{1TR}	0.
c_{TR}	0.612	Ω_{TR}	130.4
FS_{TR}	743.	$(\frac{D}{q})_{TR}$	2.
K_{TRBLK}	0.88	(da_0/dT)	0.00129
R_{TR}	5.32		

TABLE 1.- Continued.

(c) Tail

EK_{TR}	0.	i_{HTU}	2.5(HELICOPTER) 0. (FIXED WING)
FS_{DB}	728.		
FS_{HT}	660.	WL_{DB}	184.
FS_{HTU}	847.	WL_{HT}	184.
FS_{VT}	812.2 (BASIC)	WL_{HTU}	363.
		WL_{VT}	293.

(d) Engine

BL_E	82.	FS_{EI}	221.
D_{WMP}	0.	i_E	-3.5
D_{WMS}	0.	WL_E	229.
FS_E	275.		

(e) Body

Configuration	Helicopter		Compound		Fixed Wing	
Center of Gravity	FWD	AFT	FWD	AFT	FWD	AFT
W	19600.		26200.		25165.	
S_W	-		370.		370.	
FS_{CG}	296.0	313.5	296.1	308.3	296.1	309.1
WL_{CG}	230.4	230.8	224.5	225.3	221.4	222.1
I_X	8691.	8564.	25596.	25367.	24280.	24105.
I_Y	95886.	96918.	106529.	107822.	105225.	106520.
I_Z	89492.	90698.	114536.	116093.	114519.	116034.
I_{XZ}	6849.	3377.	4845.	1714.	4785.	1848.

TABLE 1.- Continued.

(f) Controls

A_{1SL}	-8.	K_{TMJET}	5.
A_{1SU}	8.	K_{TMRE}	5.
B_{CPUDR}	5.	K_{TMRUD}	0.
B_{CPULG}	5.	K_{TMTTR}	0.
B_{CPULT}	5.	K_{TRTHO}	0.78
B_{1SL}	-11.	K_{TW1}	0.167
B_{1SU}	15.	MFCPU	66.7
C_{TW}	0.5	MHCPU	66.7
DFCPU	33.3	T_{HRL}	-6.5
DHCPU	33.3	T_{HRU}	25.
HSCPU	0.5	T_{HOL}	5.2
i_{HTLL}	-8.	T_{HOU}	20.4
i_{HTUL}	8.	T_{RG}	3.0
i_{WL}	-9.	WRL	1.6
i_{WU}	15.	δ_{AL}	-10.
K_{AG}	1.9	δ_{AU}	10.
K_{ASAIL}	2.	δ_{DBL}	0.
K_{ASTHO}	-0.19	δ_{DBU}	58.
K_{BSTHO}	0.	δ_{EL}	-15.
K_{CPUDR}	1.	δ_{EU}	15.
K_{CPULG}	1.	δ_{FL}	0.
K_{CPULT}	1.	δ_{FU}	30.
K_{RDTHO}	0.5	δ_{PEL}	24.
K_{TLIN1}	1.	δ_{PEU}	110.
K_{TMAIL}	1.25	δ_{REL}	70.
K_{TMA1S}	5.	δ_{REU}	110.
K_{TMB1S}	5.	δ_{RL}	-25.
K_{TMELV}	0.625	δ_{RU}	25.

TABLE 1.- Concluded.

(g) Miscellaneous Parameters

BL_{PS}	20.			FS_{WT}	309.
FS_{PS}	133.			WL_{WT}	223.
WL_{PS}	233.				

TABLE 2.- Wing-Fuselage Induced Velocities at the Rotor.

(a) V_{NOW} $(r/R_{MR}, \psi_{MAP})$ =

r/R_{MR} \ ψ_{MAP}	0	30	60	90	120	150	180
.1	.560	.390	-.053	-.117	-.495	-1.150	-1.180
.2	1.350	.650	.330	-.042	-.360	-.750	-2.370
.3	1.060	.740	.300	-.059	-.330	-.870	-2.120
.4	.690	.540	.300	-.067	-.280	-.670	-1.550
.5	.540	.410	.240	-.076	-.220	-.560	-1.570
.6	.420	.360	.180	-.065	-.160	-.436	-1.310
.7	.360	.280	.130	-.040	-.112	-.310	-.880
.8	.280	.210	.110	-.015	-.074	-.207	-.530
.9	.200	.160	.074	-.003	-.050	-.140	-.310
1.0	.140	.120	.055	.005	-.034	-.094	-.186

(b) V_{TOW} $(r/R_{MR}, \psi_{MAP})$ =

r/R_{MR} \ ψ_{MAP}	0	30	60	90	120	150	180
.1	0	-1.100	-1.510	-1.530	-1.486	-1.141	0
.2	0	-1.180	-1.040	-.947	-1.000	-1.160	0
.3	0	-.684	-.730	-.732	-.716	-1.020	0
.4	0	-.386	-.510	-.548	-.502	-.753	0
.5	0	-.250	-.364	-.414	-.360	-.608	0
.6	0	-.165	-.266	-.315	-.265	-.475	0
.7	0	-.114	-.205	-.240	-.200	-.341	0
.8	0	-.082	-.154	-.178	-.153	-.236	0
.9	0	-.077	-.120	-.133	-.120	-.163	0
1.0	0	-.059	-.093	-.103	-.094	-.114	0

TABLE 3.- Rotor Segment Aerodynamic Coefficients.

Lift Coefficient

C_{LY} (α_{TRANS}, M) =

α_{TRANS} \ M	0	.1	.2	.3	.4	.5	.6	.7	.8	.9	1.0
0	0	0	0	0	0	0	0	0	0	0	0
2	.166	.188	.202	.214	.210	.234	.242	.300	.175	.158	.200
4	.332	.376	.404	.430	.442	.467	.484	.545	.350	.317	.400
6	.498	.565	.606	.645	.664	.700	.725	.690	.500	.475	.600
8	.665	.753	.808	.860	.885	.910	.900	.750	.630	.635	.800
10	.830	.940	1.010	1.075	1.070	.980	.870	.770	.730	.800	.820
12	.880	1.035	1.140	1.240	1.080	.915	.850	.760	.760	.775	.770
14	.679	.865	1.070	1.260	.970	.850	.830	.760	.760	.760	.760
16	.640	.735	.840	.980	.825	.830	.800	.800	.800	.800	.800
18	.640	.710	.770	.855	.750	.770	.780	.850	.850	.850	.850
20	.670	.715	.760	.804	.720	.730	.790	.900	.900	.900	.900
22	.710	.740	.770	.814	.750	.775	.840	.950	.950	.950	.950
24	.765	.790	.820	.860	.805	.870	.920	1.000	1.000	1.000	1.000
26	.835	.860	.890	.910	.855	.950	.990	1.040	1.040	1.040	1.040
28	.925	.940	.970	.980	.960	1.020	1.030	1.050	1.050	1.050	1.050
30	1.060	1.060	1.060	1.060	1.060	1.060	1.060	1.060	1.060	1.060	1.060

For $30^{\circ} \leq \alpha_{TRANS} \leq 182^{\circ}$, C_{LY} (α_{TRANS}) =

α_{TRANS}	30	38	46	54	62	70	78	86	94	102	110
C_{LY}	1.060	1.120	1.160	1.090	.920	.700	.450	.160	-.160	-.380	-.600
α_{TRANS}	118	126	134	142	150	158	166	174	182		
C_{LY}	-.760	-.930	-1.060	-1.170	-.950	-.790	-.720	-.650	.220		

TABLE 3.- Concluded.

Drag Coefficient

C_{DY} (α_{TRANS}, M) =

α_{TRANS} \ M	0	.1	.2	.3	.4	.5	.6	.7	.8	.9	1.0
0	.0085	.0074	.0070	.0070	.0070	.0072	.0074	.0078	.0190	.0650	.1500
2	.0088	.0076	.0072	.0072	.0072	.0075	.0082	.0100	.0380	.0900	.1750
4	.0099	.0083	.0078	.0078	.0080	.0087	.0101	.0300	.0740	.1260	.2100
6	.0129	.0100	.0093	.0093	.0100	.0114	.0220	.0630	.1260	.1740	.2500
8	.0168	.0129	.0124	.0116	.0134	.0250	.0600	.1120	.1750	.2200	.2800
10	.0220	.0168	.0160	.0150	.0200	.0600	.1140	.1560	.2180	.2580	.3050
12	.0350	.0300	.0250	.0250	.0600	.1250	.1640	.1940	.2490	.2850	.3250
14	.0600	.0550	.0500	.0500	.1050	.1800	.2130	.2320	.2800	.3110	.3480
16	.1050	.1050	.1050	.1050	.1650	.2300	.2580	.2720	.3120	.3400	.3700
18	.1900	.1900	.1900	.1900	.2250	.2700	.2950	.3110	.3460	.3680	.3920
20	.2920	.2920	.2920	.2920	.2920	.3150	.3320	.3540	.3820	.4000	.4240
22	.3550	.3550	.3550	.3550	.3550	.3550	.3720	.3970	.4220	.4350	.4520
24	.4000	.4000	.4000	.4000	.4000	.4000	.4180	.4440	.4630	.4720	.4900
26	.4600	.4600	.4600	.4600	.4600	.4600	.4700	.4920	.5100	.5150	.5300
28	.5400	.5400	.5400	.5400	.5400	.5400	.5400	.5500	.5600	.5620	.5700
30	.6250	.6250	.6250	.6250	.6250	.6250	.6250	.6250	.6250	.6250	.6250

For $30^{\circ} \leq \alpha_{TRANS} \leq 182^{\circ}$, C_{DY} (α_{TRANS}) =

α_{TRANS}	30	38	46	54	62	70	78	86	94	102	110
C_{DY}	.6250	.9200	1.2400	1.5010	1.7600	1.9200	2.0100	2.0600	2.0800	2.0400	1.9100

α_{TRANS}	118	126	134	142	150	158	166	174	182
C_{DY}	1.7400	1.5300	1.3000	1.0000	.7000	.4300	.2800	.0650	.0250

TABLE 4.- Rotor Lag Damper Data.

(a) $F_{\delta} = 0$ for RSRA

(b) $F'_{\dot{\delta}} =$

$\lvert\dot{\delta}\rvert$	$F'_{\dot{\delta}}$	$\lvert\dot{\delta}\rvert$	$F'_{\dot{\delta}}$
0	0	.42	2307
.02	175	.44	2314
.04	460	.46	2322
.06	760	.48	2329
.08	1240	.50	2337
.10	1780	.52	2344
.12	2100	.54	2350
.14	2160	.56	2359
.16	2170	.58	2366
.18	2185	.60	2374
.20	2200	.62	2381
.22	2215	.64	2388
.24	2225	.66	2396
.26	2235	.68	2403
.28	2242	.70	2418
.30	2255	.72	2433
.32	2265	.74	2448
.34	2275	.76	2462
.36	2280	.78	2477
.38	2290	.80	2492
.40	2300	.82	2507

TABLE 5.- Rotor Induced Velocities on the Wing-Fuselage.

χ	$EK_{WFX}(\chi)$	$EK_{WFZ}(\chi)$
-20	0	.47
-10	0	.70
0	0	.89
10	.21	1.06
20	.45	1.17
30	.73	1.22
40	1.02	1.21
50	1.32	1.15
60	1.52	1.03
70	.70	.76
80	.19	.30
90	0	0
100	0	0

TABLE 6.- Helicopter Tail-Off Lift Data.

(a) $\frac{L}{q}(\alpha_{WF})$ =

α_{WF}	$\frac{L}{q}(\alpha_{WF})$
-36	-13.75
-32	-14.75
-28	-15.00
-24	-14.75
-20	-13.50
-16	-10.20
-12	-7.00
-8	-4.25
-4	-1.25
0	1.70
4	4.50
8	7.00
12	10.00
16	12.80
20	15.60
24	18.00
28	18.75
32	19.00
36	18.50

For $-90^{\circ} \leq \alpha_{WF} < -36^{\circ}$

$$\frac{L}{q}(\alpha_{WF}) = -13.75 - .2546\,(\alpha_{WF} + 36)$$

For $36^{\circ} < \alpha_{WF} \leq 90^{\circ}$

$$\frac{L}{q}(\alpha_{WF}) = 18.50 - .3426\,(\alpha_{WF} - 36)$$

(b) $\frac{L}{q}(\psi_{WF}) = 0.$

TABLE 7.- Helicopter Tail-Off Drag Data.

(a) $\frac{D}{q}(\alpha_{WF})$ =

α_{WF}	$\frac{D}{q}(\alpha_{WF})$
-30	24.0
-25	20.5
-20	17.8
-15	15.4
-10	13.8
- 5	13.7
0	14.2
5	15.5
10	16.5
15	18.5
20	21.2
25	25.0
30	29.0

For $-90^{o} \leq \alpha_{WF} < -30^{o}$

$$\frac{D}{q}(\alpha_{WF}) = 91.4 \sin^2 (1.5 (\alpha_{WF} + 30)) + 24.0$$

For $30^{o} < \alpha_{WF} \leq 90^{o}$

$$\frac{D}{q}(\alpha_{WF}) = 86.4 \sin^2 (1.5 (\alpha_{WF} - 30)) + 29.0$$

(b) $\frac{D}{q}(\psi_{WF})$ =

For $-20^{o} \leq \psi_{WF} \leq 20^{o}$

$$\frac{D}{q}(\psi_{WF}) = 768 \sin^2 (\psi_{WF}/2) - 2.2178 \sin (\psi_{WF}/2)$$

For $-90^{o} \leq \psi_{WF} < -20^{o}$ and $20^{o} < \psi_{WF} \leq 90^{o}$

$$\frac{D}{q}(\psi_{WF}) = 235 \sin^2 (1.29(|\psi_{WF}| - 20)) + 22.77$$

TABLE 8.- Helicopter Tail-Off Pitching Moment Data.

(a) $\frac{M_M}{\bar{q}}(\alpha_{WF})$ =

α_{WF}	$\frac{M_M}{\bar{q}}(\alpha_{WF})$
-40	-310
-32	-360
-24	-400
-16	-370
- 8	-235
0	- 73
8	100
16	300
24	480
32	535
40	480

For $-90^{o} \leq \alpha_{WF} < -40^{o}$

$$\frac{M_M}{\bar{q}}(\alpha_{WF}) = -310. - 6.2\ (\alpha_{WF} + 40)$$

For $40^{o} < \alpha_{WF} \leq 90^{o}$

$$\frac{M_M}{\bar{q}}(\alpha_{WF}) = 480. - 9.6\ (\alpha_{WF} - 40)$$

TABLE 8.- Concluded.

(b) $\frac{M_M}{\bar{q}}(\psi_{WF})$ =

ψ_{WF}	$\frac{M_M}{\bar{q}}(\psi_{WF})$
-30	100
-25	104
-20	98
-15	74
-10	49
- 5	25
0	0
5	25
10	49
15	74
20	93
25	104
30	100

For $-90^\circ \leq \psi_{WF} < -30^\circ$ and $30^\circ < \psi_{WF} \leq 90^\circ$

$$\frac{M_M}{\bar{q}}(\psi_{WF}) = 1.67\ (90 - |\psi_{WF}|)$$

TABLE 9.- Helicopter Tail-Off Side Force Data.

$$\frac{Y}{\bar{q}} (\alpha_{WF}, \psi_{WF}) =$$

ψ_{WF} \ α_{WF}	-10	0	10
-35	-80.0	-80.0	-80.0
-30	-88.0	-84.0	-88.0
-25	-92.0	-85.0	-94.0
-20	-84.4	-81.5	-96.2
-15	-62.5	-57.9	-74.3
-10	-40.5	-37.9	-51.7
- 5	-21.5	-17.2	-26.8
0	0.0	0.0	0.0
5	26.1	22.7	27.5
10	45.5	41.2	53.5
15	69.6	61.0	74.0
20	94.3	84.2	96.1
25	93.5	86.0	94.0
30	86.0	85.0	87.0
35	80.0	80.0	80.0

For $-90^\circ \leq \psi_{WF} < -35^\circ$

$$\frac{Y}{\bar{q}} (\alpha_{WF}, \psi_{WF}) = -80.025 - 1.455 (\psi_{WF} + 35)$$

For $35^\circ < \psi_{WF} \leq 90^\circ$

$$\frac{Y}{\bar{q}} (\alpha_{WF}, \psi_{WF}) = 80.025 - 1.455 (\psi_{WF} - 35)$$

TABLE 10.- Helicopter Tail-Off Rolling Moment Data.

$$\frac{L_M}{\bar{q}}(\alpha_{WF}, \psi_{WF}) =$$

ψ_{WF} \ α_{WF}	-90 to -10	0	10 to 90
-50	0	0	0
-40	29	57	65
-30	22	65	102
-20	12	50	88
-10	6	25	44
0	0	0	0
10	-6	-25	-44
20	-12	-50	-88
30	-22	-65	-102
40	-29	-57	-65
50	0	0	0

For $-90^\circ \leq \psi_{WF} < -50^\circ$

$$\frac{L_M}{\bar{q}}(\alpha_{WF}, \psi_{WF}) = 5\ (\psi_{WF} + 50)$$

For $50^\circ < \psi_{WF} \leq 90^\circ$

$$\frac{L_M}{\bar{q}}(\alpha_{WF}, \psi_{WF}) = 5\ (\psi_{WF} - 50)$$

TABLE 11.- Helicopter Tail-Off Yawing Moment Data.

$$\frac{N_M}{\bar{q}}(\alpha_{WF}, \psi_{WF}) =$$

ψ_{WF} \ α_{WF}	-90 to -10	0	10 to 90
-40	-400.0	-400.0	-400.0
-36	-500.0	-500.0	-470.0
-32	-600.0	-600.0	-515.0
-28	-700.0	-700.0	-520.0
-24	-710.0	-710.0	-500.0
-20	-676.0	-676.0	-447.0
-16	-560.0	-560.0	-310.0
-12	-440.0	-440.0	-190.0
-8	-290.0	-300.0	-70.0
-4	-140.0	-140.0	-2.6
0	-25.0	44.0	42.0
4	155.0	190.0	70.0
8	280.0	330.0	150.0
12	430.0	480.0	265.0
16	560.0	620.0	400.0
20	694.0	726.0	517.0
24	725.0	755.0	545.0
28	720.0	735.0	555.0
32	635.0	640.0	535.0
36	520.0	520.0	490.0
40	400.0	400.0	400.0

For $-90^\circ \leq \psi_{WF} < -40^\circ$

$$\frac{N_M}{\bar{q}}(\alpha_{WF}, \psi_{WF}) = -20\ (\psi_{WF} + 40) - 400$$

For $40^\circ < \psi_{WF} \leq 90^\circ$

$$\frac{N_M}{\bar{q}}(\alpha_{WF}, \psi_{WF}) = -20\ (\psi_{WF} - 40) + 400$$

TABLE 12.- Fixed Wing Tail-Off Lift Data.

(a) $\frac{L}{\bar{q}}(\alpha_W, i_W)$ =

α_W \ i_W	-9	-1	7	15
-40	-199.0	-194.0	-188.0	-183.0
-38	-213.0	-201.0	-197.0	-191.0
-36	-234.0	-216.0	-205.0	-199.0
-34	-249.0	-223.0	-213.0	-207.0
-32	-265.0	-233.0	-221.0	-215.0
-30	-282.0	-244.0	-228.0	-223.0
-28	-300.0	-270.0	-245.0	-231.0
-26	-320.0	-309.0	-303.0	-246.0
-24	-338.0	-338.0	-338.0	-303.0
-22	-348.0	-348.0	-348.0	-340.0
-20	-342.0	-342.0	-342.0	-347.0
-18	-330.0	-330.0	-330.0	-340.0
-16	-306.0	-306.0	-314.0	-326.0
-14	-268.0	-274.0	-287.0	-308.0
-12	-212.0	-226.0	-241.0	-282.0
-10	-156.0	-176.0	-204.0	-240.0
-8	-102.0	-127.0	-157.0	-201.0
-6	-42.0	-75.8	-115.0	-162.0
-4	14.0	-22.4	-75.5	-119.0
-2	71.0	30.9	-29.0	-64.0
0	125.0	83.2	25.8	-10.0

TABLE 12.- Continued.

$\frac{L}{q}(\alpha_W, i_W) =$

α_W \ i_W	-9	-1	7	15
2	185.0	142.0	81.0	46.0
4	242.0	203.0	136.0	100.0
6	298.0	257.0	194.0	153.0
8	348.0	307.0	250.0	207.0
10	402.0	360.0	304.0	264.0
12	453.0	404.0	349.0	316.0
14	503.0	453.0	414.0	357.0
16	553.0	500.0	464.0	400.0
18	538.0	520.0	492.0	431.0
20	518.0	521.0	500.0	425.0
22	499.0	502.0	508.0	438.0
24	478.0	483.0	518.0	450.0
26	460.0	465.0	529.0	454.0
28	440.0	446.0	538.0	449.0
30	421.0	426.0	543.0	445.0
32	401.0	408.0	548.0	465.0
34	382.0	389.0	506.0	485.0
36	362.0	371.0	452.0	476.0
38	342.0	352.0	397.0	414.0
40	323.0	332.0	341.0	350.0

For $-90^\circ \leq \alpha_W < -40^\circ$

$$\frac{L}{q}(\alpha_W, i_W) = -347.4 - 3.86(\alpha_W - .174\, i_W)$$

For $40^\circ < \alpha_W \leq 90^\circ$

$$\frac{L}{q}(\alpha_W, i_W) = 599.4 - 6.66\,(\alpha_W - .174\, i_W)$$

TABLE 12.- Continued.

(b) $\frac{L}{\bar{q}}$ (ψ_{WF}, i_W) =

ψ_{WF} \ i_W	-9	-1	7	15
-90	61.0	22.1	7.2	-34.0
-20	61.0	22.1	7.2	-34.0
-18	54.0	19.8	6.6	-22.0
-16	47.0	17.7	6.3	-11.5
-14	39.5	15.1	5.0	-4.9
-12	32.0	12.4	3.5	-3.2
-10	24.0	9.8	1.7	-1.5
-8	16.0	7.8	3.1	2.0
-6	7.0	5.7	6.0	5.8
-4	1.9	3.3	5.4	5.8
-2	0.8	0.8	2.4	2.8
0	0	0	0	0
2	1.0	-0.8	-1.2	-1.0
4	4.5	-1.7	-3.0	-5.0
6	8.7	-1.3	-6.2	-11.0
8	13.5	0.8	-10.8	-18.5
10	18.5	2.9	-15.8	-27.0
12	26.0	5.0	-17.1	-29.0
14	33.5	7.2	-18.4	-31.0
16	40.0	8.9	-18.5	-37.5
18	46.0	10.6	-17.3	-47.5
20	52.0	12.2	-15.8	-58.0
90	52.0	12.2	-15.8	-58.0

TABLE 12.- Continued.

(c) $\frac{L}{\bar{q}}(T_J)$ =

$\alpha_N = \alpha_{WF} + i_E$

$T_J = T_P + T_S$

For $-90^\circ \leq \alpha_N < -20^\circ$

$$\frac{L}{\bar{q}}(T_J) = -.004122\ T_J$$

For $-20^\circ \leq \alpha_N < -10^\circ$

$$\frac{L}{\bar{q}}(T_J) = (.0005153\ \alpha_N + .006183)\ T_J - \delta_F(.1\ \alpha_N + 2.0)$$

For $-10^\circ \leq \alpha_N < 20^\circ$

(A) $\delta_F = 0^\circ$, $(\Delta L/\bar{q})_{flap} = 0$

(B) $\delta_F > 0^\circ$

(B1) $\alpha_N < 2^\circ$

$$(\Delta L/\bar{q})_{flap} = (.375\ \alpha_N + 3.0833)\ \delta_F - 1.8667\ \alpha_N - 28.6667$$

(B2) $\alpha_N \geq 2^\circ$

$$(\Delta L/\bar{q})_{flap} = (4.0133 - .09067\ \alpha_N)\ \delta_F - 1.8667\ \alpha_N - 28.6667$$

$$\frac{L}{\bar{q}}(T_J) = (-.0003435 - .0001374\ \alpha_N + (.04926 + .004926\ \alpha_N)\ \sin^2 i_W + .0001031\ (\Delta L/\bar{q})_{flap})T_J$$

TABLE 12.- Concluded.

(c).- Concluded.

For $20^\circ \leq \alpha_N \leq 90^\circ$

$$\frac{L}{q}(T_J) = (-.003092 + .1478 \sin^2 i_W)T_J$$

$$(d)\ \frac{L}{q}(\delta_F, \alpha_W) =$$

For $(-90^\circ + i_W) \leq \alpha_W < -10^\circ$

$$\frac{L}{q}(\delta_F,\alpha_W) = \cos^4 \psi_{WF}\left(\frac{-10}{\alpha_W} - .001562\ (\alpha_W + 10)\right)(-.0434\ \delta_F^2 + 7.48\ \delta_F) + 1.33\delta_F$$

For $-10^\circ \leq \alpha_W \leq 15^\circ$

$$\frac{L}{q}(\delta_F,\alpha_W) = \cos^4 \psi_{WF}(1.+ .01087(\alpha_W + 10))(-.0434\ \delta_F^2 + 7.48\ \delta_F) + 1.33\delta_F$$

For $15^\circ < \alpha_W \leq (90^\circ + i_W)$

$$\frac{L}{q}(\delta_F,\alpha_W) = \cos^4 \psi_{WF}\left(\frac{15}{\alpha_W} - .00222(\alpha_W - 15) + .271(1. - .0125(\alpha_W - 15))\right)(-.0434\delta_F^2 + 7.48\ \delta_F) + 1.33\ \delta_F$$

$$(e)\ \frac{L}{q}(\delta_A)_{P \text{ or } S} =$$

For $-40^\circ \leq \delta_{A_{P \text{ or } S}} < 0^\circ$

$$\frac{L}{q}(\delta_A)_{P \text{ or } S} = -3.5\ \delta_{A_{P \text{ or } S}} - .08\ (\delta_{A_{P \text{ or } S}})^2$$

For $0^\circ \leq \delta_{A_{P \text{ or } S}} \leq 40^\circ$

$$\frac{L}{q}(\delta_A)_{P \text{ or } S} = -3.05\ \delta_{A_{P \text{ or } S}} + .055\ (\delta_{A_{P \text{ or } S}})^2$$

Note: Only one aileron deflected.

TABLE 13.- Fixed Wing Tail-Off Drag Data.

(a) $\frac{D}{q}(\alpha_W, i_W)$ =

α_W \ i_W	-9	-1	7	15
-20	79.1	94.1	115.8	142.3
-18	62.5	87.4	112.4	142.0
-16	53.5	81.9	103.2	130.0
-14	44.5	71.2	93.2	118.5
-12	37.5	56.6	82.8	106.5
-10	33.0	42.3	70.6	94.5
-8	29.5	35.7	58.4	82.5
-6	27.5	29.7	48.7	70.0
-4	28.5	26.3	39.5	60.0
-2	31.5	25.7	32.0	52.5
0	35.0	27.4	30.7	45.0
2	40.0	30.2	29.5	41.5
4	47.0	35.4	32.1	38.0
6	54.0	42.0	36.8	39.0
8	65.0	50.3	42.4	43.0
10	76.5	58.3	48.1	47.5
12	91.5	70.6	57.3	55.5
14	110.5	83.4	69.3	63.5
16	129.0	97.4	82.8	75.5
18	144.5	112.9	97.0	89.0
20	149.9	126.9	110.1	100.8

For $20^\circ < |\alpha_W| \leq 90^\circ$

$$\frac{D}{q}(\alpha_W, i_W) = (28.32 + 216 \sin^2(\alpha_W - i_W))$$

$$+ (8.9714|\alpha_W| + 300.5714)\sin^2(\alpha_W + 2.6)$$

TABLE 13.- Concluded.

(b) $\frac{D}{\bar{q}}(\psi_{WF}) =$

For $-20^{\circ} \leq \psi_{WF} \leq 20^{\circ}$

$\frac{D}{\bar{q}}(\psi_{WF}) = 376.1 \sin^2\psi_{WF}$

For $20^{\circ} < |\psi_{WF}| \leq 90^{\circ}$

$\frac{D}{\bar{q}}(\psi_{WF}) = 376.1 \sin^2\psi_{WF} + 1.14 |\psi_{WF}| - 22.8$

(c) $\frac{D}{\bar{q}}(T_J) = 0.$

(d) $\frac{D}{\bar{q}}(\delta_F, \alpha_W) =$

For $(-90^{\circ} + i_W) \leq \alpha_W < -10^{\circ}$

$\frac{D}{\bar{q}}(\delta_F, \alpha_W) = 0.$

For $-10^{\circ} \leq \alpha_W \leq 10^{\circ}$

$\frac{D}{\bar{q}}(\delta_F, \alpha_W) = \cos^2\psi_{WF}(-.001565(\alpha_W + 10)^2 + .0813(\alpha_W + 10))(-.0125\ \delta_F^2 + 2.00\ \delta_F)$

For $10^{\circ} < \alpha_W \leq (90^{\circ} + i_W)$

$\frac{D}{\bar{q}}(\delta_F, \alpha_W) = \cos^2\psi_{WF}(-.0125\ \delta_F^2 + 2.00\ \delta_F)$

(e) $\frac{D}{\bar{q}}(\delta_A)_{P \text{ or } S} =$

For $-40^{\circ} \leq \delta_{A\ P \text{ or } S} \leq 40^{\circ}$

$\frac{D}{\bar{q}}(\delta_A)_{P \text{ or } S} = -.1055\ \delta_{A\ P \text{ or } S} + .00917(\delta_{A\ P \text{ or } S})^2 + .000075\ (\delta_{A\ P \text{ or } S})^3$

Note: Only one aileron deflected.

TABLE 14.- Fixed Wing Tail-Off Pitching Moment Data.

(a) $\frac{M_M}{\bar{q}}$ (α_W, i_W) =

α_W \ i_W	-9	-1	7	15
-40	-19.0	-19.0	-19.0	-19.0
-38	-60.0	-46.7	-49.7	-45.0
-36	-110.0	-83.3	-89.3	-85.0
-34	-120.0	-120.0	-129.0	-120.0
-32	-150.0	-152.0	-168.0	-160.0
-30	-180.0	-189.0	-203.0	-195.0
-28	-200.0	-222.0	-243.0	-230.0
-26	-220.0	-252.0	-283.0	-270.0
-24	-240.0	-278.0	-322.0	-305.0
-22	-260.0	-315.0	-362.0	-340.0
-20	-280.0	-348.0	-402.0	-375.0
-18	-300.0	-343.0	-434.0	-415.0
-16	-320.0	-343.0	-475.0	-450.0
-14	-320.0	-372.0	-510.0	-490.0
-12	-290.0	-424.0	-542.0	-525.0
-10	-250.0	-460.0	-551.0	-560.0
-8	-220.0	-492.0	-557.0	-600.0
-6	-150.0	-504.0	-596.0	-635.0
-4	-75.0	-462.0	-631.0	-680.0
-2	45.0	-370.0	-648.0	-740.0
0	155.0	-276.0	-605.0	-790.0

TABLE 14.- Continued.

(a) $\frac{M_M}{\bar{q}}(\alpha_W, i_W)$ =

α_W \ i_W	-9	-1	7	15
2	290.0	-180.0	-570.0	-790.0
4	425.0	-90.6	-491.0	-750.0
6	560.0	26.6	-394.0	-700.0
8	725.0	178.0	-291.0	-640.0
10	890.0	321.0	-179.0	-580.0
12	1050.0	454.0	-58.5	-530.0
14	1210.0	583.0	43.2	-455.0
16	1370.0	690.0	134.0	-370.0
18	1530.0	774.0	213.0	-320.0
20	1700.0	855.0	274.0	-255.0
22	1860.0	944.0	331.0	-190.0
24	2020.0	1029.0	410.0	-115.0
26	1970.0	1090.0	495.0	-30.0
28	1730.0	1134.0	579.0	60.0
30	1490.0	1170.0	664.0	150.0
32	1240.0	991.0	731.0	245.0
34	1000.0	804.0	640.0	340.0
36	750.0	625.0	512.0	360.0
38	505.0	443.0	388.0	315.0
40	265.0	265.0	265.0	265.0

For $-90^\circ \leq \alpha_W < -40^\circ$

$$\frac{M_M}{\bar{q}}(\alpha_W, i_W) = -754.2 - 18.38\ \alpha_W$$

For $40^\circ < \alpha_W \leq 90^\circ$

$$\frac{M_M}{\bar{q}}(\alpha_W, i_W) = 1197. - 23.30\ \alpha_W$$

TABLE 14.- Continued.

(b) $\frac{M_M}{\bar{q}}(\psi_{WF}, i_W)$ =

ψ_{WF} \ i_W	-9	-1	7	15
-30	-600	-600	-600	-600
-25	-600	-790	-760	-540
-20	-534	-804	-765	-404
-15	-327	-526	-450	-202
-10	-132	-125	-184	-108
-5	-70	-78	-58	-89
0	0	0	0	0
5	-1	-62	-78	108
10	-105	-345	-187	88
15	-275	-511	-524	-109
20	-554	-770	-689	-298
25	-580	-680	-700	-440
30	-500	-500	-500	-500

For $-90^\circ \leq \psi_{WF} < -30^\circ$

$$\frac{M_M}{\bar{q}}(\psi_{WF}, i_W) = -600 - 10\,(\psi_{WF} + 30)$$

For $30^\circ < \psi_{WF} \leq 90^\circ$

$$\frac{M_M}{\bar{q}}(\psi_{WF}, i_W) = -500 + 8.34\,(\psi_{WF} - 30)$$

TABLE 14.- Concluded.

$$(c)\ \frac{M_M}{\bar{q}}(T_J) =$$

For $T_J \leq 4000$

$K_1 = 0.$

$K_2 = -.0000938\ T_J$

For $T_J > 4000$

$K_1 = -3.625 + .00091\ T_J$

$K_2 = -.3295 - .000011388\ T_J$

$$\frac{M_M}{\bar{q}}(T_J) = K_1\ (\alpha_{WF} - 20) + K_2\ (\alpha_{WF} - 20)^2$$

$$(d)\ \frac{M_M}{\bar{q}}(\delta_F,\ \alpha_W) =$$

For $-90^\circ \leq \alpha_{WF} < (-10^\circ - i_W)$

$$\frac{M_M}{\bar{q}}(\delta_F,\alpha_W) = -\cos^8\psi_{WF}\sin^2(2.25\ \delta_F)(21.7\ i_W + 1060)\left(\frac{-10}{\alpha_W} + \frac{10\ (10 + \alpha_W)}{(-90 + i_W)(-80 + i_W)}\right)$$

For $(-10^\circ - i_W) \leq \alpha_{WF} \leq 38.9^\circ$

$$\frac{M_M}{\bar{q}}(\delta_F,\alpha_W) = \cos^8\psi_{WF}\ \sin^2(2.25\ \delta_F)(21.7\ \alpha_{WF} - 843)$$

For $38.9^\circ < \alpha_{WF} \leq 90^\circ$

$$\frac{M_M}{\bar{q}}(\delta_F,\ \alpha_W) = 0.$$

$$(e)\ \frac{M_M}{\bar{q}}(\delta_A)_{P\ \text{or}\ S} = 0.$$

TABLE 15.- Fixed Wing Tail-Off Side Force Data.

(a) $\frac{Y}{q}(\alpha_W, i_W) = 0.$

(b) $\frac{Y}{q}(\psi_{WF}, i_W) =$

ψ_{WF} \ i_W	-9	-1	7	15
-30	-117.0	-117.0	-117.0	-117.0
-28	-120.9	-120.9	-120.9	-109.2
-26	-124.8	-124.8	-124.8	-101.4
-24	-128.7	-128.7	-116.2	-93.6
-22	-121.0	-121.0	-106.5	-85.8
-20	-110.0	-110.0	-96.8	-78.0
-18	-99.0	-99.0	-87.1	-70.2
-16	-88.0	-88.0	-77.4	-62.4
-14	-77.0	-77.0	-67.8	-54.6
-12	-66.0	-66.0	-58.1	-46.8
-10	-55.0	-55.0	-48.4	-39.0
-8	-44.0	-44.0	-38.7	-31.2
-6	-33.0	-33.0	-29.0	-23.4
-4	-22.0	-22.0	-19.4	-15.6
-2	-11.0	-11.0	-9.7	-7.8

TABLE 15.- Continued.

$\frac{Y}{\bar{q}} (\psi_{WF}, i_W) =$

ψ_{WF} \ i_W	-9	-1	7	15
0	0	0	0	0
2	11.0	11.0	9.7	7.8
4	22.0	22.0	19.7	15.6
6	33.0	33.0	29.0	23.4
8	44.0	44.0	38.7	31.2
10	55.0	55.0	48.4	39.0
12	66.0	66.0	58.1	46.8
14	77.0	77.0	67.8	54.6
16	88.0	88.0	77.4	62.4
18	99.0	99.0	87.1	70.2
20	110.0	110.0	96.8	78.0
22	121.0	121.0	106.5	85.8
24	128.7	128.7	116.2	93.6
26	124.8	124.8	124.8	101.4
28	120.9	120.9	120.9	109.2
30	117.0	117.0	117.0	117.0

For $-90^\circ \leq \psi_{WF} < -30^\circ$

$$\frac{Y}{\bar{q}} (\psi_{WF}, i_W) = -175.5 - 1.95\ \psi_{WF}$$

For $30^\circ < \psi_{WF} \leq 90^\circ$

$$\frac{Y}{\bar{q}} (\psi_{WF}, i_W) = 175.5 - 1.95\ \psi_{WF}$$

TABLE 15.- Concluded.

(c) $\frac{Y}{\bar{q}}(T_J) =$

For $-90^\circ \leq \psi_{WF} < -20^\circ$ $\quad \frac{Y}{\bar{q}}(T_J) = -.0125\ T_S$

For $-20^\circ \leq \psi_{WF} < 0^\circ$ $\quad \frac{Y}{\bar{q}}(T_J) = .000625\ \psi_{WF} T_S$

For $0^\circ \leq \psi_{WF} \leq 20^\circ$ $\quad \frac{Y}{\bar{q}}(T_J) = .000625\ \psi_{WF} T_P$

For $20^\circ < \psi_{WF} \leq 90^\circ$ $\quad \frac{Y}{\bar{q}}(T_J) = .0125\ T_P$

(d) $\frac{Y}{\bar{q}}(\delta_F, \psi_{WF}) =$

For $-90^\circ \leq \psi_{WF} < -25^\circ$

$$\frac{Y}{\bar{q}}(\delta_F, \psi_{WF}) = .832\ \delta_F\left(\frac{-20}{(\psi_{WF} + 5)} + .00362\ (\psi_{WF} + 25)\right)$$

For $-25^\circ \leq \psi_{WF} \leq 25^\circ$

$$\frac{Y}{\bar{q}}(\delta_F, \psi_{WF}) = -.832\ \delta_F\left(\frac{\psi_{WF}}{25}\right)$$

For $25^\circ < \psi_{WF} \leq 90^\circ$

$$\frac{Y}{\bar{q}}(\delta_F, \psi_{WF}) = -.832\ \delta_F\left(\frac{20}{(\psi_{WF} - 5)} - .00362\ (\psi_{WF} - 25)\right)$$

(e) $\frac{Y}{\bar{q}}(\delta_A)_{P \text{ or } S} = 0.$

TABLE 16.- Fixed Wing Tail-Off Rolling Moment Data.

(a) $\frac{L_M}{\bar{q}}(\alpha_W, \psi_{WF})_0$ =

α_W \ ψ_{WF}	-90	-20	-15	-10	-5	0
-90	0	0	0	0	0	0
-30	0	0	0	0	0	0
-28	135	135	99	64	30	0
-26	270	270	197	127	60	0
-24	405	405	296	191	90	0
-22	540	540	394	254	120	0
-20	675	675	493	318	150	0
-18	755	755	535	284	115	0
-16	555	555	378	220	93	0
-14	355	355	253	162	76	0
-12	282	282	205	128	62	0
-10	200	200	150	100	50	0
-8	158	158	115	75	38	0
-6	97	97	75	52	28	0
-4	57	57	45	30	18	0
-2	19	19	16	10	8	0
0	-43	-43	-25	-10	0	0
2	-115	-115	-69	-34	-8	0
4	-168	-168	-105	-56	-16	0
6	-238	-238	-150	-80	-25	0
8	-300	-300	-193	-103	-36	0
10	-375	-375	-243	-133	-48	0
12	-468	-468	-302	-163	-62	0
14	-505	-505	-340	-198	-82	0
16	-543	-543	-384	-237	-108	0
18	-632	-632	-457	-292	-136	0
20	-835	-835	-597	-370	-169	0
22	-668	-668	-478	-296	-135	0

TABLE 16.- Continued.

(a) $\frac{L_M}{\bar{q}}(\alpha_W, \psi_{WF})_0 =$

α_W \ ψ_{WF}	-90	-20	-15	-10	-5	0
24	-501	-501	-358	-222	-101	0
26	-334	-334	-238	-148	-68	0
28	-167	-167	-119	-74	-34	0
30	0	0	0	0	0	0
90	0	0	0	0	0	0

To include wing incidence effects:

$$\frac{L_M}{\bar{q}}(\alpha_W, \psi_{WF}) = \frac{L_M}{\bar{q}}(\alpha_W, \psi_{WF})_0 - 2\psi_{WF} i_W$$

TABLE 16.- Continued.

(a) Continued.

$$\frac{L_M}{\bar{q}}(\alpha_W, \psi_{WF})_0 =$$

α_W \ ψ_{WF}	0	5	10	15	20	90
-90	0	0	0	0	0	0
-30	0	0	0	0	0	0
-28	0	-30	-64	-99	-135	-135
-26	0	-60	-127	-197	-270	-270
-24	0	-90	-191	-296	-405	-405
-22	0	-120	-254	-394	-540	-540
-20	0	-150	-318	-493	-675	-675
-18	0	-115	-284	-505	-755	-755
-16	0	-93	-220	-378	-555	-555
-14	0	-76	-162	-253	-355	-355
-12	0	-62	-128	-205	-282	-282
-10	0	-50	-100	-150	-200	-200
-8	0	-38	-75	-115	-158	-158
-6	0	-28	-52	-75	-97	-97
-4	0	-18	-30	-45	-57	-57
-2	0	-8	-10	-16	-19	-19
0	0	0	10	25	43	43
2	0	8	34	69	115	115
4	0	16	56	105	168	168
6	0	25	80	150	238	238
8	0	36	103	193	300	300
10	0	48	133	243	375	375
12	0	62	163	302	468	468
14	0	82	198	340	505	505
16	0	108	237	384	543	543
18	0	136	292	457	632	632

TABLE 16.- Continued.

(a) Continued.

$$\frac{L_M}{\bar{q}}(\alpha_W, \psi_{WF})_0 =$$

α_W \ ψ_{WF}	0	5	10	15	20	90
20	0	169	370	597	835	835
22	0	135	296	478	668	668
24	0	101	222	358	501	501
26	0	68	148	238	334	334
28	0	34	74	119	167	167
30	0	0	0	0	0	0
90	0	0	0	0	0	0

To include wing incidence effects:

$$\frac{L_M}{\bar{q}}(\alpha_W, \psi_{WF}) = \frac{L_M}{\bar{q}}(\alpha_W, \psi_{WF})_0 - 2\psi_{WF} i_W$$

TABLE 16.- Continued.

(b) $\frac{L_M}{\bar{q}}(\psi_{WF}, i_W)$ =

ψ_{WF} \ i_W	-9	-1	7	15
-20	306.0	131.0	-46.1	-220.0
-18	313.0	143.0	-39.5	-236.0
-16	317.0	151.0	-35.3	-244.0
-14	315.0	152.0	-27.9	-232.0
-12	280.0	148.0	-24.1	-207.0
-10	238.0	128.0	-19.8	-182.0
-8	199.0	103.0	-13.2	-160.0
-6	157.0	71.6	-8.5	-132.0
-4	112.0	48.0	-4.2	-100.0
-2	39.0	21.2	-1.0	-44.0
0	0.0	0.0	0.0	0.0
2	-13.0	-27.2	7.8	54.0
4	-73.0	-53.4	16.8	100.0
6	-123.0	-78.6	30.5	140.0
8	-138.0	-94.4	46.3	173.0
10	-153.0	-106.0	54.9	208.0
12	-165.0	-116.0	46.7	208.0
14	-178.0	-123.0	39.8	203.0
16	-216.0	-125.0	36.7	185.0
18	-279.0	-126.0	30.0	175.0
20	-275.0	-125.0	25.0	175.0

TABLE 16.- Continued.

For $-90^{\circ} \leq \psi_{WF} < -20^{\circ}$

$$\frac{L_M}{\bar{q}}(\psi_{WF}, i_W) = 108.9 - 21.9\, i_W + (4.903 - .313\, i_W)(\psi_{WF} + 20)$$

For $20^{\circ} < \psi_{WF} \leq 90^{\circ}$

$$\frac{L_M}{\bar{q}}(\psi_{WF}, i_W) = -106.25 + 18.75\, i_W + (4.731 - .268\, i_W)(\psi_{WF} - 20)$$

$$(c)\ \frac{L_M}{\bar{q}}(T_J, \psi_{WF}) =$$

For $-90^{\circ} \leq \psi_{WF} < -20^{\circ}$

$$\frac{L_M}{\bar{q}}(T_J, \psi_{WF}) = (-.05\, \frac{L_M}{\bar{q}}(\psi_{WF}, i_W) - 25)\ (\frac{T_J}{9600})$$

For $-20^{\circ} \leq \psi_{WF} \leq 20^{\circ}$

$$\frac{L_M}{\bar{q}}(T_J, \psi_{WF}) = \psi_{WF}(.0025\, \frac{L_M}{\bar{q}}(\psi_{WF}, i_W) + 1.25)\ (\frac{T_J}{9600})$$

For $20^{\circ} < \psi_{WF} \leq 90^{\circ}$

$$\frac{L_M}{\bar{q}}(T_J, \psi_{WF}) = (.05\, \frac{L_M}{\bar{q}}(\psi_{WF}, i_W) + 25)(\frac{T_J}{9600})$$

$$(d)\ \frac{L_M}{\bar{q}}(\delta_F, \psi_{WF}) =$$

For $-90^{\circ} \leq \psi_{WF} < -25^{\circ}$

$$\frac{L_M}{\bar{q}}(\delta_F, \psi_{WF}) = -23.3\, \delta_F\, (1 + .0154(\psi_{WF} + 25))$$

For $-25^{\circ} \leq \psi_{WF} \leq 25^{\circ}$

$$\frac{L_M}{\bar{q}}(\delta_F, \psi_{WF}) = .932\, (\psi_{WF})\delta_F$$

For $25^{\circ} < \psi_{WF} \leq 90^{\circ}$

$$\frac{L_M}{\bar{q}}(\delta_F, \psi_{WF}) = 23.3\, \delta_F\, (1 - .0154\, (\psi_{WF} - 25))$$

TABLE 16.- Concluded.

(e) $\frac{L_M}{\bar{q}}(\delta_{A_{P \text{ or } S}}, \alpha_W)$ =

α_W \ δ_A	-20	-10	0	10	20
-30	0	0	0	0	0
-25	-80	-60	0	40	40
-20	-240	-115	0	190	200
-15	-220	-125	0	375	610
-10	-370	-210	0	335	530
-5	-390	-250	0	340	505
0	-400	-260	0	345	540
5	-360	-245	0	325	555
10	-410	-240	0	290	540
15	-560	-280	0	190	410
20	-350	-170	0	65	180
25	-130	-50	0	45	90
30	-40	-25	0	140	180
35	-120	-120	0	90	90
40	-50	-50	0	10	10
45	0	0	0	0	0

For $-90^\circ \leq \alpha_W < -30^\circ$ and $45^\circ < \alpha_W \leq 90^\circ$

$\frac{L_M}{\bar{q}}(\delta_{A_{P \text{ or } S}}, \alpha_W) = 0.$

TABLE 17.- Fixed Wing Tail-Off Yawing Moment Data.

(a) $\frac{N_M}{\bar{q}}(\alpha_W, i_W) = 0.$

(b) $\frac{N_M}{\bar{q}}(\psi_{WF}, i_W) =$

ψ_{WF} \ i_W	-9	-1	7	15
-50	-120	-120	-120	-120
-48	-178	-180	-178	-175
-46	-236	-240	-236	-229
-44	-292	-291	-296	-283
-42	-347	-356	-347	-334
-40	-399	-410	-400	-384
-38	-449	-462	-450	-431
-36	-494	-509	-495	-474
-34	-537	-554	-538	-515
-32	-576	-593	-577	-552
-30	-610	-628	-611	-585
-28	-639	-658	-641	-614
-26	-664	-682	-665	-638
-24	-675	-682	-665	-638
-22	-680	-675	-641	-614
-20	-675	-660	-611	-585
-18	-610	-645	-575	-545
-16	-542	-590	-534	-505
-14	-475	-528	-483	-460
-12	-408	-454	-425	-400
-10	-340	-380	-358	-350
-8	-272	-303	-288	-285
-6	-205	-228	-219	-219
-4	-139	-152	-149	-152
-2	-70	-75	-68	-68
0	0	0	0	0

TABLE 17.- Continued.

(b) $\frac{N_M}{\bar{q}}(\psi_{WF}, i_W)$ =

ψ_{WF} \ i_W	-9	-1	7	15
2	70	75	68	68
4	139	152	149	152
6	205	228	219	225
8	272	303	288	305
10	340	380	358	375
12	408	454	425	440
14	475	528	483	500
16	542	590	534	560
18	610	645	575	610
20	675	705	611	645
22	710	738	641	672
24	764	764	660	700
26	764	764	680	700
28	738	738	709	672
30	705	705	677	645
32	666	666	640	609
34	622	622	597	569
36	572	572	549	523
38	517	517	497	474
40	458	458	441	421
42	395	395	381	364
44	329	329	319	306
46	261	261	253	245
48	191	191	187	183
50	120	120	120	120

TABLE 17.- Continued.

For $-90^{\circ} \leq \psi_{WF} < -50^{\circ}$

$$\frac{N}{\bar{q}} (\psi_{WF}, i_W) = -400 - 28(\psi_{WF} + 40)$$

For $50^{\circ} < \psi_{WF} \leq 90^{\circ}$

$$\frac{N}{\bar{q}} (\psi_{WF}, i_W) = 400 - 28 (\psi_{WF} - 40)$$

(c) $$\frac{N_M}{\bar{q}} (T_J) = 0.$$

(d) $$\frac{N_M}{\bar{q}} (\delta_F, \psi_{WF}) =$$

For $-90^{\circ} \leq \psi_{WF} < -25^{\circ}$

$$\frac{N_M}{\bar{q}} (\delta_F, \psi_{WF}) = 6.67\ \delta_F\ (1 + .0154\ (\psi_{WF} + 25))$$

For $-25^{\circ} \leq \psi_{WF} \leq 25^{\circ}$

$$\frac{N_M}{\bar{q}} (\delta_F, \psi_{WF}) = -.267\ (\psi_{WF})\ \delta_F$$

For $25^{\circ} < \psi_{WF} \leq 90^{\circ}$

$$\frac{N_M}{\bar{q}} (\delta_F, \psi_{WF}) = -6.67\ \delta_F\ (1 - .0154\ (\psi_{WF} - 25))$$

TABLE 17.- Continued.

(e) $\frac{N_M}{\bar{q}}(\delta_{A_{P \text{ or } S}}, \alpha_W)$ =

α_W \ δ_A	-20	-10	0	10	20
-30	-40	-20	0	20	40
-28	-40	-35	0	30	55
-26	-40	-40	0	40	70
-24	-40	-50	0	55	85
-22	-38	-60	0	62	100
-20	-35	-70	0	80	120
-18	-41	-100	0	60	120
-16	-77	-130	0	35	95
-14	-70	-120	0	25	80
-12	-20	-65	0	55	120
-10	47	0	0	80	130
-8	60	30	0	80	120
-6	66	38	0	60	95
-4	80	40	0	40	70
-2	85	40	0	0	60
0	105	40	0	0	35
2	118	42	0	-25	10
4	122	62	0	-30	0
6	135	80	0	-30	-20
8	155	82	0	-30	-45
10	170	90	0	-30	-60
12	177	90	0	-45	-70
14	180	90	0	-60	-80
16	160	85	0	-60	-110
18	130	65	0	-50	-115
20	130	55	0	-50	-120
22	125	60	0	-68	-130
24	120	80	0	-85	-125

TABLE 17.- Concluded.

(e) Concluded.

α_W \ δ_A	-20	-10	0	10	20
26	120	90	0	-80	-110
28	120	50	0	-50	-90
30	120	30	0	-30	-60
32	120	35	0	-32	-62
34	120	40	0	-40	-65
36	120	48	0	-45	-80
38	120	52	0	-50	-100
40	120	60	0	-58	-118

For $-90^\circ \leq \alpha_W < -30^\circ$

$$\frac{N_M}{\bar{q}} (\delta_{A_{P \text{ or } S}}, \alpha_W) = .03333(\delta_{A_{P \text{ or } S}}) \alpha_W + 3.0\, \delta_{A_{P \text{ or } S}}$$

For $40^\circ < \alpha_W \leq 90^\circ$

$$\frac{N_M}{\bar{q}} (\delta_{A_{P \text{ or } S}}, \alpha_W) = .12\, (\delta_{A_{P \text{ or } S}}) \alpha_W - 10.8\, \delta_{A_{P \text{ or } S}}$$

Note: Only one aileron deflected.

TABLE 18.- Tail-Off Dynamic Derivatives.

(a) Helicopter.

$$Y_p = L_{M_p} = N_{M_p} = Y_r = L_{M_r} = N_{M_r} = M_{M_q} = 0.$$

(b) Fixed Wing.

$$Y_p = (-1.2 \frac{L}{q} (\alpha_W, i_W) - .315)/V_{XB}$$

$$L_{M_p} = (-144232 - .0276 (\frac{L}{q} (\alpha_W, i_W))^2)/V_{XB}$$

$$N_{M_p} = (2.25 L_{M_p} (\tan \alpha_W) - 90 \frac{L}{q} (\alpha_W, i_W))/V_{XB} \text{ ; where } \alpha_W \text{ limited to } \pm 25^\circ$$

$$Y_r = 0.$$

$$L_{M_r} = ((187 \frac{L}{q} (\alpha_W, i_W) + 364)/V_{XB}) - ((\frac{\frac{L_M}{q}(\psi_{WF}, i_W)}{\beta_{WF}}(57.3) + 47.4 \delta_F)(22.55/V_{XB}))$$

$$N_{M_r} = (-.055 (\frac{L}{q} (\alpha_W, i_W))^2 - 949)/V_{XB}$$

$$M_{M_q} = 0.$$

TABLE 19.- Low Speed Phasing Parameters.

(a) Helicopter.

$X_{LS} = 0.$

$Y_{LS} = 261.$

$Z_{LS} = 324.$

$L_{LS} = 0.$

$M_{LS} = 0.$

$N_{LS} = 0.$

(b) Fixed Wing.

$X_{LS} = 0.$

$Y_{LS} = 261.$

$Z_{LS} = 1335.$

$L_{LS} = 0.$

$M_{LS} = 0.$

$N_{LS} = 0.$

TABLE 20.- Longitudinal Variable Moment Arm For Vertical Tail.

$$FS_{VT} = K(812.2 + (0.82A)(\frac{\delta_F}{30}))$$

where

$K = K_1 + K_2\alpha_{WF}$

K - nondimensional

K_1 - nondimensional

K_2 - 1/deg

A - in

812.2 - in (FS_{VT} basic)

0.82 - nondimensional

30 - deg

(a) K_1 =

For $-90^\circ \leq \alpha_{WF} < -5^\circ$ and $-20^\circ \leq \psi_{WF} \leq 20^\circ$

$\lvert\psi_{WF}\rvert$ \ i_W	-9	-1	7	15
0	1.000	1.000	1.000	1.000
2	1.031	1.076	1.134	1.209
4	1.027	1.087	1.163	1.250
6	1.005	1.067	1.146	1.233
8	0.972	1.034	1.111	1.200
10	0.927	0.989	1.066	1.155
12	0.877	0.940	1.018	1.105
14	0.824	0.886	0.964	1.051
16	0.769	0.830	0.903	0.995
18	0.738	0.797	0.871	0.950
20	1.000	1.000	1.000	1.000

TABLE 20.- Continued.

For $-5^{\circ} \leq \alpha_{WF} \leq 15^{\circ}$ and $-20^{\circ} \leq \psi_{WF} \leq 20^{\circ}$

$\lvert\psi_{WF}\rvert$ \ i_W	-9	-1	7	15
0	1.000	1.000	1.000	1.000
2	0.985	1.030	1.088	1.163
4	0.952	1.012	1.088	1.175
6	0.914	0.976	1.055	1.142
8	0.876	0.938	1.015	1.104
10	0.838	0.900	0.977	1.066
12	0.800	0.863	0.941	1.028
14	0.763	0.825	0.903	0.990
16	0.726	0.787	0.860	0.952
18	0.715	0.774	0.848	0.927
20	1.000	1.000	1.000	1.000

For $15^{\circ} < \alpha_{WF} \leq 90^{\circ}$ and $-20^{\circ} \leq \psi_{WF} \leq 20^{\circ}$

$\lvert\psi_{WF}\rvert$ \ i_W	-9	-1	7	15
0	1.000	1.000	1.000	1.000
2	0.847	0.892	0.950	1.025
4	0.727	0.787	0.863	0.950
6	0.643	0.705	0.784	0.871
8	0.588	0.650	0.727	0.816
10	0.571	0.633	0.710	0.799
12	0.571	0.634	0.712	0.799
14	0.580	0.642	0.720	0.807
16	0.599	0.660	0.733	0.825
18	0.648	0.707	0.781	0.860
20	1.000	1.000	1.000	1.000

TABLE 20.- Continued.

For $-90^{\circ} \leq \alpha_{WF} \leq 90^{\circ}$ and $20^{\circ} < |\psi_{WF}| \leq 90^{\circ}$

$$K_1 = 1.0$$

(b) K_2 =

For $-5^{\circ} \leq \alpha_{WF} \leq 15^{\circ}$ and $-20^{\circ} \leq \psi_{WF} \leq 20^{\circ}$

$\lvert\psi_{WF}\rvert$	K_2
0	0.
2	-.0092
4	-.0150
6	-.0181
8	-.0192
10	-.0178
12	-.0153
14	-.0122
16	-.0085
18	-.0045
20	0.

For $-90^{\circ} \leq \alpha_{WF} < -5^{\circ}$ and $20^{\circ} < |\psi_{WF}| \leq 90^{\circ}$

or

$15^{\circ} < \alpha_{WF} \leq 90^{\circ}$ and $20^{\circ} < |\psi_{WF}| \leq 90^{\circ}$

$$K_2 = 0.$$

(c) A =

For $-15^{\circ} \leq \alpha_{WF} \leq 15^{\circ}$ and $-90^{\circ} \leq \psi_{WF} \leq 90^{\circ}$

TABLE 20.- Concluded.

α_{WF}	A
-15	0.
-10	140.02
-5	212.80
0	275.00
5	215.00
10	0.
15	0.

For $15^{\circ} < |\alpha_{WF}| \leq 90^{\circ}$ and $-90^{\circ} \leq \psi_{WF} \leq 90^{\circ}$

$$A = 0.$$

TABLE 21.- Rotor Induced Velocities On The Tail.

(a) Upper Horizontal Tail

(1) $EK_{TXU}\ (\chi, a_{1SF})$ =

χ \ a_{1SF}	-10	0	10
-20	-.19	-.18	-.17
-10	-.23	-.22	-.21
0	-.27	-.25	-.23
10	-.32	-.29	-.26
20	-.36	-.32	-.28
30	-.40	-.35	-.30
40	-.44	-.37	-.31
50	-.44	-.38	-.32
60	-.40	-.37	-.32
70	-.26	-.32	-.31
80	0	-.20	-.25
90	.33	0	-.13
100	.64	.27	.10

TABLE 21.- Continued.

(2) EK_{TZU} (χ, a_{1SF}) =

χ \ a_{1SF}	-10	0	10
-20	0	0	0
-10	0	0	0
0	0	0	0
10	.08	.07	.05
20	.18	.16	.12
30	.31	.26	.20
40	.47	.38	.28
50	.69	.54	.40
60	1.00	.74	.55
70	1.37	1.02	.74
80	1.80	1.40	1.00
90	2.28	1.86	1.37
100	2.82	2.40	1.86

TABLE 21.- Continued.

(b) Lower Horizontal Tail

(1) $EK_{TX}(\chi, a_{1SF})$ =

χ \ a_{1SF}	-10	0	10
-20	0	0	0
-10	0	0	0
0	0	-.36	-.43
10	.17	-.20	-.63
20	.34	-.04	-.52
30	.52	.13	-.33
40	.71	.32	-.14
50	.92	.52	.06
60	1.15	.75	.28
70	1.39	1.02	.54
80	.33	.74	.85
90	-.74	-.32	.64
100	-1.00	-.60	.30

TABLE 21.- Concluded.

(2) EK_{TZ} (χ, a_{1SF}) =

χ \ a_{1SF}	-10	0	10
-20	1.74	0	0
-10	1.74	0	0
0	1.74	.80	0
10	1.74	1.76	.70
20	1.74	1.81	1.48
30	1.74	1.84	1.80
40	1.74	1.88	1.97
50	1.74	1.94	2.11
60	1.74	2.00	2.22
70	1.74	2.02	2.32
80	1.48	1.67	2.40
90	1.15	1.33	1.74
100	.90	1.06	1.30

TABLE 22.- Helicopter Tail Downwash Data.

$\varepsilon_{WTU}(\alpha_{WF})$ =

α_{WF}	ε_{WTU}
-8	0
-4	.20
0	.60
4	.60
8	.60
12	.50
16	.35
20	.25
24	.15
28	0

For $-90^{o} \leq \alpha_{WF} < -8^{o}$

or

$28^{o} < \alpha_{WF} \leq 90^{o}$

$\varepsilon_{WTU} = 0.$

TABLE 23.- Fixed Wing Tail Downwash Data.

(a) Upper Horizontal Tail

$$\varepsilon_{WTU}(\alpha_W, i_W, \delta_F)_0 = \Delta\varepsilon(\alpha_W, i_W) + \Delta\varepsilon(\delta_F, i_W)$$

(1) $\Delta\varepsilon(\alpha_W, i_W)$ =

α_W \ i_W	-9	-1	7	15
-16	0	0	0	0
-12	0.1	0.1	0.1	0.1
-8	1.6	0.8	0.8	0.8
-4	3.6	1.7	1.4	1.4
0	6.0	3.1	2.1	2.1
4	7.6	4.8	2.7	2.7
8	11.0	7.2	3.6	3.4
12	15.6	9.6	4.7	4.1
16	19.6	12.4	6.2	4.7
20	22.2	16.4	9.6	5.9
24	24.5	20.3	14.0	8.6
28	23.1	23.0	18.4	13.0
32	21.2	23.7	21.7	18.0
36	18.9	22.3	22.6	21.4
40	16.3	20.0	22.3	22.7
44	13.4	17.0	20.5	22.4
48	10.2	13.5	17.3	20.6
52	6.8	9.5	12.6	16.6
56	3.5	5.1	6.9	10.0
60	0	0	0	0

For $-90^\circ \leq \alpha_W < -16^\circ$ or $60^\circ < \alpha_W \leq 90^\circ$

$$\Delta\varepsilon(\alpha_W, i_W) = 0.$$

TABLE 23.- Continued.

$$(2)\ \Delta\epsilon(\delta_F,\ i_W) = K\left(\frac{L}{q}\ (\delta_F,\ \alpha_W)\right)$$

where

$$K = .003484 + .001035\ i_W + .00004541\ i_W^2 - .000005697\ i_W^3$$

$\frac{L}{q}\ (\delta_F,\ \alpha_W)$ is defined in Table 7, part d.

(3) Downwash effect at low speeds.

$$\epsilon_K = .0119\ (V_{XB} - 101.268)$$

if $\epsilon_K \geq 1.$, then $\epsilon_K = 1.$

if $\epsilon_K \leq 0.$, then $\epsilon_K = 0.$

$$\epsilon_{WTU}(\alpha_W,\ i_W,\ \delta_F) = \epsilon_{WTU}(\alpha_W,\ i_W,\ \delta_F)_0\ \epsilon_K$$

TABLE 23.- Continued.

(b) Lower Horizontal Tail

$$\varepsilon_{WT}(\alpha_W, i_W, \delta_F)_0 = \Delta\varepsilon\ (\alpha_W, i_W) + \Delta\varepsilon\ (\delta_F, i_W)$$

(1) $\Delta\varepsilon\ (\alpha_W, i_W)$ =

α_W \ i_W	-9	-1	7	15
-40	0	0	0	0
-38	-1.3	-1.0	-0.7	-0.5
-36	-3.1	-1.9	-1.3	-1.0
-34	-4.2	-3.0	-1.9	-1.5
-32	-5.4	-3.9	-2.6	-1.9
-30	-6.1	-4.9	-3.1	-2.4
-28	-6.6	-5.7	-3.7	-2.7
-26	-7.0	-6.2	-4.2	-3.2
-24	-7.4	-6.4	-4.7	-3.4
-22	-7.4	-6.6	-5.0	-3.8
-20	-7.1	-6.6	-5.4	-4.1
-18	-6.2	-6.6	-5.8	-4.3
-16	-5.5	-6.4	-6.0	-4.6
-14	-4.4	-5.7	-6.2	-4.7
-12	-3.3	-4.8	-5.5	-4.9
-10	-2.2	-3.8	-4.6	-4.9
-8	-1.0	-2.5	-3.8	-4.8
-6	0.3	-1.4	-2.8	-3.9
-4	1.7	-0.2	-1.8	-3.1
-2	2.7	1.0	-0.8	-2.3
0	3.7	2.2	0.1	-1.4
2	4.4	3.3	1.0	-0.6
4	5.2	4.3	1.9	0.3
6	5.8	5.0	3.0	1.2

TABLE 23.- Continued.

α_W \ i_W	-9	-1	7	15
8	6.3	5.5	4.1	1.8
10	6.6	6.1	5.0	2.9
12	5.8	6.7	6.0	3.7
14	5.9	7.0	6.8	4.6
16	5.6	7.0	7.7	5.3
18	5.2	6.6	8.1	6.3
20	4.7	6.2	7.9	7.1
22	4.3	5.7	7.5	8.1
24	3.8	5.1	7.0	8.9
26	3.3	4.6	6.3	9.0
28	2.9	4.0	5.7	8.4
30	2.4	3.4	4.9	7.2
32	1.9	2.8	4.1	5.9
34	1.4	2.2	3.1	4.7
36	0.9	1.5	2.1	3.3
38	0.4	0.8	1.1	1.7
40	0	0	0	0

For $-90^\circ \leq \alpha_W < 40^\circ$ or $40^\circ < \alpha_W \leq 90^\circ$

$$\therefore \quad \Delta\epsilon(\alpha_W, i_W) = 0.$$

$$(2)\ \Delta\epsilon(\delta_F, i_W) = K\left(\frac{L}{q}(\delta_F, \alpha_W)\right)$$

where

$$K = .02984 - .0004819\, i_W - .0003062\, i_W^2 + .00001904\, i_W^3$$

$\frac{L}{q}(\delta_F, \alpha_W)$ is defined in Table 7, part d.

TABLE 23.- Concluded.

(3) Downwash effect at low speeds.

$$\varepsilon_K = .0119\ (V_{XB} - 101.268)$$

if $\varepsilon_K \geq 1$, then $\varepsilon_K = 1.$

if $\varepsilon_K \leq 0.$, then $\varepsilon_K = 0.$

$$\varepsilon_{WT}(\alpha_W,\ i_W,\ \delta_F) = \varepsilon_{WT}(\alpha_W,\ i_W,\ \delta_F)_0\ \varepsilon_K$$

TABLE 24.- Helicopter Tail Sidewash Data.

$\sigma_{WT}(\beta_{WF})$ =

β_{WF}	$\sigma_{WT}(\beta_{WF})$	β_{WF}	$\sigma_{WT}(\beta_{WF})$
-60	0	4	2.2
-56	-2.2	8	4.1
-52	-4.1	12	5.7
-48	-5.7	16	6.7
-44	-6.7	20	7.4
-40	-7.4	24	7.9
-36	-7.9	28	8.0
-32	-8.0	32	8.0
-28	-8.0	36	7.9
-24	-7.9	40	7.4
-20	-7.4	44	6.7
-16	-6.7	48	5.7
-12	-5.7	52	4.1
-8	-4.1	56	2.2
-4	-2.2	60	0
0	0		

For $-90^{o} \leq \beta_{WF} < -60^{o}$

or

$60^{o} < \beta_{WF} \leq 90^{o}$

$\sigma_{WT}(\beta_{WF}) = 0.$

TABLE 25.- Fixed Wing Tail Sidewash Data.

$\sigma_{WT}(\beta_{WF})_0 =$

β_{WF}	$\sigma_{WT}(\beta_{WF})_0$	β_{WF}	$\sigma_{WT}(\beta_{WF})_0$
-60	0	4	1.8
-56	-1.8	8	3.0
-52	-3.0	12	3.9
-48	-3.9	16	4.6
-44	-4.6	20	5.0
-40	-5.0	24	5.2
-36	-5.2	28	5.4
-32	-5.4	32	5.4
-28	-5.4	36	5.2
-24	-5.2	40	5.0
-20	-5.0	44	4.6
-16	-4.6	48	3.9
-12	-3.9	52	3.0
-8	-3.0	56	1.8
-4	-1.8	60	0
0	0		

For $-90^\circ \leq \beta_{WF} < -60^\circ$ or

$60^\circ < \beta_{WF} \leq 90^\circ$

$$\sigma_{WT}(\beta_{WF})_0 = 0.$$

TABLE 25.- Concluded.

Engine thrust effects on sidewash.

$$C_{TE} = T_J/(q_{WF}S_W)$$

$$\sigma_K = 2.(C_{TE} - .2) + 1.$$

if $\sigma_K \geq 1.6$, then $\sigma_K = 1.6$

if $\sigma_K \leq 1.0$, then $\sigma_K = 1.0$

$$\sigma_{WT}(\beta_{WF}) = \sigma_{WT}(\beta_{WF})_0 \sigma_K$$

TABLE 26.- Helicopter Tail Dynamic Pressure Ratio Data.

(a) Horizontal Tail

$$K_{QHTU} = \left(\frac{q_{HTU}}{\bar{q}}\ (\alpha_{WF})\right)^{1/2}$$

For $10^{\circ} \leq \alpha_{WF} \leq 46^{\circ}$

$$\frac{q_{HTU}}{\bar{q}}\ (\alpha_{WF}) = .4 + .0333|\alpha_{WF} - 28|$$

For $-90^{\circ} \leq \alpha_{WF} < 10^{\circ}$ or $46^{\circ} < \alpha_{WF} \leq 90^{\circ}$

$$\frac{q_{HTU}}{\bar{q}}\ (\alpha_{WF}) = 1.0$$

(b) Vertical Tail

$$K_{QVT} = \left(\frac{q_{VT}}{\bar{q}}(\psi_{WF}) + \frac{q_{VT}}{\bar{q}}\ (\alpha_{WF},\ |\psi_{WF}|)\right)^{1/2}$$

(1) $\frac{q_{VT}}{\bar{q}}\ (\psi_{WF}) =$

For $-17.5^{\circ} \leq \psi_{WF} \leq 17.5^{\circ}$

$$\frac{q_{VT}}{\bar{q}}\ (\psi_{WF}) = .68 + .01314\ |\psi_{WF}|$$

For $-90^{\circ} \leq \psi_{WF} < -17.5^{\circ}$

$$\frac{q_{VT}}{\bar{q}}\ (\psi_{WF}) = .91 - .00124\ (\psi_{WF} + 17.5)$$

For $17.5^{\circ} < \psi_{WF} \leq 90^{\circ}$

$$\frac{q_{VT}}{\bar{q}}\ (\psi_{WF}) = .91 + .00124\ (\psi_{WF} - 17.5)$$

TABLE 26.- Concluded.

(2) $\frac{q_{VT}}{\bar{q}} (\alpha_{WF}, |\psi_{WF}|)$

α_{WF} / $\lvert\psi_{WF}\rvert$	-90 to -20	-10	0	10	20 to 90
0	.065	.030	0	-.100	-.200
10	.055	.030	0	-.100	-.200
20	.035	.020	0	-.100	-.160
30	0	0	0	0	0

For $30^{\circ} < |\psi_{WF}| \leq 90^{\circ}$

$$\frac{q_{VT}}{\bar{q}} (\alpha_{WF}, |\psi_{WF}|) = 0.$$

TABLE 27.- Fixed Wing Tail Dynamic Pressure Ratio Data.

(a) Upper Horizontal Tail

$$K_{QHTU} = \left(\frac{q_{HTU}}{\bar{q}}(\alpha_{WF}, \alpha') + \frac{q_{HTU}}{\bar{q}}(T_J) + \frac{q_{HTU}}{\bar{q}}(\delta_F)\right)^{1/2}$$

$\alpha' = 20 - .4\, i_W$ and $K_{NAC} = T_J/6490$

$$(1)\ \frac{q_{HTU}}{\bar{q}}(\alpha_{WF}, \alpha') =$$

For $\alpha' \leq \alpha_{WF} \leq (\alpha' + 18^o)$

$$\frac{q_{HTU}}{\bar{q}}(\alpha_{WF}, \alpha') = .67 + .03644\,|\alpha' - \alpha_{WF} + 9|$$

For $-90^o \leq \alpha_{WF} < \alpha'$ or $(\alpha' + 18^o) < \alpha_{WF} \leq 90^o$

$$\frac{q_{HTU}}{\bar{q}}(\alpha_{WF}, \alpha') = 1.0$$

$$(2)\ \frac{q_{HTU}}{\bar{q}}(T_J) =$$

For $\alpha' \leq \alpha_{WF} \leq (\alpha' + 18^o)$

$$\frac{q_{HTU}}{\bar{q}}(T_J) = (.33 - .03644\,|\alpha' - \alpha_{WF} + 9|)K_{NAC}$$

For $-90^o \leq \alpha_{WF} < \alpha'$ or $(\alpha' + 18^o) < \alpha_{WF} \leq 90^o$

$$\frac{q_{HTU}}{\bar{q}}(T_J) = 0.$$

$$(3)\ \frac{q_{HTU}}{\bar{q}}(\delta_F) = \left(\frac{q_{HTU}}{\bar{q}}(\delta_F)_0\right)\left(\frac{\delta_F}{30}\right)$$

where $\frac{q_{HTU}}{\bar{q}}(\delta_F)_0 = 0.$

TABLE 27.- Continued.

(b) Lower Horizontal Tail

$$K_{QHT} = \left(\frac{q_{HT}}{\bar{q}}(\alpha_{MAP}, i_W) + \frac{q_{HT}}{\bar{q}}(T_J) + \frac{q_{HT}}{\bar{q}}(\delta_F)\right)^{1/2}$$

$$\alpha_{MAP} = \alpha_{WF} - .4\, i_W \quad \text{and} \quad K_{NAC} = T_J/6490$$

$$(1)\ \frac{q_{HT}}{\bar{q}}(\alpha_{MAP}, i_W) =$$

α_{MAP} \ i_W	-9	-1	7	15
-35	1.000	1.000	1.000	1.000
-28	.885	.885	.885	.885
-21	.885	.885	.885	.885
-14	.925	.925	.925	.925
-7	.930	.930	.930	.930
0	.920	.920	.920	.920
7	.900	.890	.900	.900
14	.850	.860	.870	.870
21	.745	.820	.860	.845
28	.825	.845	.880	.865
35	1.000	1.000	1.000	1.000

For $-90^\circ \leq \alpha_{MAP} < -35^\circ$ or $35^\circ < \alpha_{MAP} \leq 90^\circ$

$$\frac{q_{HT}}{\bar{q}}(\alpha_{MAP}, i_W) = 1.0$$

TABLE 27.- Continued.

$$(2)\ \frac{q_{HT}}{\bar{q}}(T_J) =$$

For $-25.5^\circ \leq \alpha_{MAP} \leq -7.5^\circ$

$$\frac{q_{HT}}{\bar{q}}(T_J) = (.6 - (.087 - .00000838\ T_J)|\alpha_{MAP} + 21|)K_{NAC}$$

If $\frac{q_{HT}}{\bar{q}}(T_J) < 0.$, then $\frac{q_{HT}}{\bar{q}}(T_J) = 0.$

For $-90^\circ \leq \alpha_{MAP} < -25.5^\circ$ or $-7.5^\circ < \alpha_{MAP} \leq 90^\circ$

$$\frac{q_{HT}}{\bar{q}}(T_J) = 0.$$

$$(3)\ \frac{q_{HT}}{\bar{q}}(\delta_F) = \left(\frac{q_{HT}}{\bar{q}}(\delta_F)_0\right)\left(\frac{\delta_F}{30}\right)$$

$$\frac{q_{HT}}{\bar{q}}(\delta_F)_0 =$$

α_W \ T_J	0	8200	16,400
-25	0	0	0
-15	-.06	-.06	-.06
-5	-.07	.33	.59
5	-.09	.35	.60
15	-.08	0	.20
25	0	0	0

For $-90^\circ \leq \alpha_W < -25^\circ$ or $25^\circ < \alpha_W \leq 90^\circ$

$$\frac{q_{HT}}{\bar{q}}(\delta_F)_0 = 0.$$

TABLE 27.- Continued.

(c) Vertical Tail

$$K_{QVT} = \left(\frac{q_{VT}}{\bar{q}}(\psi_{WF}, i_W) + \frac{q_{VT}}{\bar{q}}(\alpha_{WF}, |\psi_{WF}|) + \frac{q_{VT}}{\bar{q}}(T_J) + \frac{q_{VT}}{\bar{q}}(\delta_F)\right)^{1/2}$$

$$K_{NAC} = T_J/6490$$

(1) $\frac{q_{VT}}{\bar{q}}(\psi_{WF}, i_W) =$

ψ_{WF} \ i_W	-9	-1	7	15
-30	.95	.95	.95	.95
-20	.73	.85	.91	.93
-10	.83	.92	.94	.87
0	.77	.87	.92	.91
10	.73	.84	.90	.93
20	.80	.85	.92	.94
30	.95	.95	.95	.95

For $-90^\circ \leq \psi_{WF} < -30^\circ$

$$\frac{q_{VT}}{\bar{q}}(\psi_{WF}, i_W) = .95 - .00083\,(\psi_{WF} + 30)$$

For $30^\circ < \psi_{WF} \leq 90^\circ$

$$\frac{q_{VT}}{\bar{q}}(\psi_{WF}, i_W) = .95 + .00083\,(\psi_{WF} - 30)$$

TABLE 27.- Concluded.

(2) $\frac{q_{VT}}{\bar{q}} (\alpha_{WF}, |\psi_{WF}|) =$

α_{WF} / $\lvert\psi_{WF}\rvert$	-90 to -20	-10	0	10	20 to 90
0	.065	.030	0	-.100	-.200
10	.055	.030	0	-.100	-.200
20	.035	.020	0	-.100	-.160
30	0	0	0	0	0

For $30^\circ < |\psi_{WF}| \leq 90^\circ$

$$\frac{q_{VT}}{\bar{q}} (\alpha_{WF}, |\psi_{WF}|) = 0.$$

(3) $\frac{q_{VT}}{\bar{q}} (T_J) =$

For $-90^\circ \leq \psi_{WF} < -30^\circ$

$$\frac{q_{VT}}{\bar{q}} (T_J) = (.06 + .001 (\psi_{WF} + 30))K_{NAC}$$

For $-30^\circ \leq \psi_{WF} \leq 30^\circ$

$$\frac{q_{VT}}{\bar{q}} (T_J) = .06 K_{NAC}$$

For $30^\circ < \psi_{WF} \leq 90^\circ$

$$\frac{q_{VT}}{\bar{q}} (T_J) = (.06 - .001 (\psi_{WF} - 30))K_{NAC}$$

(4) $\frac{q_{VT}}{\bar{q}} (\delta_F) = (\frac{q_{VT}}{\bar{q}} (\delta_F)_0)(\frac{\delta_F}{30})$

where $\frac{q_{VT}}{\bar{q}} (\delta_F)_0 = 0.$

TABLE 28.- Drag Brake Dynamic Pressure Ratio Data.

For Helicopter:

$K_{QDB} = K_{QVT}$ of helicopter.

For Fixed Wing:

$K_{QDB} = K_{QHT}$ of fixed wing.

TABLE 29.- Fixed Wing Lower Horizontal Tail Data.

(a) $\frac{L_{HT}}{\bar{q}} (\alpha_{HTT}, \delta_E)_0 =$

α_{HTT} \ δ_E	-30	-20	-10	0	10	20	30
-30	-60.0	-60.0	-60.0	-60.0	-60.0	-60.0	-60.0
-28	-74.0	-74.0	-74.0	-74.0	-70.0	-66.0	-64.0
-26	-88.0	-88.0	-88.0	-83.0	-73.0	-69.0	-65.0
-24	-103.0	-103.0	-103.0	-88.0	-76.0	-70.0	-62.0
-22	-118.0	-118.0	-107.0	-92.0	-78.0	-69.0	-60.0
-20	-131.0	-129.0	-113.0	-93.0	-78.0	-64.0	-53.0
-18	-139.0	-132.0	-115.0	-92.0	-73.0	-56.0	-41.0
-16	-143.0	-131.0	-111.0	-87.0	-66.5	-44.0	-29.0
-14	-141.0	-128.0	-106.0	-80.0	-54.5	-32.0	-17.0
-12	-135.0	-121.0	-98.0	-72.0	-42.5	-20.0	-5.0
-10	-127.0	-112.0	-89.5	-60.0	-30.5	-8.0	7.0
-8	-115.0	-100.0	-77.5	-48.0	-18.5	4.0	19.0
-6	-103.0	-88.0	-65.5	-36.0	-6.5	16.0	31.0
-4	-91.0	-76.0	-53.5	-24.0	5.5	28.0	43.0
-2	-79.0	-64.0	-41.5	-12.0	17.5	40.0	55.0
0	-67.0	-52.0	-29.5	0.0	29.5	52.0	67.0
2	-55.0	-40.0	-17.5	12.0	41.5	64.0	79.0
4	-43.0	-28.0	-5.5	24.0	53.5	76.0	91.0

TABLE 29.- Continued.

(a) $\frac{L_{HT}}{\bar{q}}(\alpha_{HTT}, \delta_E)_0$ =

α_{HTT} \ δ_E	-30	-20	-10	0	10	20	30
6	-31.0	-16.0	6.5	36.0	65.5	88.0	103.0
8	-19.0	-4.0	18.5	48.0	77.5	100.0	115.0
10	-7.0	8.0	30.5	60.0	89.5	112.0	127.0
12	5.0	20.0	42.5	72.0	98.0	121.0	135.0
14	17.0	32.0	54.5	80.0	106.0	128.0	141.0
16	29.0	44.0	66.5	87.0	111.0	131.0	143.0
18	41.0	56.0	73.0	92.0	115.0	132.0	140.0
20	53.0	64.0	78.0	93.0	113.0	129.0	131.0
22	60.0	69.0	78.0	92.0	107.0	118.0	118.0
24	62.0	70.0	76.0	88.0	103.0	103.0	103.0
26	65.0	69.0	73.0	83.0	88.0	88.0	88.0
28	64.0	66.0	69.0	74.0	74.0	74.0	74.0
30	60.0	60.0	60.0	60.0	60.0	60.0	60.0

For $-90^\circ \leq \alpha_{HTT} < -30^\circ$

$$\frac{L_{HT}}{\bar{q}}(\alpha_{HTT}, \delta_E)_0 = -90 - \alpha_{HTT}$$

For $30^\circ < \alpha_{HTT} \leq 90^\circ$

$$\frac{L_{HT}}{\bar{q}}(\alpha_{HTT}, \delta_E)_0 = 90 - \alpha_{HTT}$$

$$\frac{L_{HT}}{\bar{q}}(\alpha_{HTT}, \delta_E) = \frac{L_{HT}}{\bar{q}}(\alpha_{HTT}, \delta_E)_0 - (-1.27 + .62\,\alpha_W - .053\,i_W^2\,(\frac{i_W}{|i_W|}) - .021\,\delta_F\alpha_{WF})$$

TABLE 29.- Concluded.

(b) $\frac{D_{HT}}{\bar{q}}(\alpha_{HTT}, \delta_E) =$

For $-10^\circ + .25\,\delta_E \leq \alpha_{HTT} \leq 10^\circ + .25\,\delta_E$

$$\frac{D_{HT}}{\bar{q}}(\alpha_{HTT}, \delta_E) = .0434\,(\alpha_{HTT} - .25\,\delta_E)^2 - .013|\alpha_{HTT} - .25\,\delta_E| + 1.16 - .03743|\delta_E| + .00936\,\delta_E^2$$

For $-25^\circ + .25\,\delta_E \leq \alpha_{HTT} < -10^\circ + .25\,\delta_E$

or

$10^\circ + .25\,\delta_E < \alpha_{HTT} \leq 25^\circ + .25\,\delta_E$

$$\frac{D_{HT}}{\bar{q}}(\alpha_{HTT}, \delta_E) = -.049\,(\alpha_{HTT} - .25\,\delta_E)^2 + 3.6118|\alpha_{HTT} - .25\,\delta_E| - 25.489 + .00936\,\delta_E^2 - .03743|\delta_E|$$

For $-90^\circ \leq \alpha_{HTT} < -25^\circ + .25\,\delta_E$

or

$25^\circ + .25\,\delta_E < \alpha_{HTT} \leq 90^\circ$

$$\frac{D_{HT}}{\bar{q}}(\alpha_{HTT}, \delta_E) = 160\,\sin^2(\alpha_{HTT} - .25\,\delta_E) + 5.604$$

TABLE 30.- Helicopter Horizontal Tail Data.

(a) $\frac{L_{HTU}}{\bar{q}} (\alpha_{HTTU}) =$

α_{HTTU}	$\frac{L_{HTU}}{\bar{q}} (\alpha_{HTTU})$
-30	-17.80
-28	-18.40
-26	-19.00
-24	-19.50
-22	-20.10
-20	-20.60
-18	-21.40
-16	-22.00
-14	-21.50
-12	-18.75
-10	-16.00
-8	-12.80
-6	-9.60
-4	-6.40
-2	-3.20
0	0.00
2	3.20
4	6.40
6	9.60
8	12.80
10	16.00
12	18.75
14	21.50
16	22.00

TABLE 30.- Concluded.

α_{HTTU}	$\frac{L_{HTU}}{\bar{q}}(\alpha_{HTTU})$
18	21.40
20	20.60
22	20.10
24	19.50
26	19.00
28	18.40
30	17.80

For $-90^{\circ} \leq \alpha_{HTTU} < -30^{\circ}$

$$\frac{L_{HTU}}{\bar{q}}(\alpha_{HTTU}) = -.2967\ (90 + \alpha_{HTTU})$$

For $30^{\circ} < \alpha_{HTTU} \leq 90^{\circ}$

$$\frac{L_{HTU}}{\bar{q}}(\alpha_{HTTU}) = .2967\ (90 - \alpha_{HTTU})$$

(b) $\frac{D_{HTU}}{\bar{q}}(\alpha_{HTTU}) =$

For $-10^{\circ} \leq \alpha_{HTTU} \leq 10^{\circ}$

$$\frac{D_{HTU}}{\bar{q}}(\alpha_{HTTU}) = .0138\ \alpha_{HTTU}^2 - .003|\alpha_{HTTU}| + .33$$

For $-90^{\circ} \leq \alpha_{HTTU} < -10^{\circ}$ or $10^{\circ} < \alpha_{HTTU} \leq 90^{\circ}$

$$\frac{D_{HTU}}{\bar{q}}(\alpha_{HTTU}) = 56.64\ \sin^2(\alpha_{HTTU}) - .023$$

TABLE 31.- Fixed Wing Upper Horizontal Tail Data.

(a) $\frac{L_{HTU}}{\bar{q}}(\alpha_{HTTU}) =$

α_{HTTU}	$\frac{L_{HTU}}{\bar{q}}(\alpha_{HTTU})$
-30	-11.4
-28	-11.7
-26	-12.0
-24	-12.2
-22	-12.3
-20	-12.4
-18	-12.4
-16	-12.2
-14	-11.9
-12	-11.4
-10	-10.5
-8	-8.8
-6	-6.6
-4	-4.4
-2	-2.2
0	0
2	2.2
4	4.4
6	6.6
8	8.8

TABLE 31.- Concluded.

α_{HTTU}	$\frac{L_{HTU}}{\bar{q}}(\alpha_{HTTU})$
10	10.5
12	11.4
14	11.9
16	12.2
18	12.4
20	12.4
22	12.3
24	12.2
26	12.0
28	11.7
30	11.4

For $-90^{\circ} \leq \alpha_{HTTU} < -30^{\circ}$

$$\frac{L_{HTU}}{\bar{q}}(\alpha_{HTTU}) = -.173(90 + \alpha_{HTTU})$$

For $30^{\circ} < \alpha_{HTTU} \leq 90^{\circ}$

$$\frac{L_{HTU}}{\bar{q}}(\alpha_{HTTU}) = .19(90 - \alpha_{HTTU})$$

(b) $\frac{D_{HTU}}{\bar{q}}(\alpha_{HTTU}) =$

For $-10^{\circ} \leq \alpha_{HTTU} \leq 10^{\circ}$

$$\frac{D_{HTU}}{\bar{q}}(\alpha_{HTTU}) = .62 - .086|\alpha_{HTTU}| + .0272\,\alpha^2_{HTTU}$$

For $-90^{\circ} \leq \alpha_{HTTU} < -10^{\circ}$ or $10^{\circ} < \alpha_{HTTU} \leq 90^{\circ}$

$$\frac{D_{HTU}}{\bar{q}}(\alpha_{HTTU}) = 27.176 \sin^2(\alpha_{HTTU}) + 1.661$$

TABLE 32.- Helicopter-Fixed Wing Vertical Tail Data.

(a) $\frac{L_{VT}}{\bar{q}}(\alpha_{VTT}, \delta_R)$ =

α_{VTT} \ δ_R	-30	-20	-10	0	10	20	30
-30	-80	-80	-80	-80	-80	-80	-80
-25	-99	-93	-89	-81	-80	-79	-69
-20	-94	-86	-78	-70	-62	-55	-48
-15	-80	-70	-62	-52	-45	-34	-27
-10	-64	-55	-46	-35	-28	-16	-7
-5	-48	-38	-29	-18	-8	2	12
0	-30	-20	-10	0	10	20	30
5	-8	0	10	18	28	36	46
10	12	20	29	36	44	52	63
15	32	40	47	52	60	68	76
20	52	58	64	70	76	82	89
25	71	76	80	84	87	92	99
30	80	80	80	80	80	80	80

For $-90^\circ \leq \alpha_{VTT} < -30^\circ$

$$\frac{L_{VT}}{\bar{q}}(\alpha_{VTT}, \delta_R) = -1.33\ (90 + \alpha_{VTT})$$

For $30^\circ < \alpha_{VTT} \leq 90^\circ$

$$\frac{L_{VT}}{\bar{q}}(\alpha_{VTT}, \delta_R) = 1.33\ (90 - \alpha_{VTT})$$

TABLE 32.- Continued.

(b) $\frac{D_{VT}}{\bar{q}}(\alpha_{VTT}, \delta_R) =$

For $-20^\circ \leq \alpha_{VTT} \leq 20^\circ$

$$\frac{D_{VT}}{\bar{q}}(\alpha_{VTT}, \delta_R) = .0031529 \left(\frac{L_{VT}}{\bar{q}}(\alpha_{VTT}, \delta_R)\right)^2 - .018652 \left(\frac{L_{VT}}{\bar{q}}(\alpha_{VTT}, \delta_R)\right) + 2.93 + .00465\,\delta_R^2 - .0305\,|\delta_R|$$

For $-90^\circ \leq \alpha_{VTT} < -20^\circ$

or

$20^\circ < \alpha_{VTT} \leq 90^\circ$

$$\frac{D_{VT}}{\bar{q}}(\alpha_{VTT}, \delta_R) = 203 \sin^2(\alpha_{VTT}) - 2.38 + .4\,\delta_R \left(\frac{\alpha_{VTT}}{|\alpha_{VTT}|}\right)$$

TABLE 32.- Concluded.

(c) $\frac{L_{MVT}}{\bar{q}}(\alpha_{VTT}, \delta_R)$ =

α_{VTT} \ δ_R	-30	-20	-10	0	10	20	30
-30	300	300	300	300	300	300	300
-25	480	470	460	420	380	360	320
-20	520	470	410	380	330	280	240
-15	400	340	290	250	200	160	120
-10	320	270	210	160	110	60	10
-5	230	160	110	70	20	-40	-90
0	140	70	20	-20	-70	-130	-180
5	50	-30	-30	-120	-180	-230	-290
10	-70	-150	-190	-220	-280	-340	-400
15	-190	-270	-310	-350	-410	-460	-500
20	-330	-390	-440	-480	-530	-570	-600
25	-400	-430	-460	-490	-500	-530	-560
30	-400	-400	-400	-400	-400	-400	-400

For $-90^\circ \leq \alpha_{VTT} < -30^\circ$

$$\frac{L_{MVT}}{\bar{q}}(\alpha_{VTT}, \delta_R) = 450 + 5\,\alpha_{VTT}$$

For $30^\circ < \alpha_{VTT} \leq 90^\circ$

$$\frac{L_{MVT}}{\bar{q}}(\alpha_{VTT}, \delta_R) = -600.1 + 6.67\,\alpha_{VTT}$$

TABLE 33.- Drag Brake Data.

(a) $\frac{L_{DB}}{\bar{q}} (\delta_{DB}) =$

For $0^{o} \leq \delta_{DB} \leq 55^{o}$

$\frac{L_{DB}}{\bar{q}} (\delta_{DB}) = 0.$

(b) $\frac{D_{DB}}{\bar{q}} (\delta_{DB}) =$

For $0^{o} \leq \delta_{DB} \leq 55^{o}$

$\frac{D_{DB}}{\bar{q}} (\delta_{DB}) = .25\ \delta_{DB}$

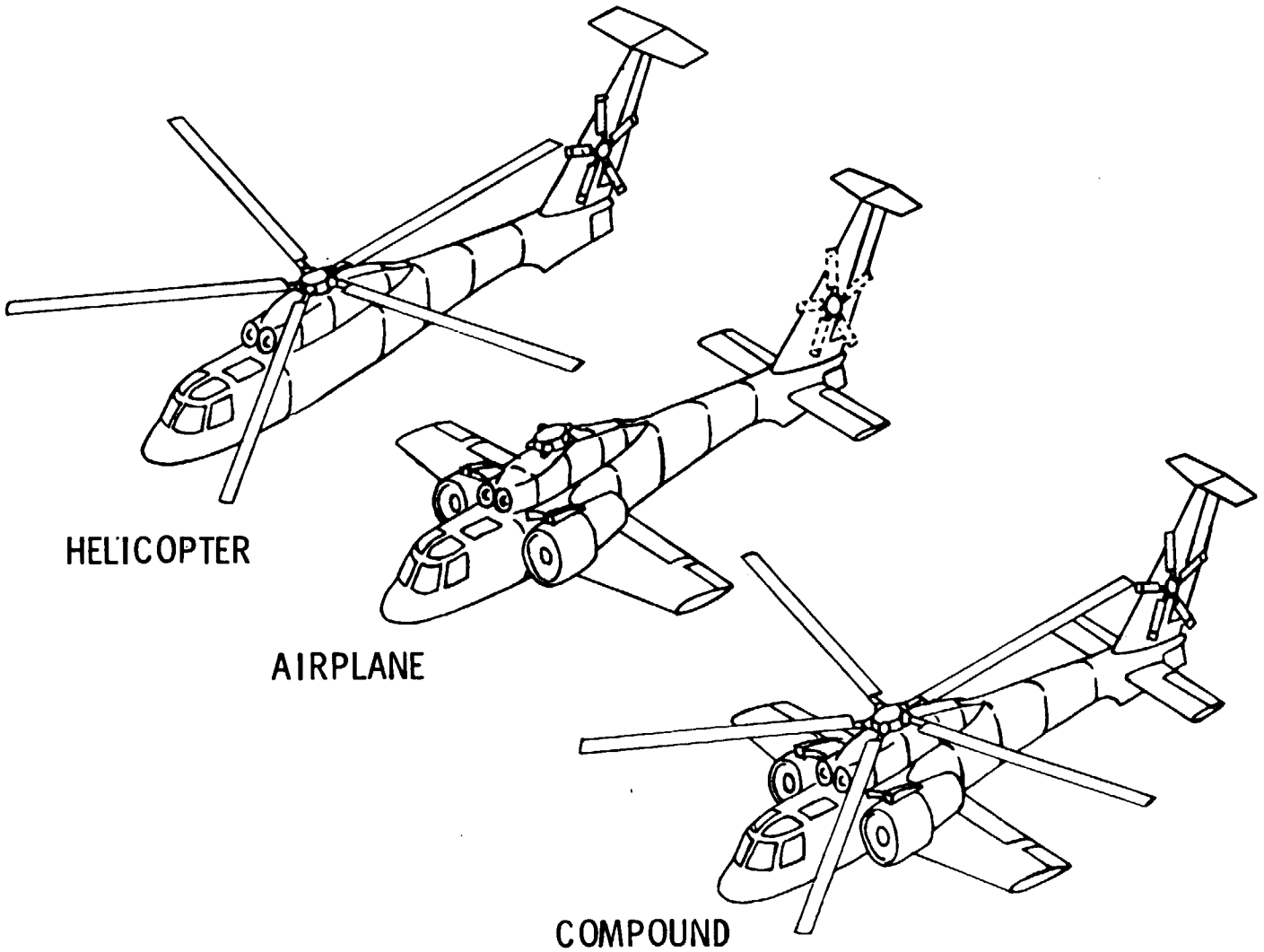

FIGURE 1. - RSRA Configurations Simulated.

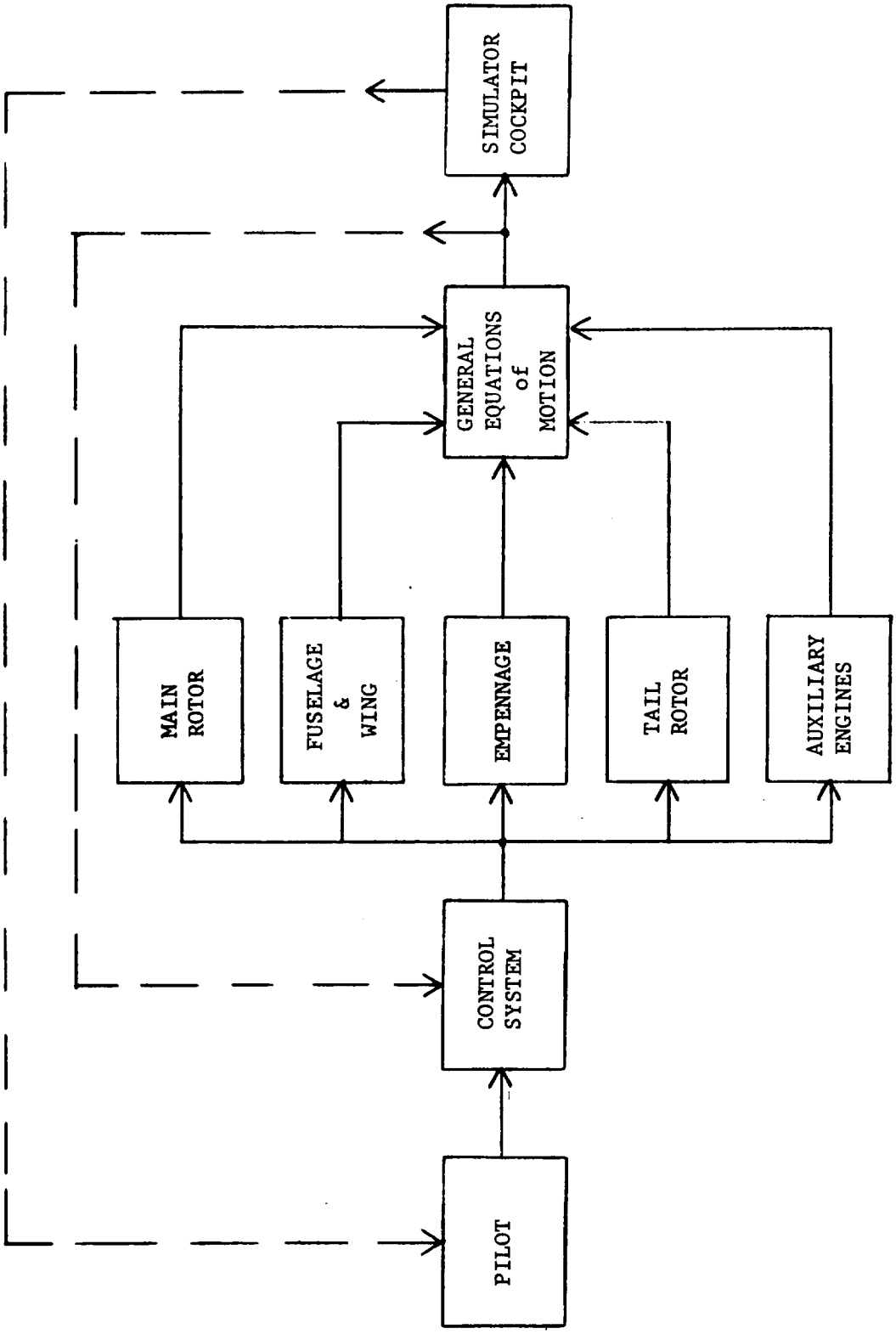

FIGURE 2. - Simplified Block Diagram of RSRA Simulation.

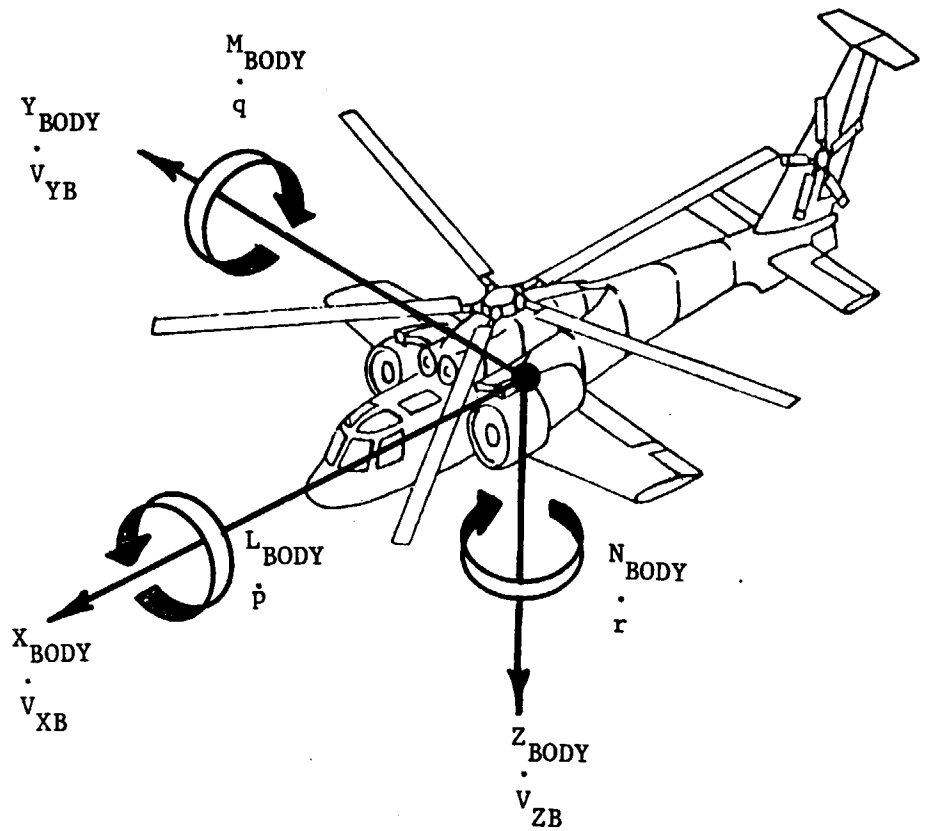

FIGURE 3. - Body Axes System.

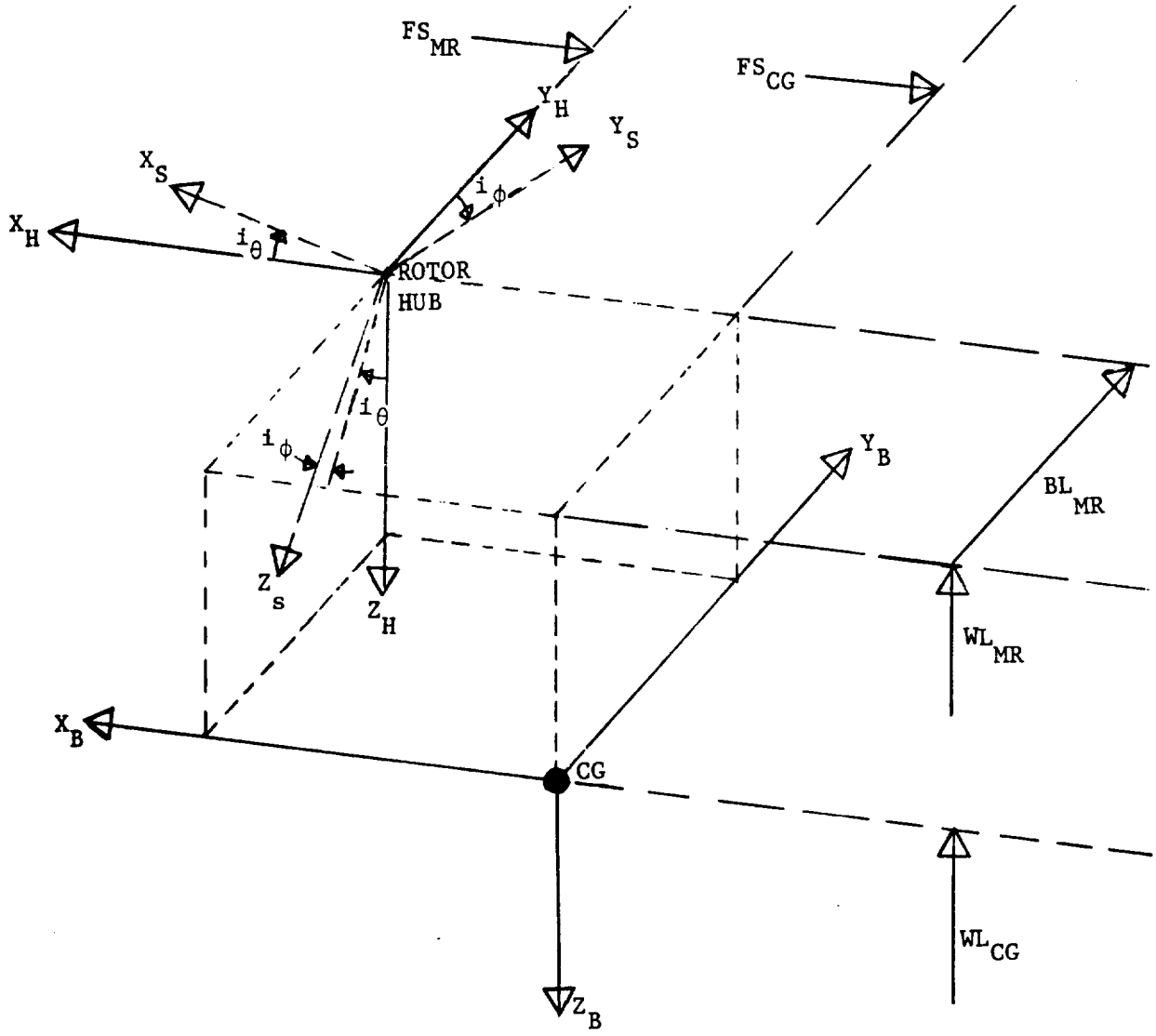

X_B, Y_B, Z_B	Body Axes System
X_H, Y_H, Z_H	Hub Axes System
X_S, Y_S, Z_S	Shaft Axes System

FIGURE 4. - Body Axes to Shaft Axes Transformation.

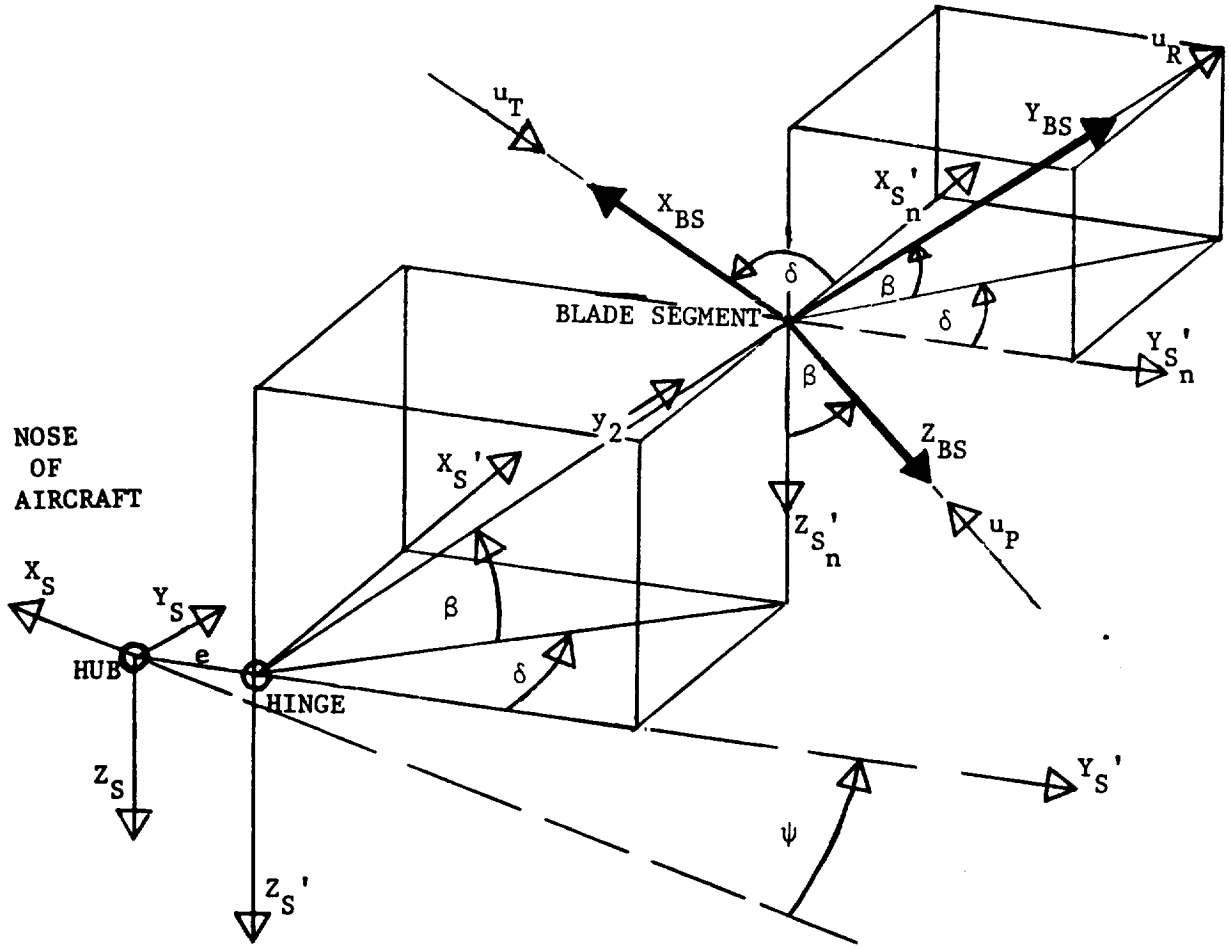

X_S, Y_S, Z_S	Shaft Axes System
X_S', Y_S', Z_S'	Rotating Shaft Axes System
X_{BS}, Y_{BS}, Z_{BS}	Blade Span Axes System

u_T, u_R, u_P Blade Element Velocities along X_{BS}, Y_{BS}, Z_{BS} respectively

δ and β are Euler Angles with δ rotation about Z_S', then β rotation about X_{BS}

FIGURE 5. - Shaft Axes to Rotating Blade Span Axes Transformation.

$$\alpha_Y = \phi_Y + \theta_Y$$

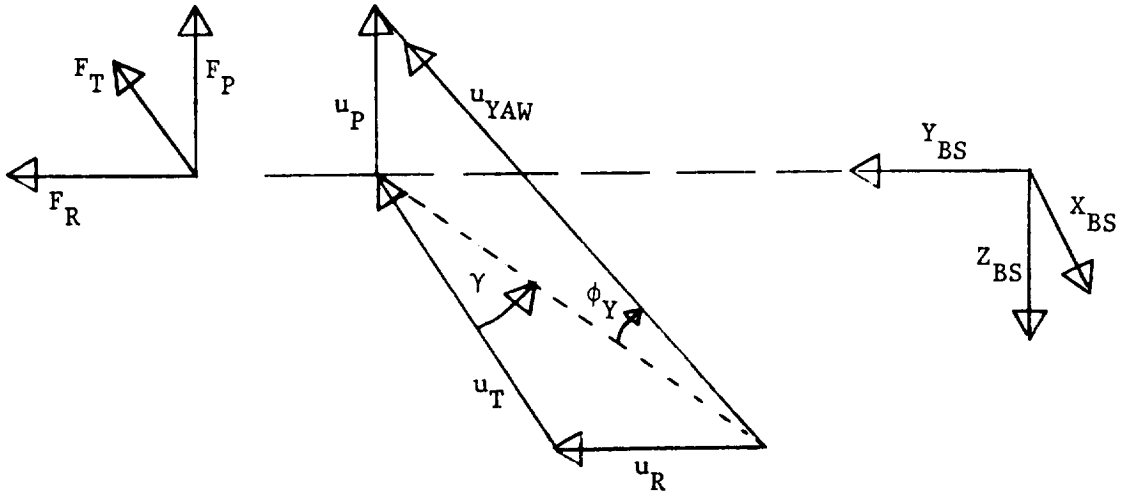

a) INFLOW COMPONENT

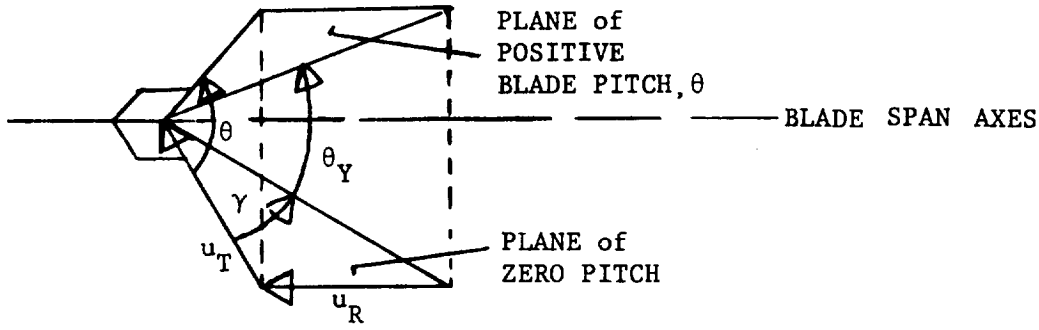

b) BLADE PITCH COMPONENT

X_{BS}, Y_{BS}, Z_{BS} Blade Span Axes System

FIGURE 6. - Definition of Yawed Angle of Attack, α_Y.

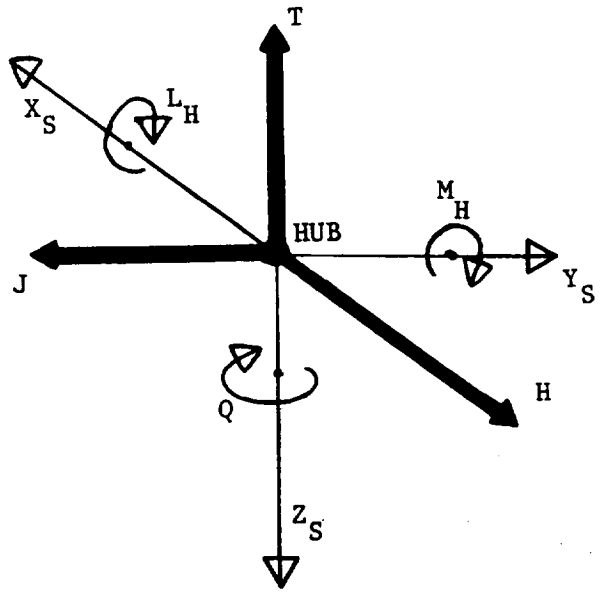

X_S, Y_S, Z_S Shaft Axes System

FIGURE 7. - Total Rotor Forces and Moments in the Fixed Shaft Axes System.

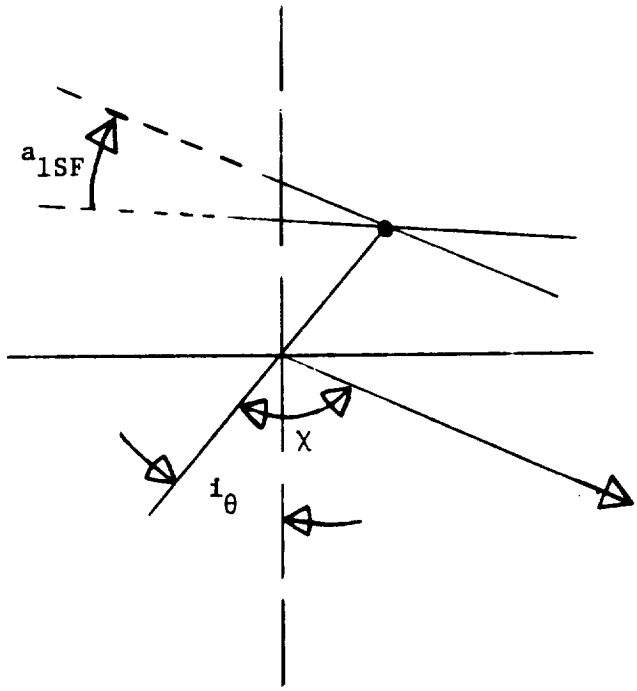

FIGURE 8. - Rotor Wake Skew Angle.

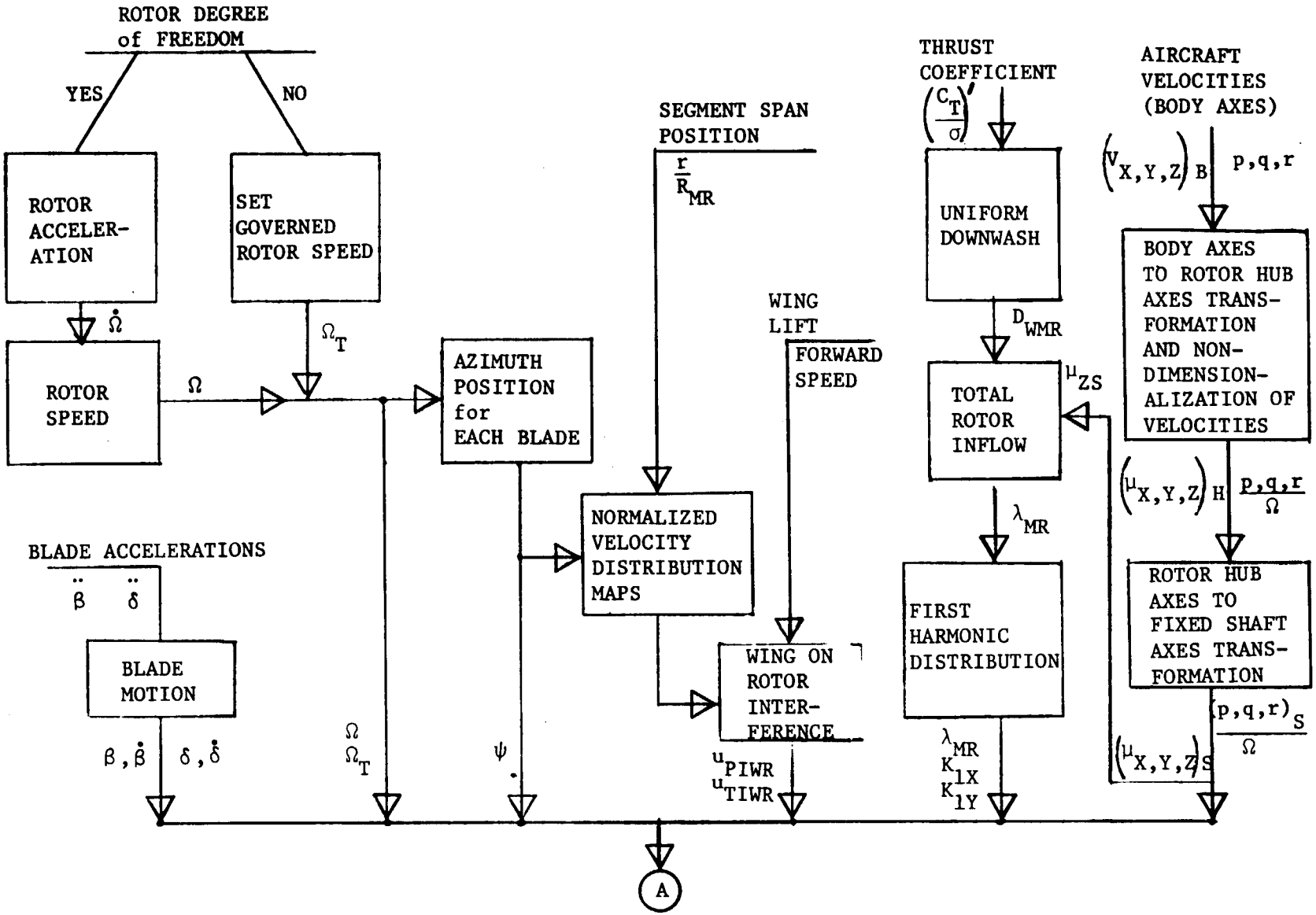

FIGURE 9. - Rotor Model Block Diagram.

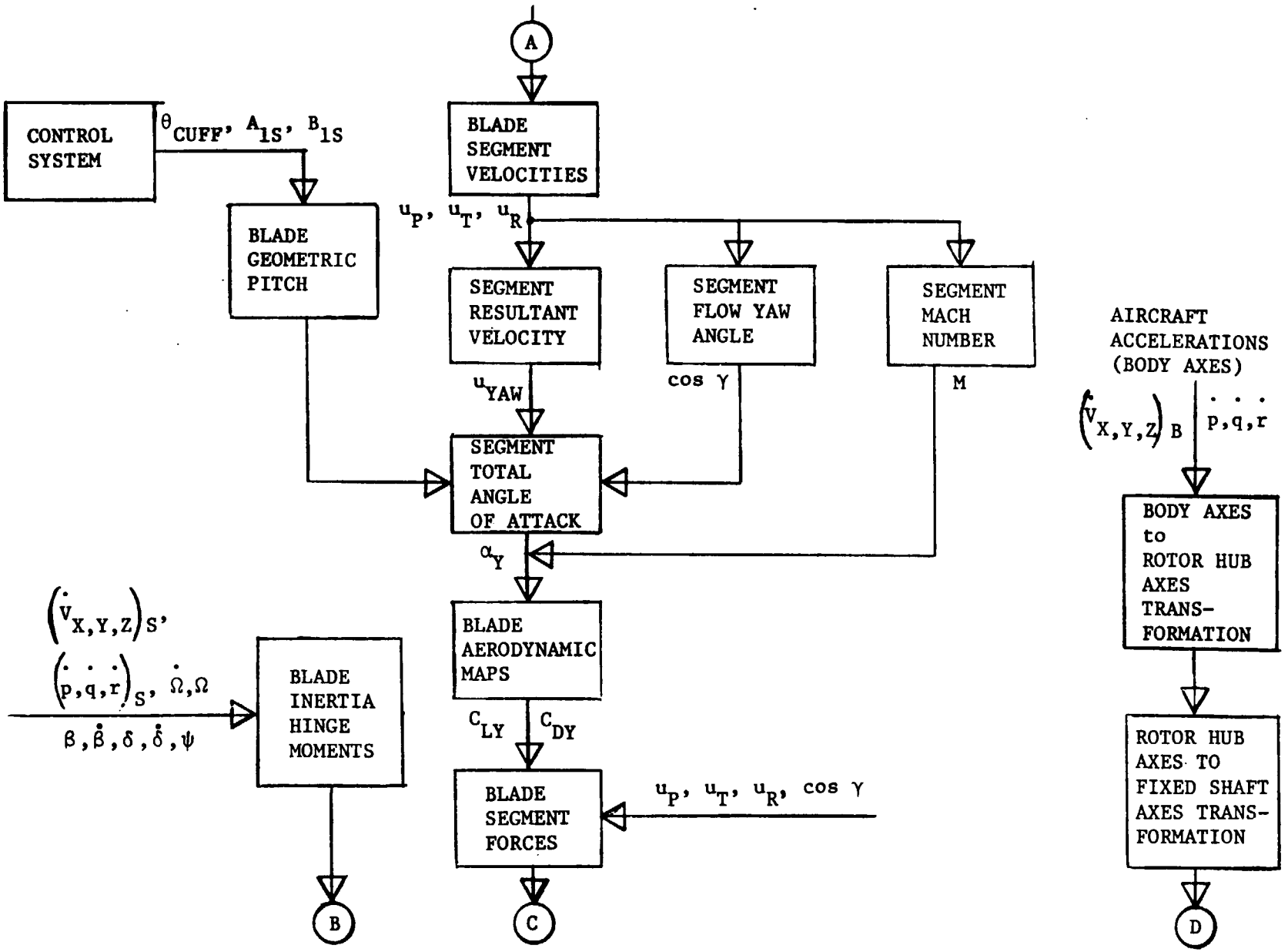

FIGURE 9. - Continued.

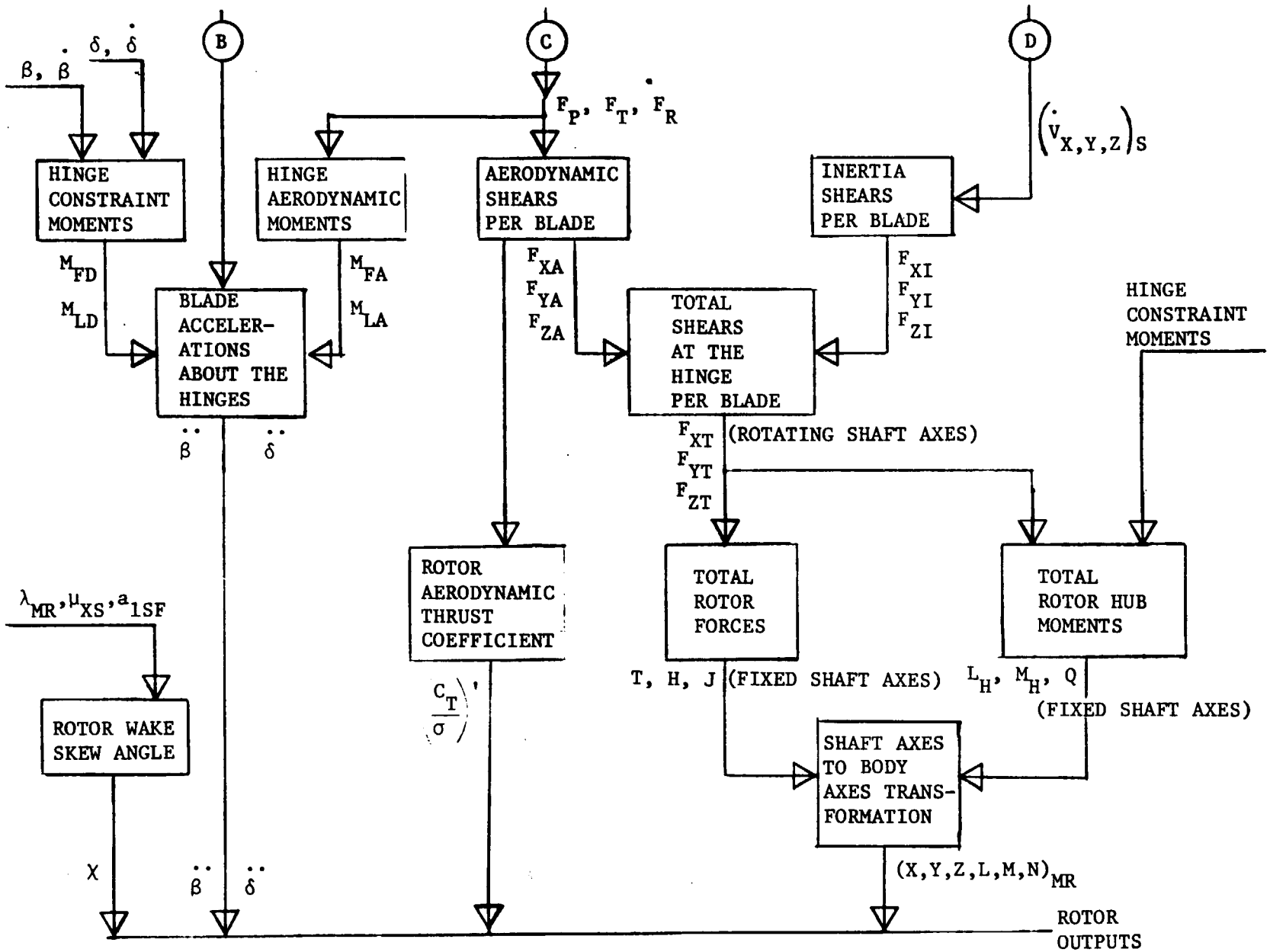

FIGURE 9. - Concluded.

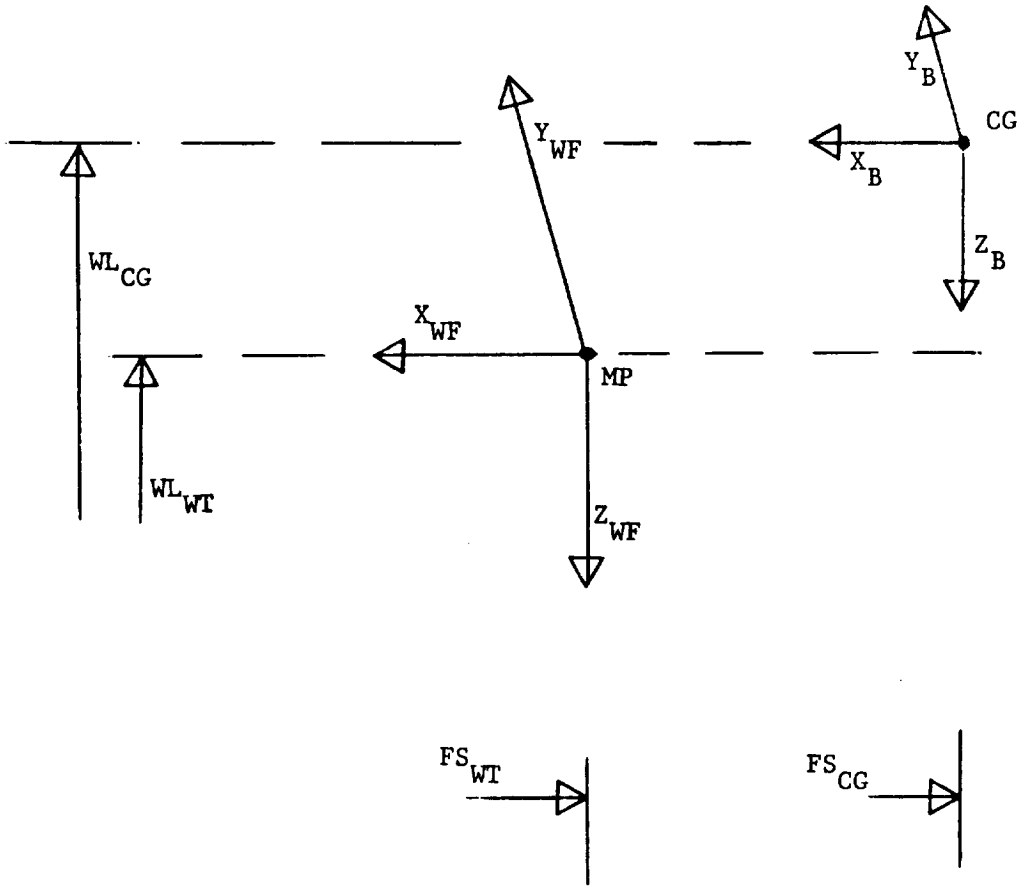

X_B, Y_B, Z_B Body Axes System

FIGURE 10. - Fuselage Geometry.

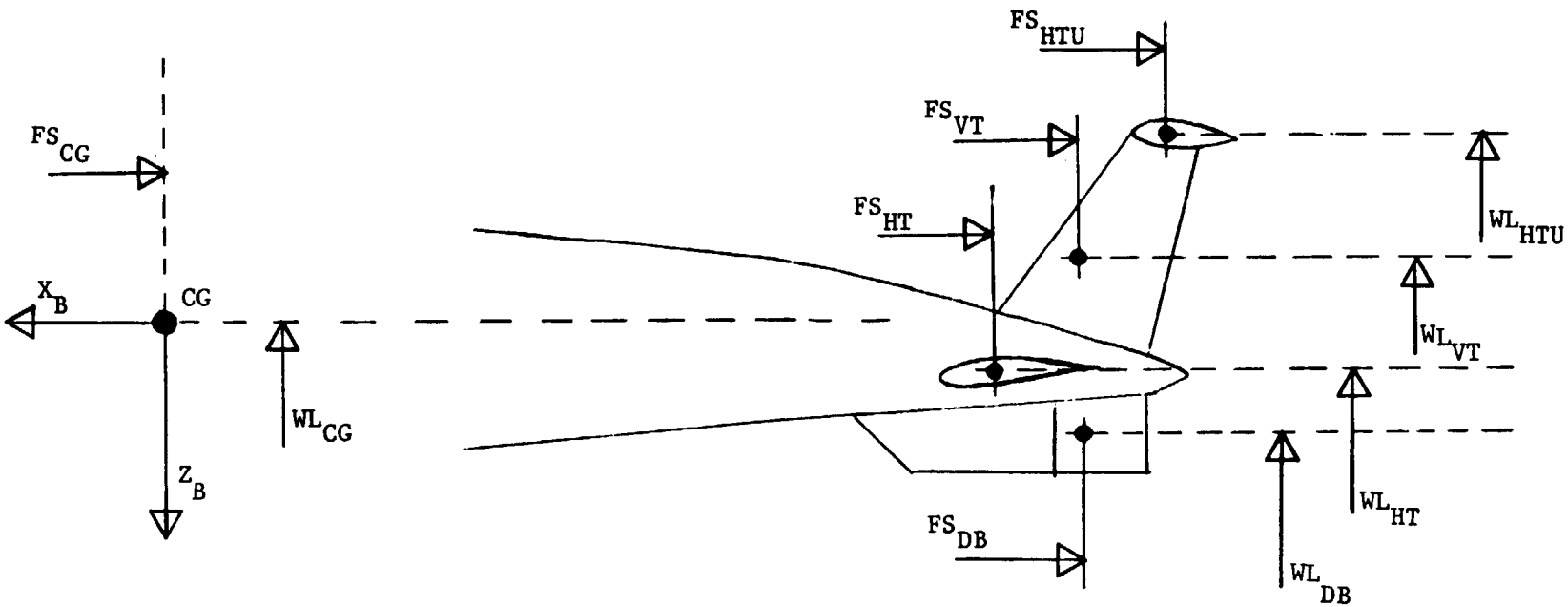

X_B, Y_B, Z_B Body Axes System

FIGURE 11. - Empennage Geometry.

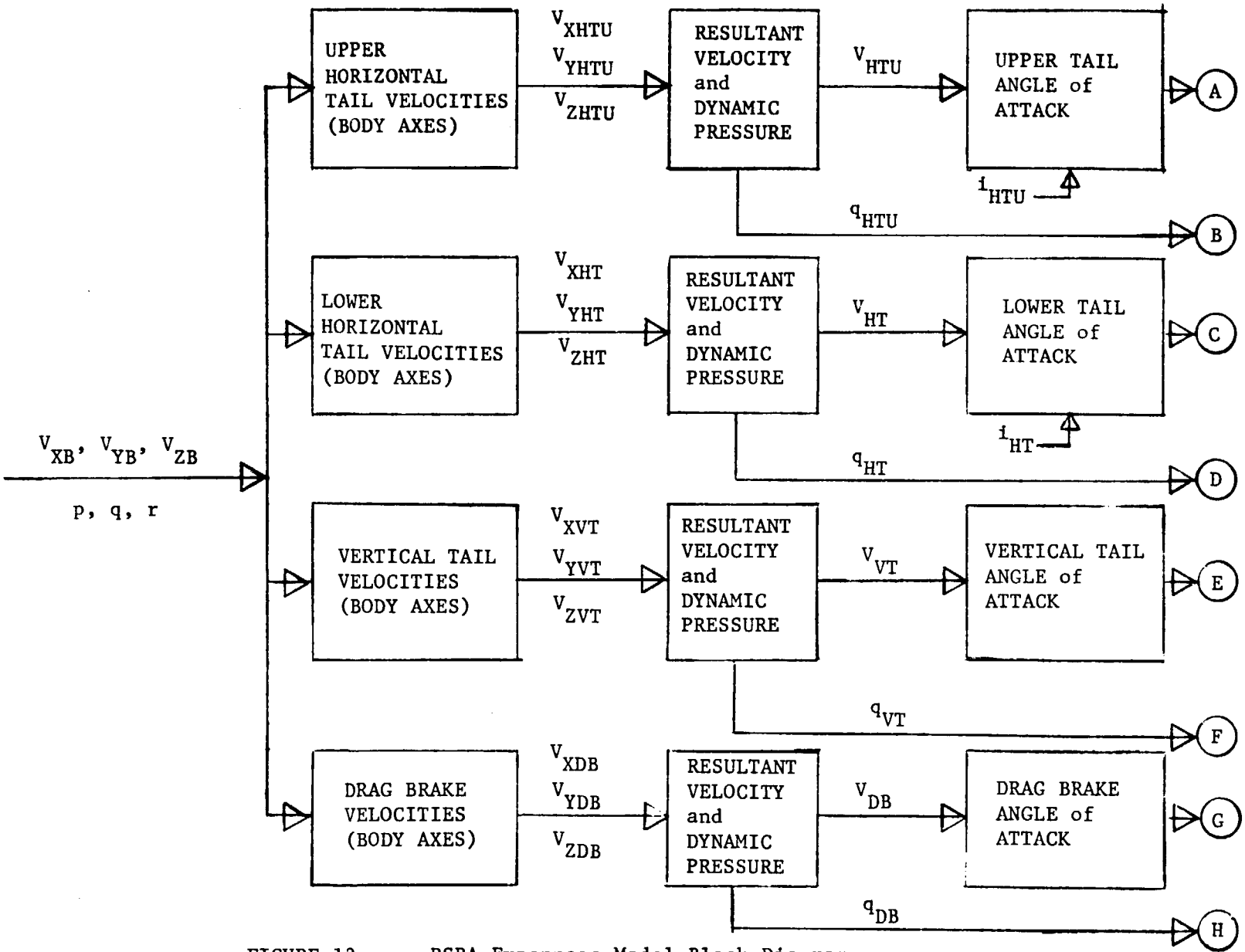

FIGURE 12. - RSRA Empennage Model Block Diagram.

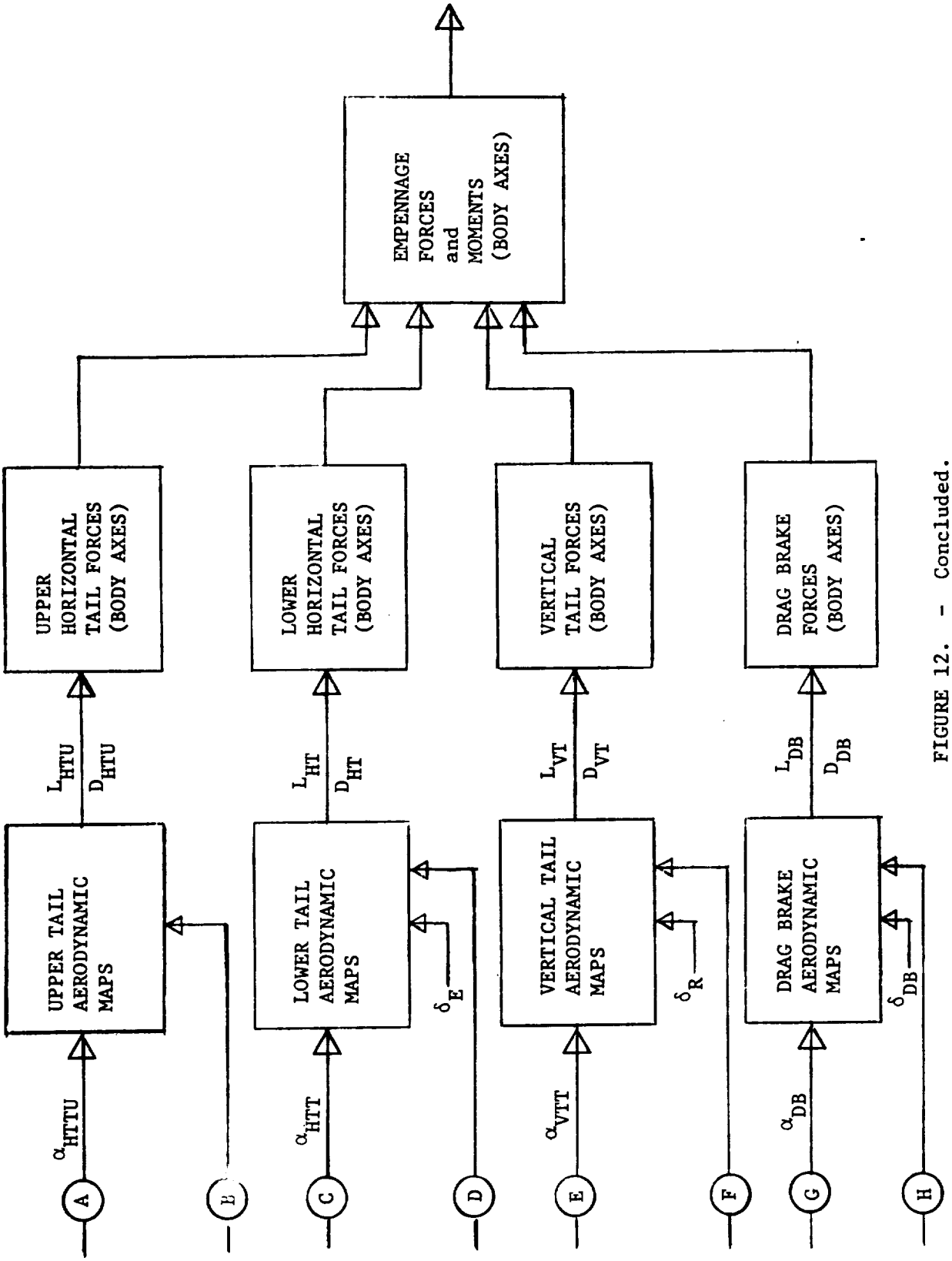

FIGURE 12. - Concluded.

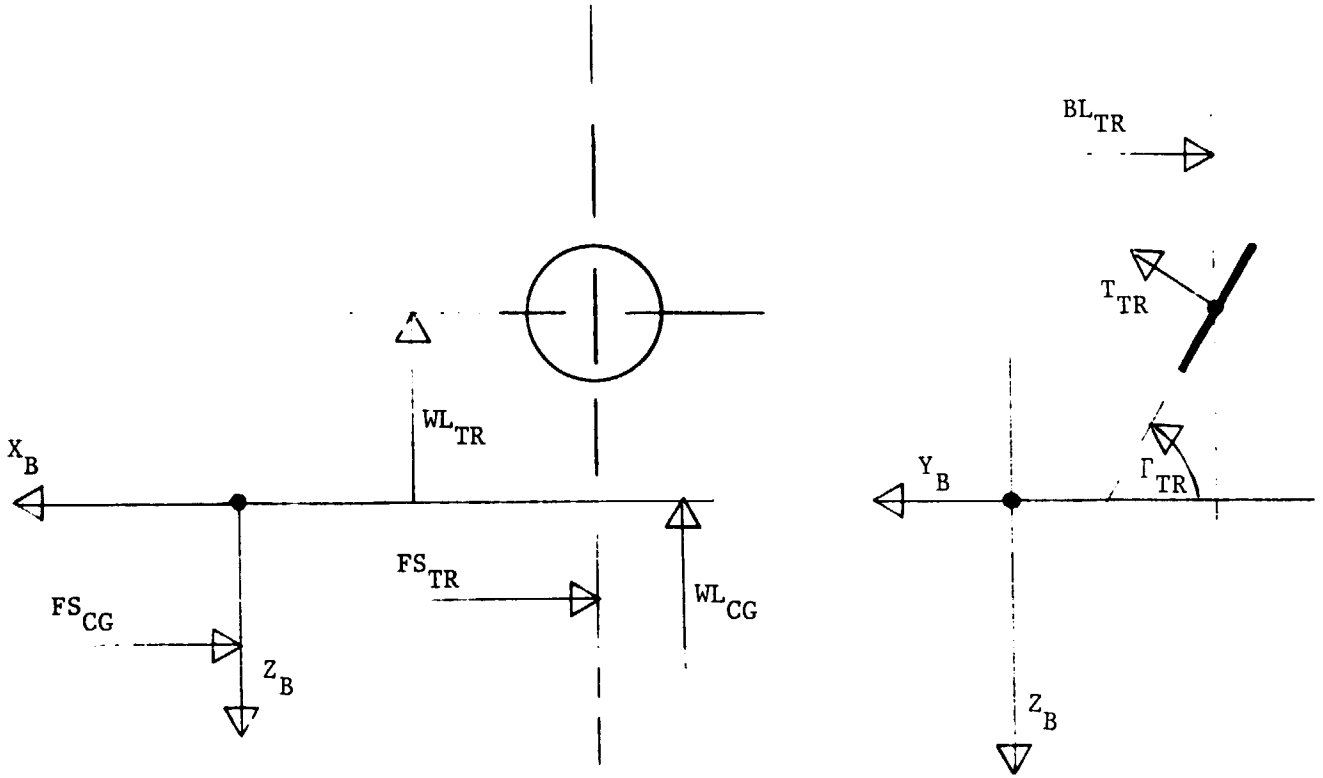

X_B, Y_B, Z_B Body Axes System

FIGURE 13. - Tail Rotor Geometry.

C-3

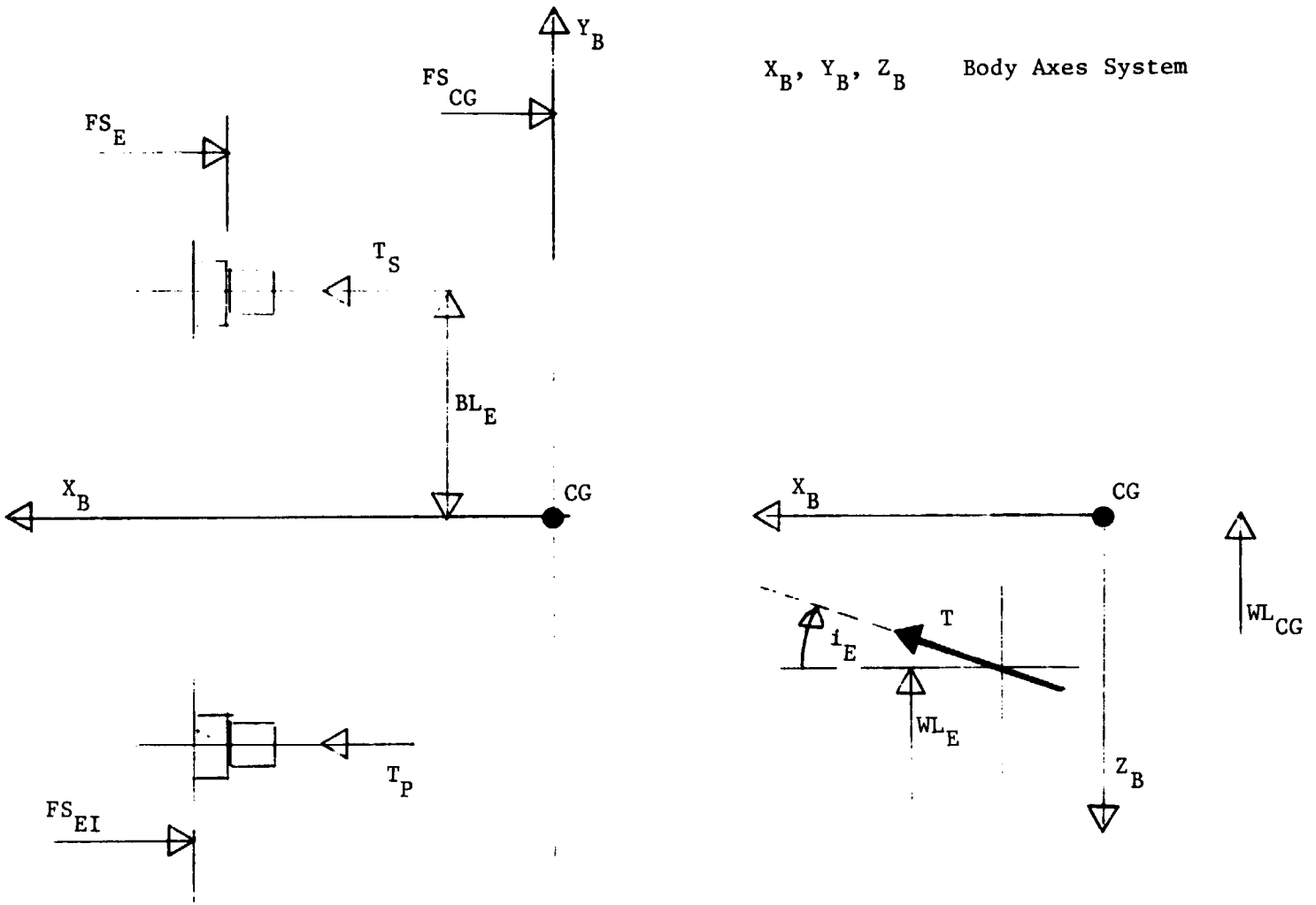

FIGURE 14. - Auxiliary Engine Geometry.

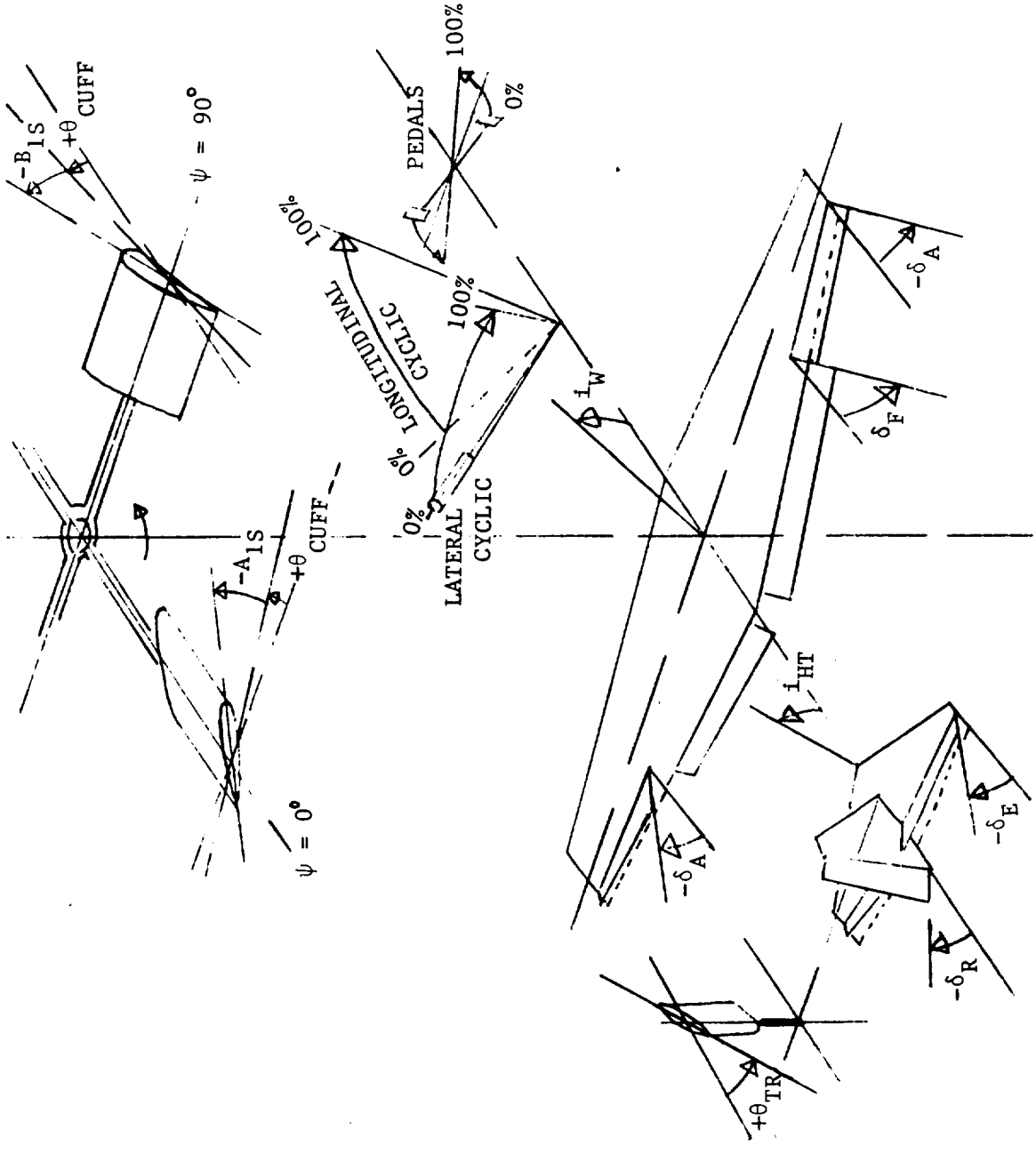

FIGURE 15. - Control System Sign Convention.

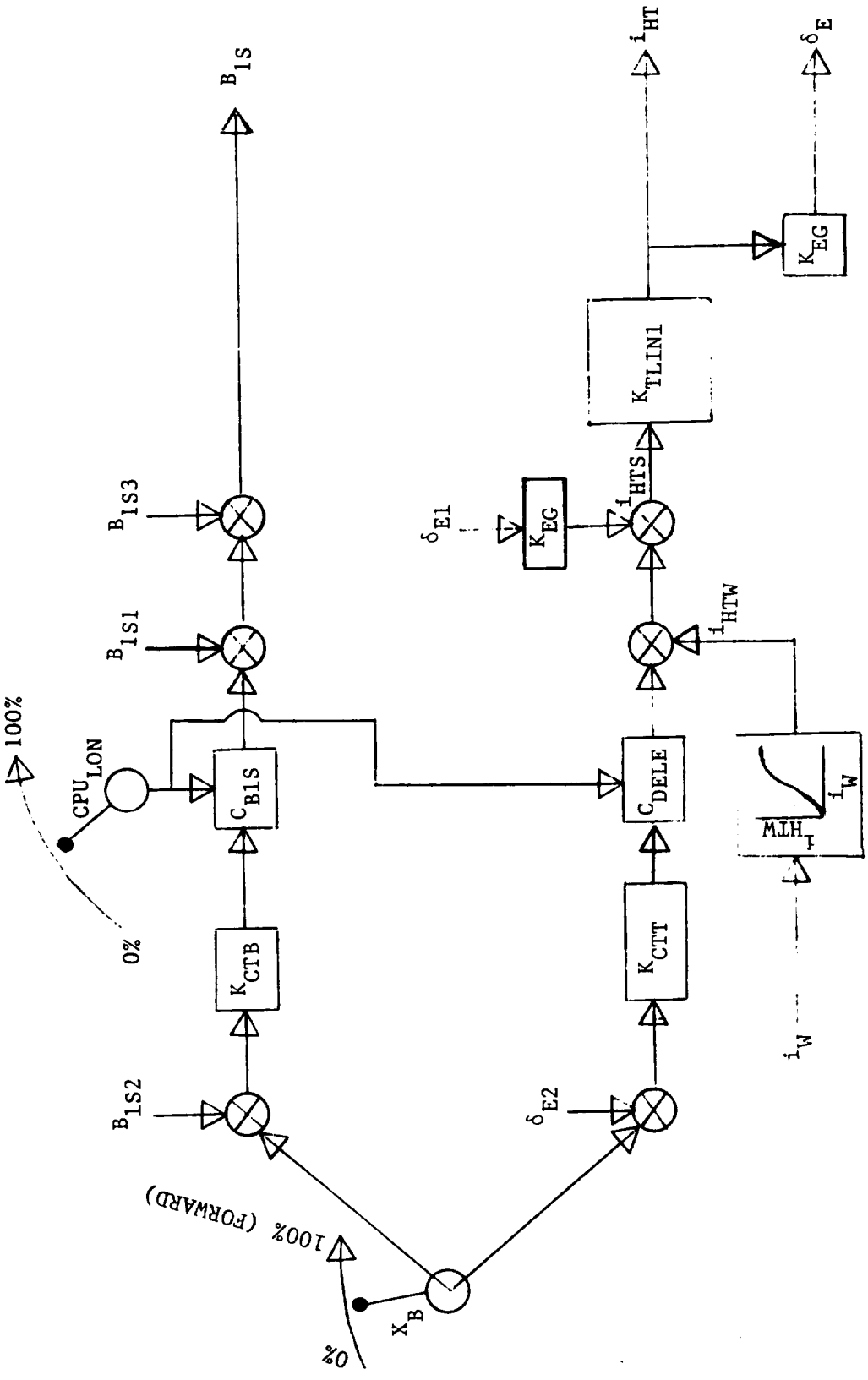

FIGURE 16. - Longitudinal Control System.

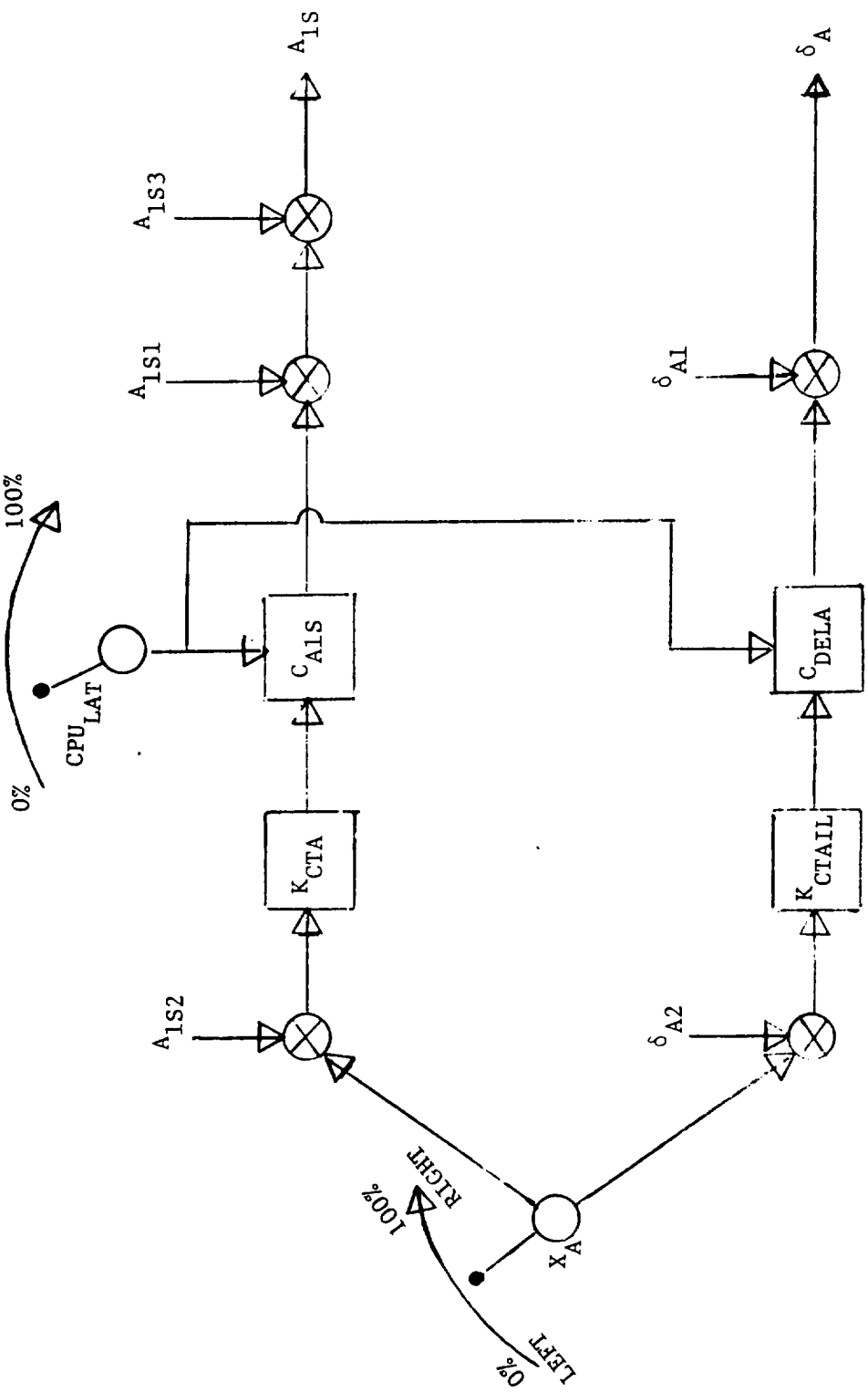

FIGURE 17. - Lateral Control System.

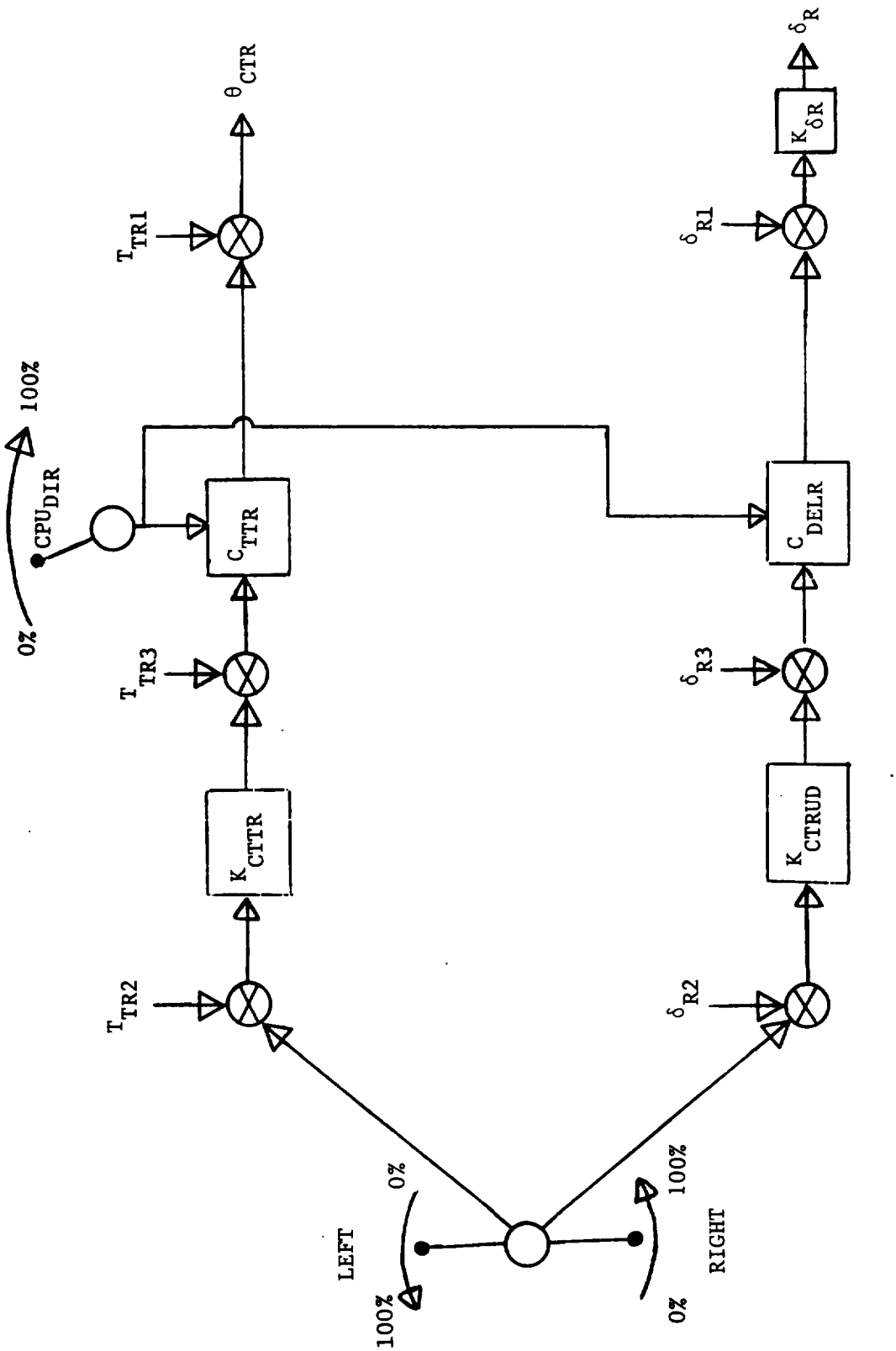

FIGURE 18. - Directional Control System.

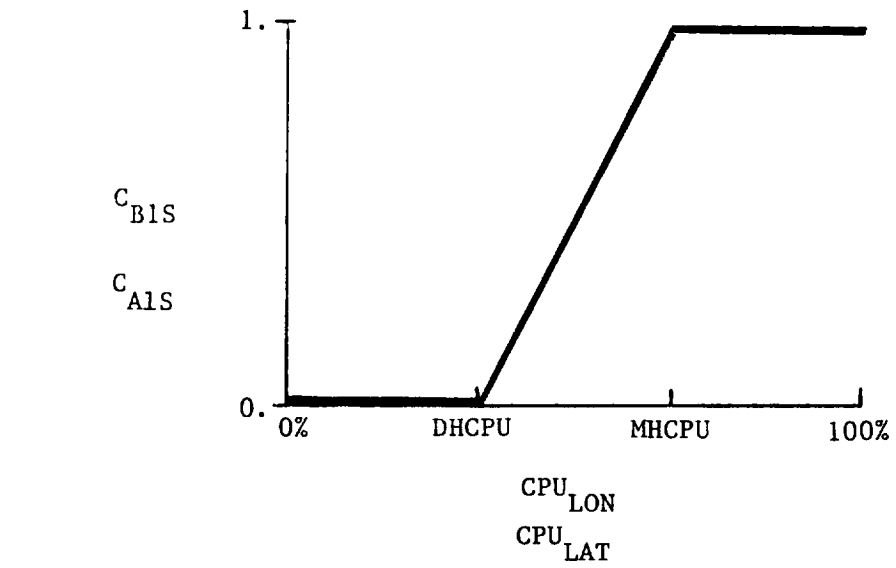

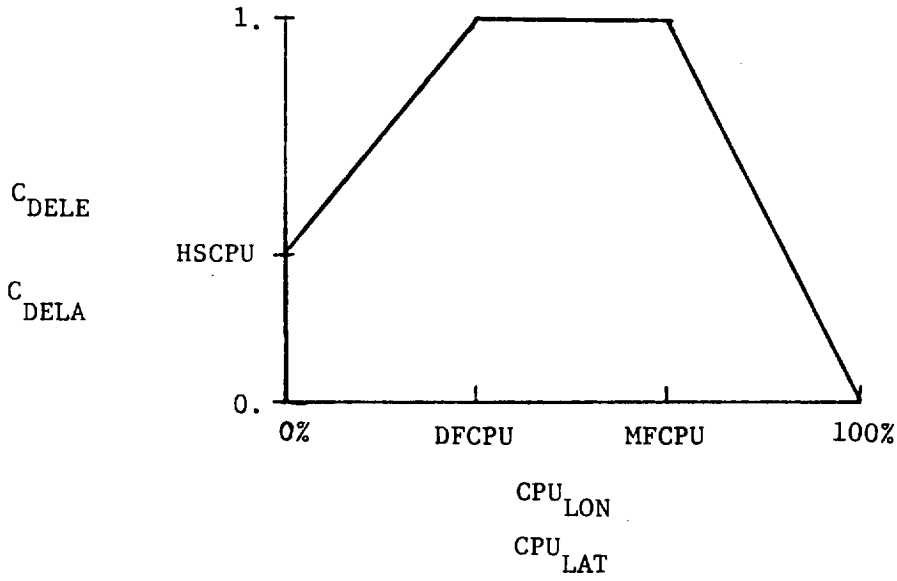

FIGURE 19. - Control Phasing Unit (CPU) Schedules.

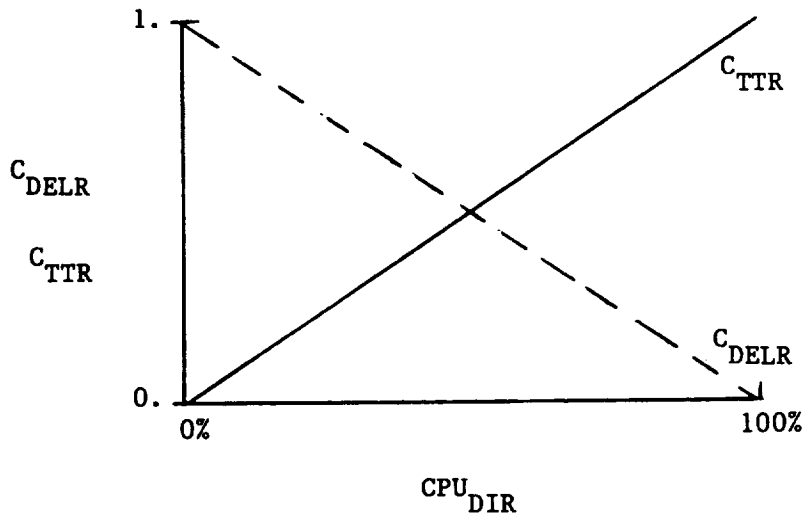

FIGURE 19. - Concluded.

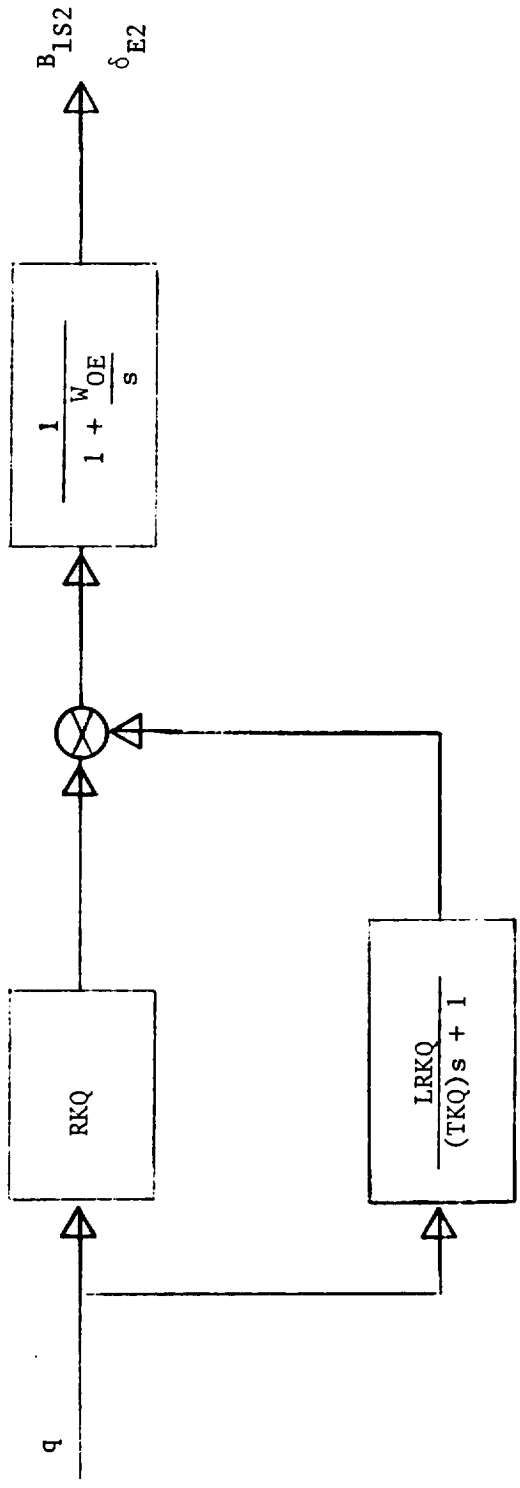

FIGURE 20. - Pitch SAS Channel.

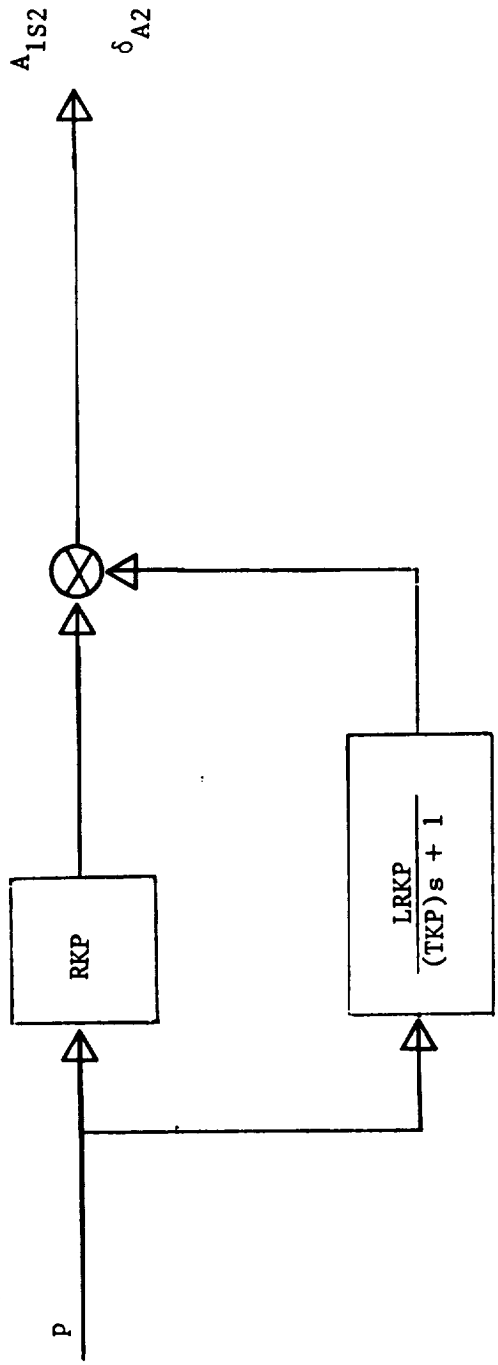

FIGURE 21. - Roll SAS Channel.

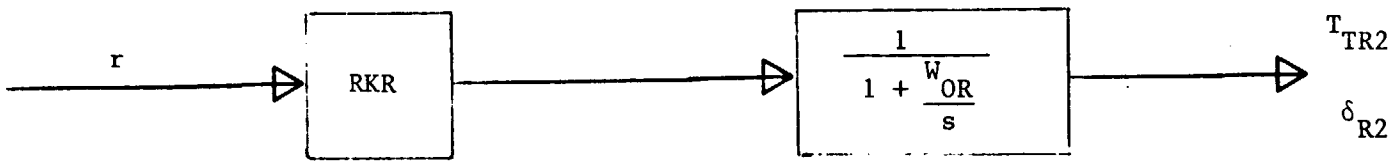

FIGURE 22. - Yaw SAS Channel.

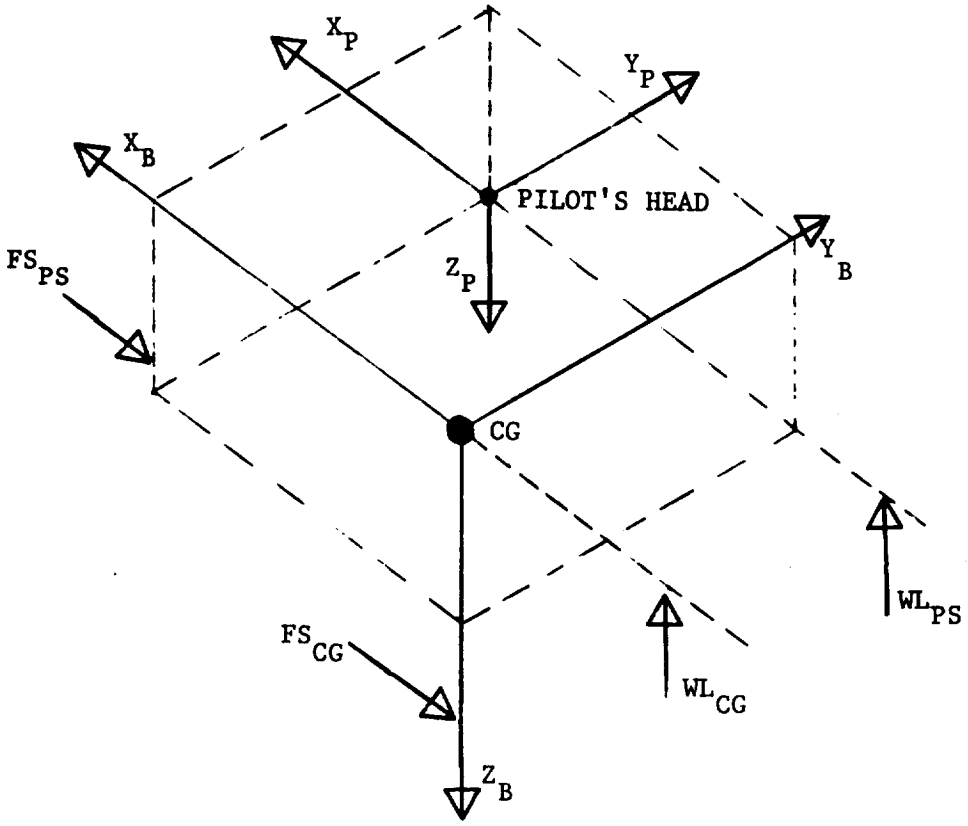

X_B, Y_B, Z_B Body Axes System

X_P, Y_P, Z_P Pilot Axes System

FIGURE 23. - Pilot Station Geometry.

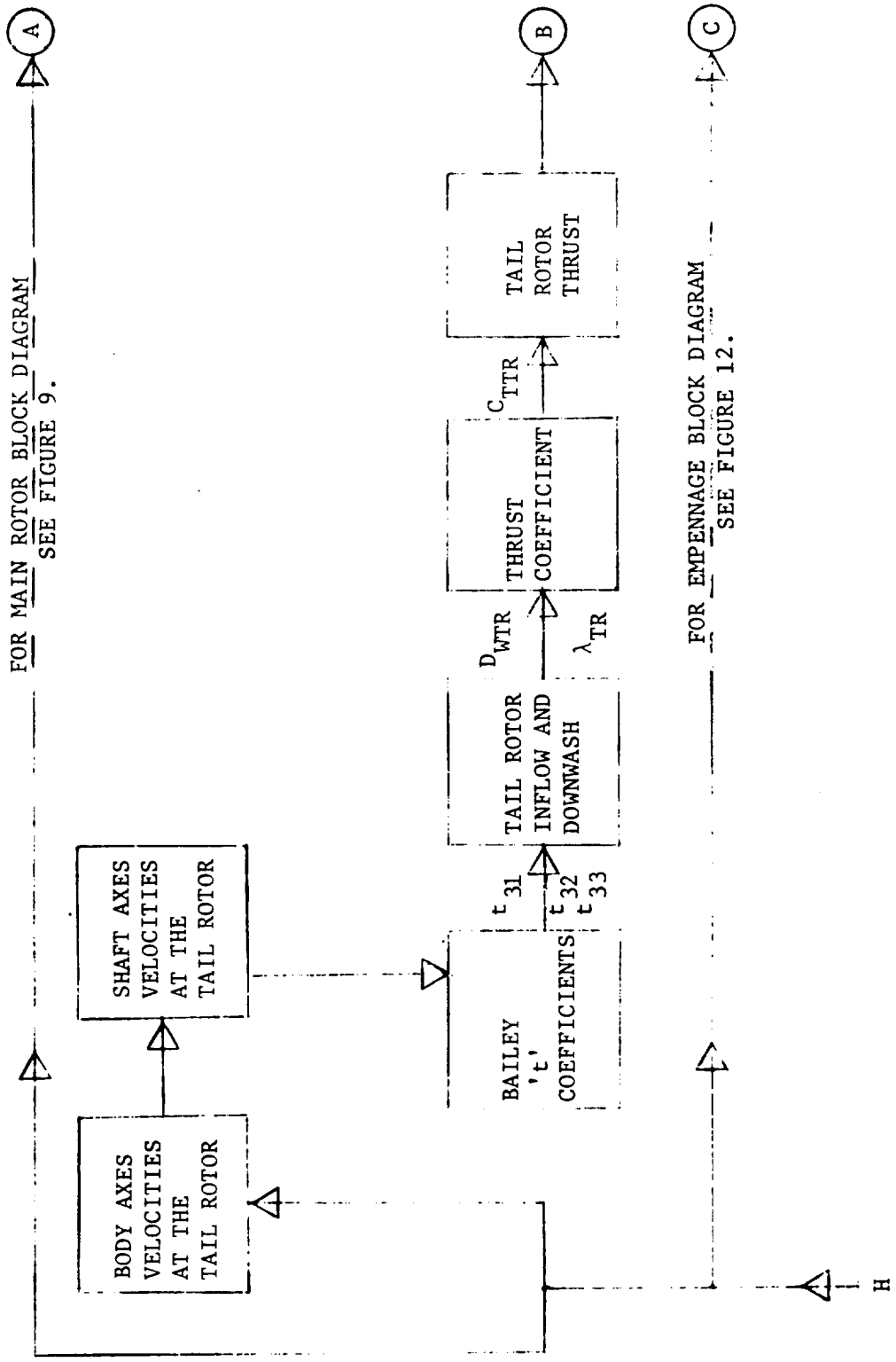

FIGURE 24. - RSRA Simulation Block Diagram.

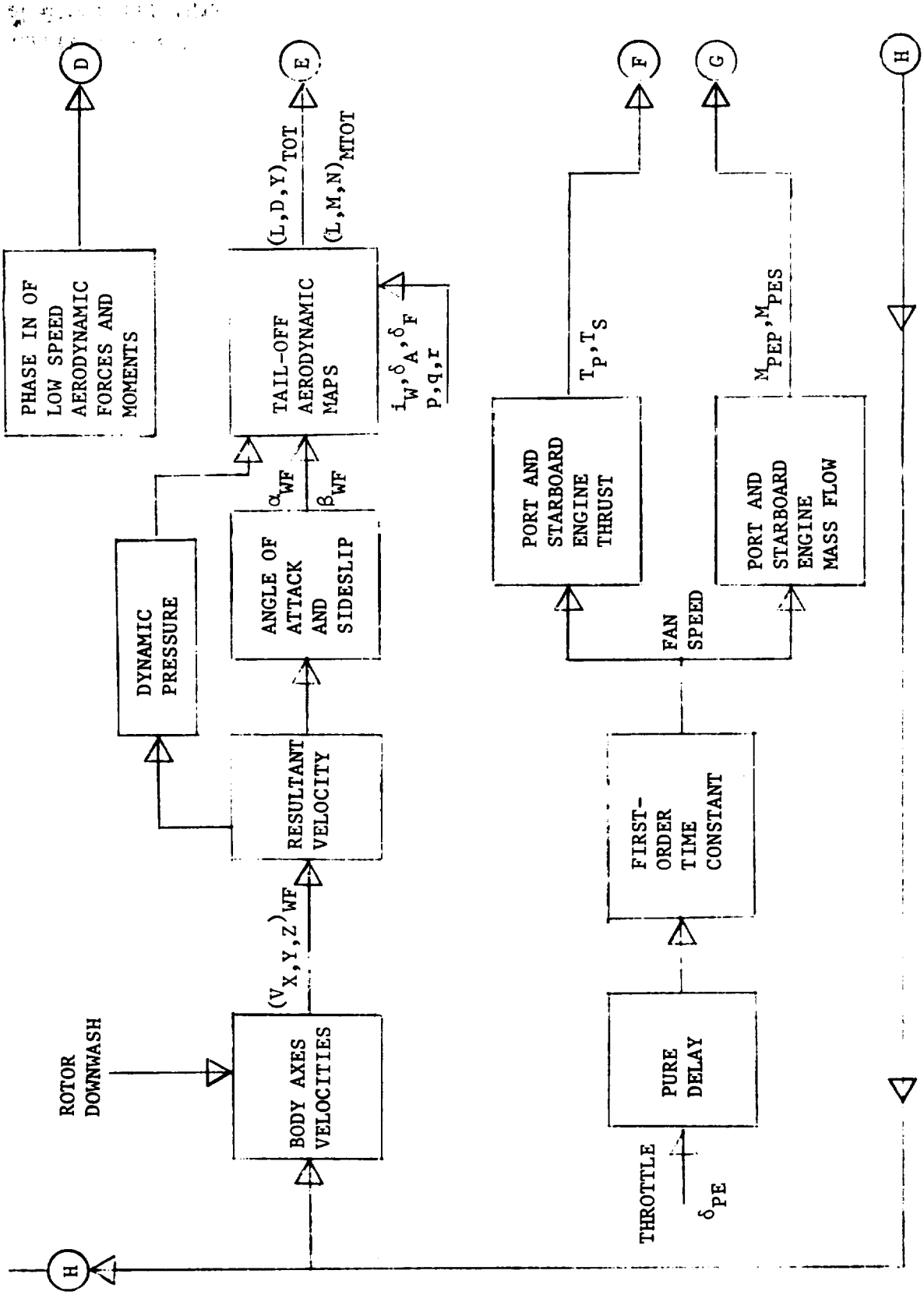

FIGURE 24. - Continued.

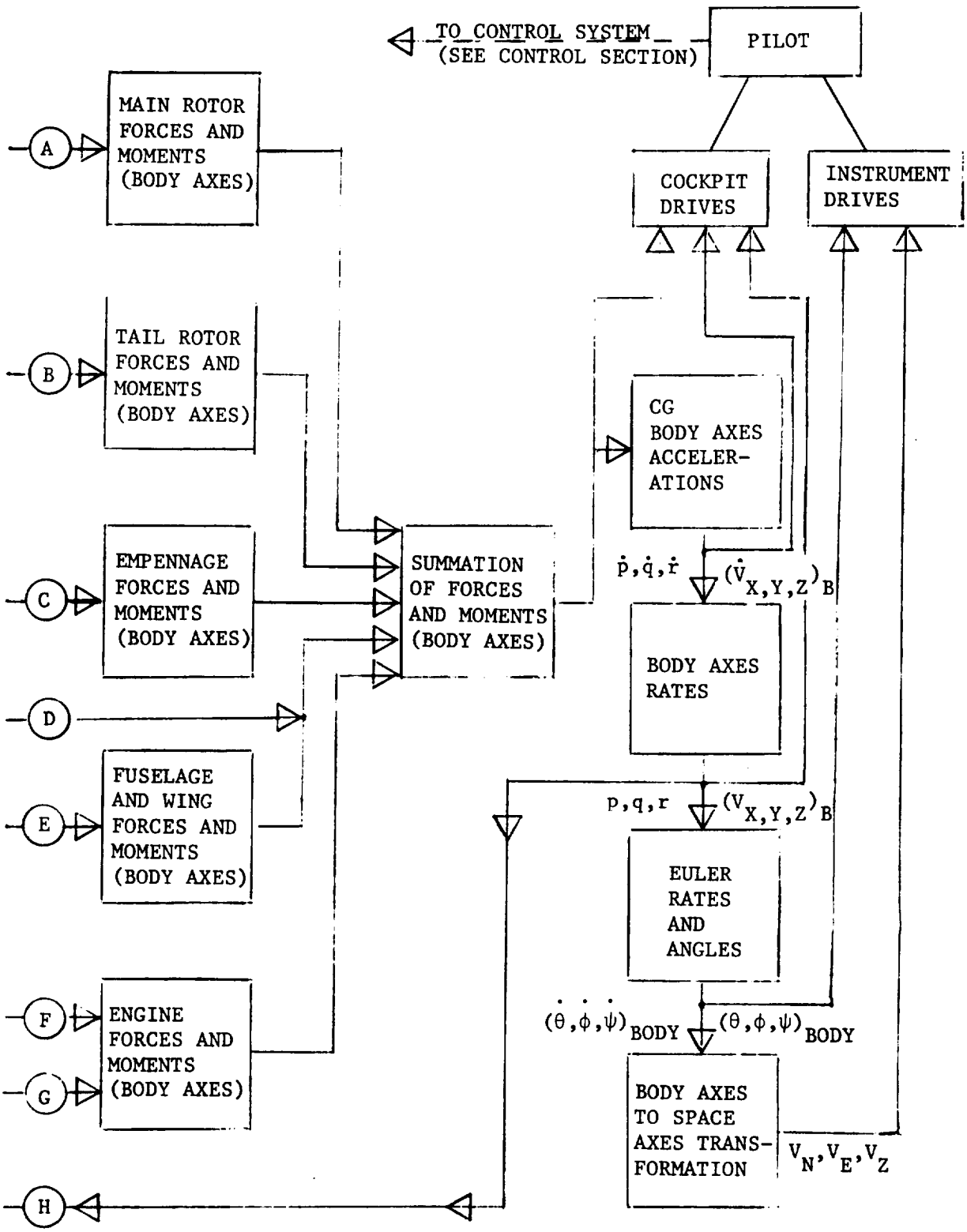

FIGURE 24. - Concluded.